



Universidade do Minho
Escola de Engenharia

Cátia Sofia Dias Oliveira

Development of biofunctionalized tubular scaffolds for vascular tissue engineering applications

Dissertação de Mestrado

Mestrado Integrado em Engenharia Biomédica

Ramo de Biomateriais, Reabilitação e Biomecânica

Trabalho realizado sob a orientação de

Professor Nuno João Meleiro Alves das Neves

Doutor Albino Manuel Pereira Martins

Junho de 2019

DECLARAÇÃO

Nome: Cátia Sofia Dias Oliveira

Endereço eletrónico: a71078@mail.alunos.uminho.pt

Telefone: +351 969444235

Número do Bilhete de Identidade: 14604429

Título da dissertação: Development of biofunctionalized tubular scaffolds for vascular tissue engineering applications

Orientador(es): Professor Nuno João Meleiro Alves das Neves
Doutor Albino Manuel Pereira Martins

Ano de conclusão: 2019

Designação do Mestrado: Mestrado Integrado em Engenharia Biomédica

Área de Especialização: Biomateriais, Reabilitação e Biomecânica

Unidade de Investigação 3B's - Biomateriais, Biodegradáveis e Biomiméticos da Universidade do Minho

É AUTORIZADA A REPRODUÇÃO INTEGRAL DESTA DISSERTAÇÃO APENAS PARA EFEITOS DE INVESTIGAÇÃO, MEDIANTE DECLARAÇÃO ESCRITA DO INTERESSADO, QUE A TAL SE COMPROMETE;

Universidade do Minho, ___/___/_____

Assinatura:

Cátia Sofia Dias Oliveira

Agradecimentos

Assim chegou ao fim mais um capítulo da minha vida e, como tal, gostaria de agradecer a todas as pessoas que me ajudaram e incentivaram durante esta jornada.

Em primeiro lugar, gostaria de agradecer ao Professor Rui Reis pela oportunidade de desenvolver a minha dissertação de mestrado num centro de excelência, Instituto de Investigação em Biomateriais, Biodegradáveis e Biomiméticos (I3Bs), na Universidade do Minho.

Ao meu orientador, Professor Nuno Neves, agradeço sinceramente pela oportunidade de desenvolver este projeto sob a sua orientação. Muito obrigada pela transmissão de conhecimento, pelo espírito crítico, assim como pela força e confiança depositadas todos os dias que foram determinantes para desenvolver este projeto.

Ao meu co-orientador, Albino Martins, um obrigado por toda a ajuda, disponibilidade e conhecimento partilhado ao longo desta etapa. Obrigada por estar sempre presente, me aconselhar sempre da melhor forma e por toda a paciência que foi necessária para me ensinar. A sua orientação foi decisiva, incentivando-me sempre a resolver todos os desafios e adversidades que surgiam de cabeça erguida.

Um especial agradecimento ao Projeto SPARTAN que providenciou o financiamento necessário para a elaboração desta tese. Igualmente, agradeço ao Projeto BEAM (Master Joint Mobility Project - EU Australian cooperation in Biomedical Engineering, Grant Agreement) que permitiu a colaboração com a Universidade de Sydney onde tive a oportunidade de integrar a equipa do Professor Anthony Weiss e da Dr. Suzanne Mithieux. A eles agradeço todo o conhecimento aprendido, bem como toda a disponibilidade e incentivo que tiveram para comigo. Em particular, um especial obrigado à Kekini por toda a ajuda e amizade demonstrada ao longo dos meses. À Su um muito obrigado por me introduzir ao mundo da microscopia confocal, mostrando-se sempre incansável para comigo. Igualmente, quero agradecer à Karen e ao Ziyu que foram os melhores amigos que podia ter e que tornaram a minha temporada em Sydney ainda mais memorável. *To my peeps from the other side of the world, thank you so much for making me feel at home.* Também à Professora Natália, gostaria de expressar uma palavra de apreço pelo seu apoio e trabalho que teve em nos ajudar durante todo o processo, desde a candidatura até à partida para a maior aventura da nossa vida.

A todos os colegas de laboratório com quem tive a oportunidade de trabalhar mais de perto, quero agradecer pelo auxílio e incentivo demonstrado ao longo da minha estadia nos 3B's. À grande Catarina Silva por ser incansável para comigo, por toda a entreatada demonstrada,

estando sempre por perto sempre que precisava de algo. Um especial obrigado à Tatiana Felizardo pelos sábios conselhos de cultura de células e pelas imagens de fluorescência. À Marta Casanova pelas competências extraordinárias de estatística e pela orientação nas ELISAs. À Sara Vieira pelo companheirismo e conselhos prestados sempre que tinha alguma dúvida. À Sara Amorim pela disponibilidade nas análises do SurPass e pelo seu *know-how* da química. Agradeço também ao Emanuel Fernandes pelo esclarecimento sobre os ensaios mecânicos e à Elsa Ribeiro e Belinha pela aquisição das imagens de microscopia de SEM. A todo o staff dos 3B's, muito obrigada por me terem recebido tão bem.

Às meninas da *Library Crew* que me acompanharam desde o primeiro dia nesta aventura não há palavras suficientes para vos agradecer. Obrigada por serem pacientes, por me motivarem sempre que me sentia desmotivada e por todas as gargalhadas e brincadeiras partilhadas ao longo desta viagem. À Taipas, à Rita, à Vera, à Britney e à minha companheira de aventuras na Austrália, Helena um grande obrigado por me aturarem e pelo companheirismo demonstrado.

Uma palavra especial a todas as minhas amigas que me acompanharam durante toda a minha vida. À melhor colega de casa e melhor amiga, Marta, que sempre me ajudou com os meus dilemas e me aconselhou sempre da melhor forma nos bons e maus momentos. À Vera também quero expressar uma palavra de gratidão pelo apoio, amizade e aventuras vividas durante estes anos. Às minhas amigas que a universidade me deu quero também agradecer por todos os inesquecíveis momentos vividos ao longo destes 5 anos que foram cruciais para tornar a minha experiência ainda mais incrível. A elas, Maia, Cardia, Mel, Silva, Mondim, Tininha, Veet, Marinela, Diness, Vilaça e Fontes estou grata por todas as aventuras, gargalhas e, sobretudo, pelo apoio e amizade.

À minha família quero também expressar uma palavra de gratidão por terem sido sempre incansáveis ao longo desta etapa. Em particular, ao meu pai e mãe por todo o apoio, dedicação, encorajamento e amor demonstrados todos os dias, incentivando-me sempre a ser melhor a cada dia. Igualmente, ao Filipe, agradeço-lhe por me aturar nos piores momentos e por estar sempre presente nos melhores momentos, apoiando-me sempre em todas as decisões.

Com alguma tristeza e nostalgia, chego ao fim desta longa viagem que vivi intensamente e, por isso, termino esta fase e toda a minha vida académica com a certeza que foram fundamentais para a minha aprendizagem pessoal e crescimento profissional - *You can check out any time you like, but you can never leave.*

Resumo

Um dos maiores problemas associados à substituição de vasos sanguíneos de pequeno diâmetro é a insuficiência de enxertos vasculares com propriedades mecânicas e biológicas adequadas. Embora existam enxertos vasculares sintéticos na prática clínica, estes substitutos apresentam trombogenicidade e são demasiado rígidos comparativamente aos vasos sanguíneos nativos. Uma rápida endotelização e propriedades mecânicas semelhantes aos vasos sanguíneos humanos são requisitos essenciais que um excerto vascular deve possuir. Neste trabalho, estruturas tubulares fibrosas foram produzidas por *electrospinning* (*eTF scaffolds*) e funcionalizadas para imobilizar tropoelastina na superfície interna, proporcionando um ambiente biomimético para promover a endotelização.

A morfologia foi analisada por microscopia eletrônica de varrimento (SEM), a eficiência da funcionalização da superfície pela quantificação dos grupos amina (-NH₂) e pela carga de superfície, e as propriedades mecânicas foram analisadas por testes uniaxiais à tração. A tropoelastina foi imobilizada a uma concentração de 20 µg/mL através dos seus grupos -NH₂ nos *eTF scaffolds* activados, bem como pelos seus grupos carboxílicos (-COOH) nos *scaffolds* aminolisados, de forma a expor diferentes conformações para a ligação com as células. A quantidade de tropoelastina imobilizada em ambos os substratos foi quantificada através do método microBCA. Por último, os *eTF scaffolds* foram semeados com uma linha celular de células endoteliais da veia umbilical humana durante 7 dias para estudar a endotelização. Desta forma, a atividade metabólica, a proliferação celular, a síntese proteica e de VEGF, bem como a morfologia celular e a manutenção do fenótipo dos *eTF scaffolds* foram investigadas.

Os resultados experimentais demonstraram que os *eTF scaffolds* possuem uma espessura de 240.85 ± 46.91 µm e uma superfície interna 33.55% porosa com diâmetros de fibras na ordem do micro ao submicro, tamanhos de poros inferiores a 23 µm e áreas de poros até 70 µm². Os *eTF scaffolds* foram efetivamente funcionalizados através da inserção de 0.5 ± 0.04 nmol de grupos NH₂ na superfície e pelas diferenças observadas na carga de superfície. Os *eTF scaffolds* não tratados, activados e aminolisados suportaram tensões e alongamentos mais elevados na direção axial do que na radial. Estes resultados obtidos são compatíveis com os valores reportados para os vasos sanguíneos nativos. A exposição dos grupos -COOH da tropoelastina induziu um aumento da atividade metabólica e crescimento das células endoteliais. Quando expostos os grupos -NH₂, uma influência significativa na síntese proteica foi observada. Além disso, os *eTF scaffolds* promoveram a manutenção do fenótipo e a formação de uma monocamada de células

endoteliais na superfície após 7 dias de cultura. De um modo geral, estes resultados confirmam que estes *eTF scaffolds* biofuncionais são adequados para aplicação vascular, uma vez que apresentam propriedades mecânicas adequadas e uma rápida endotelização.

Keywords: *Electrospinning*, Enxertos vasculares por engenharia de tecidos, Biofuncionalização, Tropoelastina, Propriedades mecânicas, Endotelização.

Abstract

One of the major problems related to small-diameter blood vessels replacement is the lack of vascular grafts with suitable mechanical and biological properties. Although there are synthetic vascular grafts in clinical use, these substitutes present thrombogenic behaviour and are too stiff compared to native vessels. Rapid endothelialization and matched mechanical properties are important functional requirements that vascular grafts should accomplish. Herein, an electrospun tubular fibrous (eTF) scaffold was fabricated and functionalized to immobilize tropoelastin at the luminal surface, providing a biomimetic environment to enhance endothelialization.

The morphology was assessed by scanning electron microscopy, the effectiveness of surface functionalization by NH_2 groups quantification and surface charge measurements, and the mechanical properties by uniaxial tensile tests. Tropoelastin was immobilized at $20 \mu\text{g}/\text{mL}$ by its - NH_2 functional groups on activated scaffolds, as well as by its - COOH functional groups on aminolysed scaffolds, in an attempt to expose different conformations of tropoelastin for cell binding. The amount of immobilized tropoelastin on both substrates was quantified by microBCA assay. These constructs were cultured with a cell line of human umbilical vein endothelial cells (HUVECs) for 7 days, to study the endothelialization of eTF scaffolds by evaluating their metabolic activity, proliferation, total protein synthesis, VEGF secretion, as well as cell morphology and phenotype maintenance.

Our experimental characterization demonstrated that the eTF scaffolds have a thickness of $240.85 \pm 46.91 \mu\text{m}$ and their luminal surface was 33.55 % porous mix of micro to submicro fibers diameters, pore sizes less than $23 \mu\text{m}$ and pore areas up to $70 \mu\text{m}^2$. The eTF scaffolds were successfully functionalized by the insertion of $0.5 \pm 0.04 \text{ nmol}/\text{mg}$ of NH_2 groups at their surface and confirmed by the differences observed in surface charge. Untreated, activated and aminolysed scaffolds supported higher stresses and strains in axial direction rather than in radial direction. These values are compatible to those of native blood vessels. The exposure of tropoelastin - COOH groups promoted endothelial cells metabolic activity and growth, whereas when exposed its - NH_2 groups a significant influence on protein synthesis was observed. Additionally, eTF scaffolds promoted phenotype maintenance and endothelial cell coverage just after 7 days of culture. Altogether, the results confirm that biofunctional eTF scaffolds are suitable for vascular application since they presented adequate mechanical properties and a rapid endothelialization.

Keywords: Electrospinning, Tissue-Engineered Vascular Graft, Biofunctionalization, Tropoelastin, Mechanical properties, Endothelialization.

Table of Contents

Agradecimientos.....	iii
Resumo.....	v
Abstract.....	vii
Table of Contents	viii
List of Abbreviations	xi
List of Figures.....	xiii
List of Tables.....	xvi
List of Equations.....	xvii
CHAPTER I. General Introduction	1
1.1 The blood vessels.....	3
1.1.1. Architecture of native blood vessels.....	3
1.1.2. Vascular cells	6
1.2 Cardiovascular diseases	7
1.3 Functional requirements of blood vessel substitutes.....	8
1.3.1 Hemocompatibility of blood vessel substitutes.....	9
1.4 Treatment modalities.....	11
1.5 Tissue engineering	12
1.6 Tissue-engineered vascular grafts strategies.....	13
1.6.1 Cell sources.....	13
1.6.2 Cell-sheet approaches.....	15
1.6.3 Scaffold-based approaches	15
1.6.4 Processing techniques	19
1.6.5 Surface modification	23
1.7 Purpose of the work	27
1.8 References.....	29
CHAPTER II. Materials and Methods	41
2.1 Materials.....	43
2.1.1 Polycaprolactone	43
2.1.2 Tropoelastin	44
2.2 Electrospinning	45
2.2.2 Electrospinning parameters	46

2.2.3	Production of electrospun tubular fibrous (eTF) scaffolds	47
2.3	Functionalization of eTF scaffolds.....	48
2.3.1	Optimisation of surface functionalisation	49
2.3.2	Amine groups (NH ₂) quantification.....	50
2.4	eTF scaffolds characterization.....	51
2.4.1.	Scanning Electron Microscopy (SEM).....	51
2.4.2.	Uniaxial tensile testing	52
2.5	Tropoelastin immobilization	56
2.6	Chemical characterization of the biofunctionalized eTF scaffolds.....	57
2.6.1.	Quantification of immobilized tropoelastin.....	57
2.6.2.	Surface charge properties	58
2.7	Cell biology assays	60
2.7.1.	Cell source	60
2.7.2.	Cell culture and seeding.....	60
2.7.3.	Metabolic activity	61
2.7.4.	Cell proliferation	62
2.7.5.	Total Protein synthesis	62
2.7.6.	Soluble VEGF quantification	63
2.7.7.	Cells morphology	64
2.7.8.	Immunocytochemistry.....	64
2.8	Statistical analysis	65
2.9	References	66
CHAPTER III. Tubular fibrous scaffold functionalized with tropoelastin as a small-diameter vascular graft		73
3.1	Abstract	75
3.2	Introduction.....	76
3.3	Materials and methods	79
3.3.1.	Production of electrospun tubular fibrous scaffolds	79
3.3.2.	Surface functionalization	79
3.3.3.	Scaffolds characterization	80
3.3.4.	Tropoelastin immobilization at luminal surface	81
3.3.5.	Chemical characterization of biofunctionalized scaffolds	81
3.3.6.	Cell biology assays.....	82

3.3.7.	Statistical analysis	85
3.4	Results.....	86
3.4.1.	Scaffolds characterization	86
3.4.2.	Characterization of functionalized scaffolds	87
3.4.3.	Uniaxial tensile properties	89
3.4.4.	Characterization of biofunctionalized scaffolds.....	91
3.4.5.	Biological performance	92
3.5	Discussion	98
3.6	Conclusions	101
3.7	References.....	101
CHAPTER IV.	General Conclusions and Future Work.....	107
4.1.	General conclusions	109
4.2.	Future work.....	110

List of Abbreviations

μg	Microgram	ECs	Endothelial cells
μL	Microliter	EDC	1-(3-Dimethylaminopropyl)-3-ethylcarbodiimide hydrochloride
μm	Micrometer	EDTA	Ethylenediaminetetraacetic acid
Pg	Picogram	ELISA	Enzyme-linked Immunosorbent Assay
E	Tensile strain	EOCs	Endothelial outgrowth cells
Σ	Tensile stress	EPCs	Endothelial progenitor cells
2-IT	2-Iminothiolane	ePTFE	Expanded polytetrafluoroethylene
	A	ESCs	Embryonic stem cells
ASA	Acetylsalicylic acid	eTF	Electrospun Tubular Fibrous
ASCs	Adipose stem cells		F
	B	FBS	Fetal Bovine Serum
BCA	Bicinchoninic acid	FDA	Food and Drug Administration
BSA	Bovine Serum Albumin		G
	C	GAGs	Glycoaminoglycans
CABG	Coronary artery bypass graft		H
CAG	Cysteine-Alanine-Glycine	hiPSCs	Human induced pluripotent stem cells
	D	HMD	Hexamethylenediamine
DES	Drug Eluting Stents	HUVECs	Human Umbilical Vein Endothelial Cells
DMAP	Dimethylaminopyridine	PBS	Phosphate Buffered Saline
DMEM	Dulbecco 's Modified Eagle Medium	PGS	Poly(glycerol sebacate)
DNA	Deoxyribonucleic acid		K
DPBS	Dulbecco's Phosphate Buffered Saline	KCL	Potassium Chloride
dsDNA	double-stranded DNA		M
DTNB	5,5'-dithiobis-(2-nitrobenzoic acid	M	Molar
DTT	Dithiothreitol		
	E		
E	Young 's modulus		
ECM	Extracellular matrix		

MES	2-N-morpholino) ethanesulfonic acid hydrate)	PLCL	Poly(L-lactide-co-E-caprolactone)
mL	Milliliter	PLGA	Poly(lactic-co-[glycolic acid])
Mm	Millimeter	PLLA	Isomer of PLA
mM	Millimolar	PU	Polyurethane
MPa	Mega Pascal		R
MSCs	Mesenchymal stem cells	RGD	arginine–glycine–aspartic acid
		rpm	Revolutions per minute
			S
MTS	3-(4,5-dimethylthiazol-2-yl)-5-(3-carboxymethoxyphenyl)-2-(4-sulfophenyl)-2H-tetrazolium)	SDF-1 α	Stromal cell-derived factor-1 α
		SEM	Scanning Electron Microscopy
		SMCs	Smooth muscle cells
			T
N	Newton	TEVGs	Tissue-engineered Vascular Grafts
NaCL	Sodium Chloride		Thermally Induced Phase
NaOH	Sodium Hydroxide	TIPS	Separation
NHS	N-hydroxysulfosuccinimide	TNB	2-nitro-5-thiobenzoic acid
Nm	Nanometer		U
Nmol/mg	Nanomol per milligram	UV	Ultra-violet
			V
PCAM-1	Platelet Endothelial Cell Adhesion Molecule	VEGF	Vascular endothelial growth factor
PCL	Polycaprolactone		
PCU	Polycarbonate urethane		
PDGF	Platelet-derived growth factor		
PDS	Polydioxanone		
PEEUU	Poly(ester-urethane)urea		
PEGMA	Poly(ethyleneglycol)methacrylate;		
PES	Polyethersulfone		
PET	Polyethylene terephthal		
PGA	Polyglycolic acid		
PHVB	Poly(3-hydroxybutyrate-co-3-hydroxyvalerate)		
PLA	Poly(lactic acid)		

List of Figures

Chapter I. General Introduction

- Figure 1. 1** - Structure of an artery, illustrating the cellular and extracellular components distributed within the three tunics. Adapted from ref. [1]..... 4
- Figure 1. 2** - Development of atherosclerosis. (a) A healthy artery. (b) The infiltration and migration of leucocytes into the intima. (c) The migration of SMCs from the media to the intima layer and proliferation of intimal SMCs and ECM proteins, resulting in the formation of plaque. (d) Disruption of the plaque which leads to the formation of thrombus. Adapted from ref. [9]..... 8
- Figure 1. 3** - The coronary artery bypass graft. The use of a non-vital vessel (A) to provide a new path for blood flow (B). Adapted from ref. [29]..... 11
- Figure 1. 4** - Tissue-engineered vascular grafts strategy. Adapted from ref. [35]..... 13

Chapter II. Materials and Methods

- Figure 2. 1** - PCL chemical structure. Adapted from ref. [10]. 43
- Figure 2. 2** - Tropoelastin structure which includes two functionally distinct regions, N and C terminal, separated by a bridge responsible for the mechanical coupling. Adapted from ref. [17]. 45
- Figure 2. 3** - Schematic representation of the electrospinning setup used to produce eTF scaffolds..... 48
- Figure 2. 4** - Schematic representation of activation (NaOH treatment) and aminolysis (HMD treatment) reactions on eTF scaffolds surface..... 49
- Figure 2. 5** - Typical tensile specimen with an enlarged ends and reduced gauge section. Adapted from ref. [53]..... 53
- Figure 2. 6** - Stress-strain curve for a ductile material. Adapted from ref. [52]..... 54
- Figure 2. 7** - Specimens preparation (A) and specimens mounting (B) for uniaxial tensile testing. 55
- Figure 2. 8** - Schematic representation of tropoelastin immobilization on activated (A) and aminolysed (B) eTF scaffolds surface. 56
- Figure 2. 9** - Chemical reaction for the EDC/NHS coupling. Adapted from ref. [55]. 57
- Figure 2. 10** - Schematic representation of charge distribution in the zeta potential measurement. Adapted from ref. [58]. 59

Chapter III. Tubular fibrous scaffold functionalized with tropoelastin as a small-diameter vascular graft

Figure 3. 1- Electrospun tubular fibrous (eTF) scaffolds. Macrostructure (A and B) and SEM micrographs of the cross-section (C and D).	86
Figure 3. 2 - SEM micrographs of eTF scaffolds along axial (A) and radial (B) directions. Fibers morphology analysis: fiber orientation of axial and radial directions (C), fiber diameter frequency (D), pore size frequency (E) and pore area frequency (F).	87
Figure 3. 3 - SEM micrographs of the activated (A) and aminolysed (B) surfaces. Frequency distribution of fibers diameter of activated (C) and aminolysed (D) surfaces. NH_2 groups quantification on untreated, activated and aminolysed eTF scaffolds (E). Data were analyzed by the one-way ANOVA test, followed by the Tukey 's HSD test ($p < 0.05$): a denotes significant differences compared to untreated condition and b denotes significant differences compared to activated condition. The data is expressed as the mean \pm standard deviation.	88
Figure 3. 4 - Stress-Strain curves of untreated, activated and aminolysed eTF scaffolds, tested in dry and hydrated conditions: axial direction (A) and radial direction (B).	89
Figure 3. 5 - Uniaxial tensile properties of untreated, activated and aminolysed eTF scaffolds under axial and radial directions, tested in dry (1) and hydrated (2) conditions: Young 's modulus (A), maximum stress (B) and strain at maximum stress (C). Data were analysed by the Krustal-Wallis tes Wallis test, followed by the Tukey's HSD test ($p < 0.01$): a denotes significant differences compared to untreated and b denotes significant differences compared to activated condition. The data is expressed as median \pm interquartile range.	90
Figure 3. 6 - Maximum immobilization capacity of tropoelastin at the surface of activated (OH-TE) and aminolysed ($\text{NH}_2\text{-TE}$) eTF scaffolds. Data were analysed by the Krustal-Wallis test, followed by the Tukey's HSD test ($p < 0.01$): a denotes significant differences compared to concentration 0 $\mu\text{g/mL}$; b denotes significant differences compared to concentration 5 $\mu\text{g/mL}$; c denotes significant differences compared to concentration 10 $\mu\text{g/mL}$. The data is expressed as median \pm interquartile range.	91
Figure 3. 7 - Surface zeta potential of untreated, activated (OH), aminolysed (NH_2) and tropoelastin-immobilized on activated (OH-TE) or on aminolysed ($\text{NH}_2\text{-TE}$) eTF scaffolds along pH.	92

Figure 3. 8 - Metabolic activity (A) and DNA quantification (B) of human endothelial cells seeded on untreated, activated (OH), aminolysed (NH₂) and tropoelastin-immobilized on activated (OH-TE) or on aminolysed (NH₂-TE) eTF scaffolds after 1, 3 and 7 days of culture. Data were analysed by the Krustal-Wallis test, followed by the Tukey ' s HSD test (p<0.01): **a** denotes significant differences compared to the untreated condition. 94

Figure 3. 9 - Total protein synthesis (A) and soluble VEGF production (B) human endothelial cells seeded on untreated, activated (OH), aminolysed (NH₂) and tropoelastin-immobilized on activated (OH-TE) or on aminolysed (NH₂-TE) eTF scaffolds after 1, 3 and 7 days of culture. Data were analysed by the Krustal-Wallis test, followed by the Tukey ' s HSD test (p<0.01): **a** denotes significant differences compared to the untreated condition; **b** denotes significant differences compared to the activated condition; **c** denotes significant differences compared to the aminolysed condition and **d** denotes significant differences compared to the OH-TE condition. 95

Figure 3. 10 - Morphological analysis by SEM of human endothelial cells cultured on untreated, activated (OH), aminolysed (NH₂) and tropoelastin-immobilized on activated (OH-TE) or on aminolysed (NH₂-TE) eTF scaffolds surface after 1, 3 and 7 days of culture. Scale bar: 100 μm (250x magnification) and 10 μm (1000x magnification). 96

Figure 3. 11 - Fluorescent images of human endothelial cells seeded on untreated, activated (OH), aminolysed (NH₂) and tropoelastin immobilized on activated (OH-TE) or on aminolysed (NH₂-TE) eTF scaffolds surface after 1, 3 and 7 days of culture. Cell nuclei are stained in blue by DAPI and the CD31 endothelial cell marker is stained in green. Scale bar: 50 μm. 97

List of Tables

Chapter I. General Introduction

Table 1. 1 - Characteristics of the blood vessels. Adapted from ref. [1]	5
Table 1. 2 - Summary of some processing techniques, materials and cell sources explored to produce TEVGs.....	21
Table 1. 3 - Summary of the surface modification strategies applied for TEVGs.....	24

Chapter II. Materials and Methods

Table 2. 1 - Electrospinning parameters tested for optimization of eTF scaffolds production ...	47
Table 2. 2 - Concentrations and incubation times of both NaOH and HMD solutions tested for optimization of nanofibers surface functionalization	50

Chapter III. Tubular fibrous scaffold functionalized with tropoelastin as a small-diameter vascular graft

Table 3. 1 - Uniaxial tensile mechanical properties: Young 's modulus and maximum stress of some native human blood vessels.....	77
---	----

List of Equations

Chapter II. Materials and Methods

Determination of the amine groups (NH_2) (Equation 2. 1).....	51
Determination of Tensile Stress (Equation 2. 2)	53
Determination of Tensile Strain (Equation 2. 3).....	53
Determination of Young ' s Modulus (Equation 2. 4)	54

CHAPTER I.

General Introduction

Chapter I. General Introduction

1.1 The blood vessels

The vascular system of the human body is composed of blood vessels whose function is to facilitate blood distribution to and from the heart, tissues and organs. The blood vessels form a branched system of arteries and veins which differs in function and structural organization [1].

An artery is a larger blood vessel which transports the oxygenated blood from the heart to the organs and tissues where it branches into smaller vessels, called arterioles [1]. The arterioles divide into tiny capillaries to distribute the blood within the organs and tissues, providing the supply of nutrients, oxygen and transport of CO₂ and waste [2]. Afterwards, the blood leaves the capillaries, converging into smaller veins, called venules. The venules carry the blood to a vein, a larger blood vessel which is responsible for conducting the blood back to the heart [1,2].

1.1.1. Architecture of native blood vessels

Structurally, both arteries and veins have a concentric layered structure and are composed of three distinct tissue layers called tunics. Starting from the inner layer to the outer, it is possible to identify the tunica intima, the tunica media and the tunica adventitia. These layers present different cellular and protein composition, having specific roles in the maintenance of the normal vascular function [1,3].

Concerning the vascular wall composition, collagen is the load bearing protein which establishes the structural basis of the vessels and, thus, provides strength and flexibility to the vessel. Along with collagen, elastin is also an important element of the vascular walls since it provides resilience and passive elastic recoil without energy input [4]. The following Figure 1. 1 represents the structure and characteristics of an artery.

The tunica intima, or tunica interna, is composed of the endothelium, the basement membrane and the connective tissue. The endothelium consists of a single layer of endothelial cells (ECs) and is the layer lining the vascular wall. Next to the endothelium, the basement membrane, or basal lamina, is a thin extracellular layer composed mainly of collagen, proteoglycans and glycoproteins. This membrane binds the endothelium to the subendothelial layer which consists of loose connective tissue, where smooth muscle cells (SMCs) can be present [1].

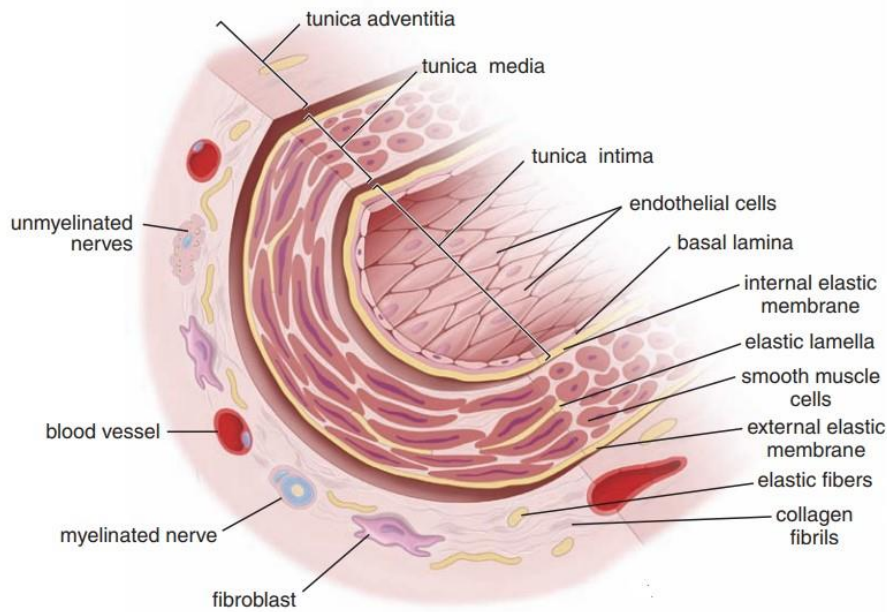


Figure 1. 1 - Structure of an artery, illustrating the cellular and extracellular components distributed within the three tunics. Adapted from ref. [1].

The tunica media is the intermediate layer of the vessel wall. This layer consists of circumferentially organized layers of SMCs that are responsible for the contractile function of the vessel [1,3]. Elastin, arranged in circular concentric layers, reticular fibers, and proteoglycans are interposed between the SMCs in the tunica media [1]. These components provide strength to the vessel and act as effectors of vascular tone [2].

The tunica adventitia is a considerable sheath of connective tissue composed mainly by longitudinally arranged collagenous fibers containing fibroblasts and perivascular nerve cells, that provides rigidity to the vessel walls. The outer layers of the tunica adventitia are found with the surrounding connective tissue outside the vessel in order to hold it in place [1,3].

Both arteries and veins can be distinguished by the composition and thickness of the vascular wall, as suggested in the Table 1. 1. For instance, arteries with diameter superior of 10 mm are called elastic arteries because they are composed of multiple sheets of elastin in their walls, which allow them to stretch and recoil without permanent deformation. Additionally, the medium arteries display lower diameters and are known as muscular arteries due to the higher content of SMCs in comparison with elastin in the middle layer [1]. These arteries present two additional layers, the internal and external elastic membrane, which separate the tunica intima and media, and the tunica media and adventitia, respectively, to provide elasticity to the vessel, as illustrated in Table 1. 1 [1,3]. In contrast, the vascular wall layers of veins are more similar and thinner than arteries. For small vessels as arterioles and venules, the vascular wall is composed of

few layers of SMCs, while in capillaries the structure of the layers might be less obvious or absent [2,3].

Table 1. 1 - Characteristics of the blood vessels. Adapted from ref. [1]

Blood Vessels		Diameter	Tunicas composition		
			Intima	Media	Adventitia
Arteries	Large Artery	>10 mm	Endothelium Connective tissue SMCs	SMCs Elastic lamellae	Connective tissue Elastic fibers
	Medium artery	2-10 mm	Endothelium Connective tissue SMCs Internal elastic membrane	SMCs Collagen fibers External elastic membrane	Connective tissue Some elastic fibers
	Arteriole	10-100 μ m	Endothelium Connective tissue SMCs	SMCs (1-2 cell layers)	Unclear sheet of connective tissue
	Capillary	4-10 μ m	Endothelium	None	None
Veins	Large vein	>10 mm	Endothelium Connective tissue SMCs	SMCs Collagen fibers	Connective tissue Some elastic fibers SMCs
	Medium vein	1-10 mm	Endothelium SMCs Collagen fibers	SMCs Collagen fibers	Connective tissue Some elastic fibers
	Venule	50-100 μ m	Endothelium	SMCs (1-2 cell layers)	Connective tissue Some elastic fibers
	Postcapillary venule	10-50 μ m	Endothelium Pericytes	None	None

1.1.2. Vascular cells

The endothelium is the major component of the tunica intima which is formed by a continuous layer of flattened, elongated and polygonally shaped ECs that are aligned in the direction of the blood flow. These cells play an important role in blood homeostasis and participate in the structural and functional integrity of the vascular wall [1]. Moreover, ECs are responsible for maintaining a selective permeability barrier which allows the movement of small and large molecules from the blood to the tissues and vice versa [2,5].

One of the most important properties of the vessels is the presence of a non-thrombogenic barrier between blood platelets and subendothelial tissue. The maintenance of this barrier is achieved by the production of anticoagulants (e.g. thrombomodulin), agents that prevent coagulation, and anti-thrombogenic substances (e.g. prostacyclin), agents that prevent or interfere with platelet aggregation and formation of clots [1]. ECs regulate the expression of binding sites for anticoagulant and anti-thrombogenic factors at cell surface, maintaining the blood fluidity and controlling the activity of anticoagulants pathways, under physiological conditions. Upon vascular injury, these anticoagulant mechanisms are interrupted and the procoagulant pathways are induced to produce prothrombogenic agents (e.g. Von Willebrand factor) promoting clot formation to restore vascular integrity [6].

The endothelium is also important in the modulation of blood flow and vascular resistance. ECs secrete and uptake several vasoactive substances, such as nitric oxide (NO), endothelin and angiotensin II, in response to physical stimuli which induce constriction and dilation, regulating the blood flow [6]. Vascular ECs also regulate the SMCs growth not only by the synthesis of several stimulating growth factors as platelet-derived growth factor (PDGF) but also by the synthesis of inhibiting growth factors as heparin. At the luminal surface, ECs express a variety of surface adhesion molecules and receptors crucial to regulate the immune responses by controlling the interaction between lymphocytes and endothelial surface. The maintenance of extracellular matrix (ECM) is achieved by the synthesis of type IV collagen, laminin and proteoglycans [1,5].

The mechanical properties of native arteries rely on the presence of contractile vascular SMCs, elastin, collagen and proteoglycans within the tunica media. SMCs respond to stimuli from the ECs and cytokines from the blood, contracting or dilating [7]. The shear stresses produced between the blood flow and endothelium increase the production of NO by ECs. Once synthesized, NO diffuses to the tunica media to induce the relaxation of SMCs and, consequently, the vessel dilation. To cause vasoconstriction, endothelins are also produced by ECs to reduce the luminal

diameter of the vessel and increase vascular resistance, promoting the contraction of SMCs and, consequently, the vessel contraction [1]. SMCs are primarily responsible for the ECM proteins synthesis, namely, elastin and collagen, in this layer. Elastin confers elasticity, as well as act as regulator of SMCs proliferation, whereas the radially aligned collagen fibers provide appropriate stiffness to withstand the physiological stress. Moreover, proteoglycans, such as heparan sulfate, chondroitin sulfate and dermatan sulfate, play a crucial role on the compressibility of the artery wall [7].

Tunica adventitia participates in vessel structure and function, mediated mainly by the presence of adventitial fibroblasts which are also responsible for collagen synthesis [7]. Particularly, this layer influences growth and repair of the vessel wall and mediates communication between ECs and SMCs. Also, lymphatic vessels and nerves can be found to control the lumen size and vascular remodelling, as well as populations of macrophages and mast cells mediate immune response [8]. Incorporated within the media and the adventitia layers can be found the vasa vasorum which is a network of blood vessels responsible for oxygen and nutrients supply to cells present in both layers [7].

1.2 Cardiovascular diseases

Diseases of the cardiovascular system are the major causes of morbidity and mortality worldwide. Coronary heart disease, also known as ischemic heart disease, is the most common type of vascular disease which is mainly caused by atherosclerotic changes in the walls of coronary arteries. This promotes the artery occlusion and, consequently, the restriction to the blood flow and oxygen supply to the cardiac muscle [1].

Atherosclerosis develops primarily in the tunica intima of blood vessels and is responsible for functional and structural changes in the vessel wall (Figure 1. 2) [9]. In its early stage, the damaged endothelium has increased permeability to the circulating low-density lipoproteins (LDL, responsible for cholesterol transport), ECM proteins and cells such as blood leukocytes and monocytes [5,9]. These molecules can penetrate and become entrapped within the tunica intima. Also, as SMCs and fibroblasts migrate to the lesion to replace dead ECs, the resultant layer of fibrous connective tissue becomes thicker which leads to the development of atheromatous plaques [1,10]. As these plaques progress, the integrity of endothelium is lost, narrowing the arteries enough to impair the blood flow. Eventually, the disruption of the plaques may occur, resulting in the formation of thrombus and, consequently, in the artery obstruction which can cause

severe damages on the patient. Alternatively, the plaque can break off and travel with the bloodstream as an embolus until it blocks a smaller artery more distant [1].

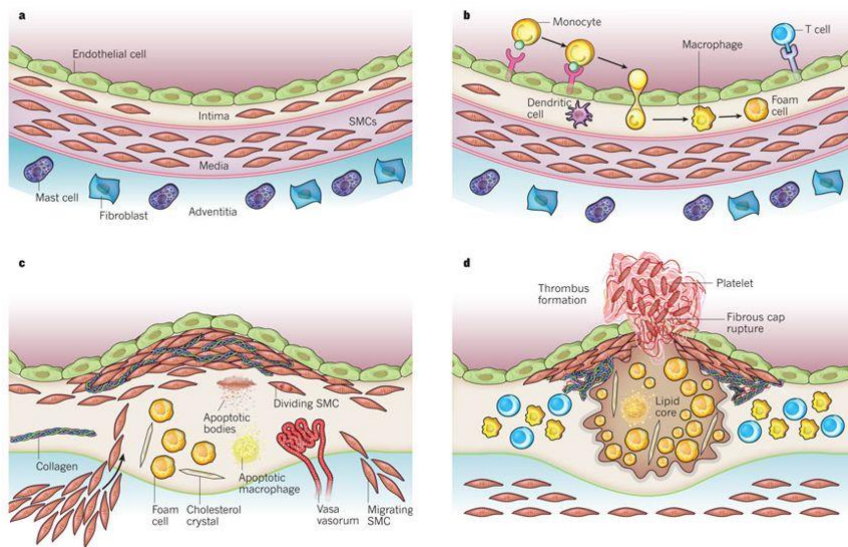


Figure 1. 2 - Development of atherosclerosis. (a) A healthy artery. (b) The infiltration and migration of leukocytes into the intima. (c) The migration of SMCs from the media to the intima layer and proliferation of intimal SMCs and ECM proteins, resulting in the formation of plaque. (d) Disruption of the plaque which leads to the formation of thrombus. Adapted from ref. [9].

The endothelium dysfunction may also lead to the reduction of the artery compliance. Compliance is the ability of an artery to expand, when the blood is pumped through it from the heart, and then to recoil after the blood passage, facilitating the blood flow [1]. In atherosclerosis, the compliance is reduced increasing the pressure and the resistance within the vessel [1,10].

1.3 Functional requirements of blood vessel substitutes

There are several requirements that a vascular graft needs to meet, aiming to be considered ideal for blood vessel substitute. It should be biocompatible, non-immunogenic, non-thrombogenic and induce an acceptable healing response. Additionally, it should possess suitable mechanical properties, such as physiological compliance, and the ability to withstand the cyclic hemodynamic stress without failure [11–13].

Thrombogenic complications are in the short-term the primary cause of graft failure [13]. Since the endothelium contacts the blood, it is required a vessel substitute with a confluent endothelium, as well as vasoactive properties to provide an antithrombotic lumen [11,14]. As such, ECs must adhere to the graft to allow the formation of an anti-thrombogenic luminal continuous

surface [11]. A rapid endothelialization plays a critical role in reducing thrombosis and keeping long-term patency due to the anti-inflammatory and anticoagulation functions of the ECs [12].

The graft should mimic the ECM morphology with suitable pore size, porosity and interconnectivity in order to allow cells infiltration, adhesion, proliferation and synthesis of their own ECM [12,15]. Regarding the pore size, larger pores may induce excessive fibrous tissue infiltration and lead to blood leakage, compromising the endothelial coverage and the mechanical properties [13]. On the other hand, small pores may obstruct the cell infiltration and migration, particularly, for SMCs colonization in the outer part of the vessel [15]. Furthermore, the vascular graft surface should allow cells to resist to the detachment caused by the high shear forces resulting from the blood flow and turbulence [11].

An important aspect to be considered is the mechanical properties of the vascular graft. It should possess structural and mechanical properties similar to the native blood vessels [15]. The blood vessel substitute requires a compliant material since the compliance mismatch is the basis of intimal hyperplasia [11]. The compliance mismatch between the native vessel and the vascular graft can trigger the excessive proliferation of SMCs and fibroblasts, as well as the ECM deposition in the vessel wall, leading to lumen narrowing [13]. Furthermore, the vascular graft should provide mechanical support to withstand the physiological conditions of native blood vessels over an extended period of time, without experiencing permanent deformation [15,16]. To mimic the native tissue, the engineered vascular grafts should possess burst strength higher than 1,700 mmHg to support the systemic arterial pressures. In addition to burst strength, the vascular graft must be fatigue resistance to cyclic physiological loading without noticeable dilation [17]. In fact, it should allow contractility but not undergoing plastic behaviour since it could result in aneurysm formation upon long-term implantation [11,15]. Additionally, the vascular graft must present appropriate elastic moduli to allow suture retention strength comparable with physiological values and suitable degradation kinetics properties to allow the regeneration of the vascular tissue [14,15].

1.3.1 Hemocompatibility of blood vessel substitutes

Since the hemocompatibility is one of the major requirements of blood vessel substitutes, it is crucial to understand the fundamental mechanism that induces thrombosis. When implanted, the vascular graft should not adversely interact, activate and not damaged any blood components [18].

The blood is composed of 55% plasma, 44% erythrocytes and 1% leucocytes and platelets. The blood plasma contains high amounts of proteins, such as albumin, coagulation factors and immunoglobulins. The erythrocytes are the most abundant blood cells which function is to transport the oxygen to all tissues. These cells are sensitive to rupture when exposed to exterior shear stress and changes in osmotic pressure. Platelets are the second abundant cell type in the blood and are the cellular component responsible for the coagulation cascade. These cells can rapidly recognize foreign surfaces and trigger the blood coagulation. Besides these cell types, monocytes and granulocytes are also present in the blood. These immune cells can be rapidly activated upon recognition of a foreign material to neutralize it [18].

Once the biomaterial is in contact with the blood, several reactions occur at the surface that are crucial for tissue replacement, determining the success or failure of the implant [19]. The contact of the biomaterial with the blood induces a cellular response mediated by the platelets. The cells are recruited to the implant surface where they might adhere, spread, release active compounds and recruit other cells to the implant site [20]. Consequently, an instantaneous adsorption of plasma proteins (e.g., fibrinogen, fibronectin, vitronectin, albumin) may occur to the biomaterial surface, triggering the activation of the coagulation cascade and of the complement system [21–23].

The activation of the coagulation cascade involves two enzyme based pathways, the extrinsic and intrinsic, leading to the thrombus formation. The extrinsic pathway is initiated when the blood is exposed to the damaged endothelium. The intrinsic pathway is activated by the contact between the implanted materials and the blood, followed by conformational changes in the plasma proteins. Both pathways converge, eventually, into a common pathway where the thrombin catalyses the conversion of fibrinogen to fibrin that forms crosslinked fibrils, resulting in a fibrin clot. The complement system consists of more than 20 proteins circulating in the blood and, when a foreign surface is in contact with blood, the complement factors are sequentially activated, leading to the activation of platelets, coagulation enzymes and inflammation through leukocyte activation [24]. The thrombogenicity of a blood vessel substitute is determined by the extent of the activation of these pathways [25].

The protein adsorption depends on the biomaterial surface chemical composition and topography, affecting the blood-material interactions [26]. In particular, hydrophobic surfaces have an increased complement activation in comparison to the hydrophilic surfaces [27]. Since the adhesion and activation of platelets is prevented by a healthy endothelial monolayer, a rapid

endothelialization is required to develop a EC layer on the material 's surface, preventing the thrombus formation [28].

1.4 Treatment modalities

In the early stages of plaque deposition in the lumen of blood vessels, medication can be used to prevent the progression of plaque formation. However, in many cases, the blood flow is compromised, and the use of therapeutic drugs may be no longer effective [29,30]. For severe lesions in the vessel walls, other treatments must be considered. When the plaque deposition is in the early stages but causing thoracic pain, angioplasty is performed. In this treatment, a catheter is inserted into the vessel at the narrowing point and a balloon is inflated to expand the vessel. The blocked artery is opened and begin to heal as soon as the balloon is deflated. However, if the plaque progression causes severe thoracic pain, a stent is normally included in the angioplasty procedure to prevent the collapse of the vessel [29,30].

In plaque occlusion cases, surgical procedure is required, particularly, when there is a significant narrowing of the left main coronary artery or multiple areas of coronary artery blockage [29,30]. This procedure, called coronary artery bypass graft (CABG) surgery, uses a non-vital superficial vessel from another part of the body or a synthetic vessel to insert in the blocked area to restore the blood flow in the coronary artery [29]. The following Figure 1. 3 illustrates the alternative blood flow created by the CABG surgery.

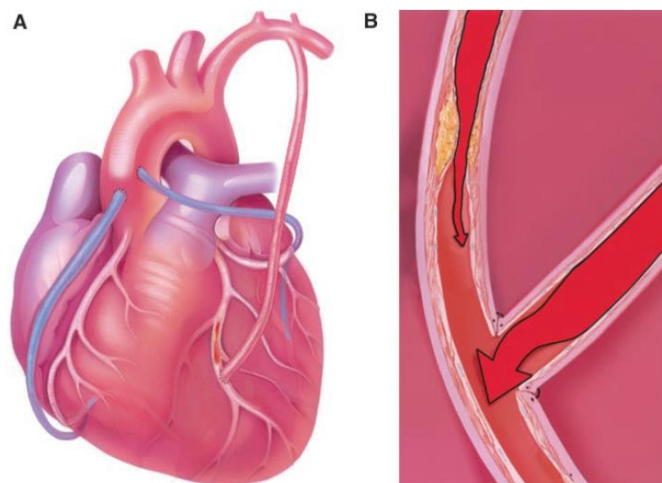


Figure 1. 3 - The coronary artery bypass graft. The use of a non-vital vessel (A) to provide a new path for blood flow (B). Adapted from ref. [29].

In CABG surgery, the surgeon uses a portion of a healthy vessel (either a muscular artery or a muscular vein) from the leg, chest or arm [29]. The most commonly used vessels for bypass surgery are the saphenous vein from the leg, the internal mammary artery from the chest and the

radial artery from the arm. Although the saphenous vein is preferred than other vessels due to its easily surgical access, this vessel is more prone to intimal hyperplasia, aneurysm and atherosclerosis [30]. In contrast, the internal mammary artery exhibits greater elasticity, the ability to vasoregulate and is less prone to atherosclerosis than the other vessels. Also, the internal mammary artery demonstrates superior patency comparing to the saphenous vein [31].

These biological grafts are suitable replacements because they are flexible, viable, non-thrombogenic, biocompatible and have adequate patency. Therefore, autologous substitutes are considered the gold standard in CABG surgery. However, the limited availability of non-affected autologous grafts in patients with vascular diseases may limit their use. This is particularly frequent in patients subjected to previous surgery or by the anatomical variability [32,33]. As alternative substitutes, allografts (donor/cadaveric) and xenografts (from bovine or porcine pulmonary valve conduit) can be also used, but their performance may be compromised by the potential immunogenic reaction [33].

Synthetic vascular grafts have emerged as commercial alternatives to the autologous vessels [33]. Currently, there are two clinically available synthetic vascular grafts: polyethylene terephthalate (PET) and expanded polytetrafluoroethylene (ePTFE) [31]. These non-degradable materials have been extensively used as medium and large diameter vessel replacement ($\varnothing > 6$ mm) with reasonable success. However, when they are applied to small-diameter vessels ($\varnothing < 6$ mm), such as the coronary artery, these grafts tend to fail, producing low patency rates. This occurs because the large diameter vessels are subject to higher flows and less resistance than small diameter vessels. Furthermore, the low blood flow and high shear stresses involved in small-diameter vessels make the synthetic graft more prone to thrombus formation and intimal hyperplasia [29,32]. In fact, synthetic surfaces display a thrombogenic behaviour and cause immune reaction, resulting in chronic inflammation. Because these polymers are stiffer, this also leads to a compliance mismatch between the rigid synthetic conduits and the native elastic vessels, and, consequently, cause intimal hyperplasia [31]. Therefore, an ideal small-diameter vascular graft for these situations is currently not available.

1.5 Tissue engineering

Tissue engineering is a promising alternative for the creation of vascular grafts. This approach combines the principles of engineering and life sciences, aiming for the creation of tissue substitutes. Generally, the tissue engineering approach relies on the seeding or encapsulation of cells, followed by culture of cells under defined *in vitro* conditions in scaffolds fabricated from

biodegradable synthetic or natural polymer [34]. The scaffold provides a temporary biomechanical structure for cells in culture to produce their own ECM, while the polymer is degrading, which facilitated the production of ECM, allowing the gradual creation of the intended tissue [32].

Functional tissue-engineered vascular grafts (TEVGs) were already extensively investigated. The cells are harvested from the patient and expanded *in vitro*, followed by their seeding onto a polymeric tubular scaffold. The construct can be placed in a bioreactor to mature the engineered vessel and, then, be implanted into the patient, replacing the damaged blood vessel (Figure 1. 4) [35]. These tubular constructs combined with viable cells represent an attractive potential solution due to their ability to grow and remodel *in vitro*, avoiding the need for autograft surgery [33].

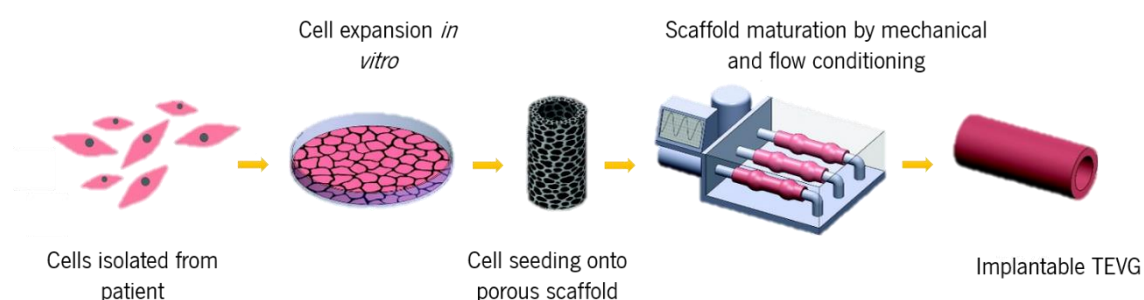


Figure 1. 4 - Tissue-engineered vascular grafts strategy. Adapted from ref. [35].

1.6 Tissue-engineered vascular grafts strategies

Several strategies have been applied to develop functional TEVGs, from cell-sheet to scaffold-based approaches, to address the vascular grafts needs. Although some of these strategies have already reached the clinical studies, the searching for an ideal small-diameter vascular graft is still underway. Aiming to create a vascular graft, a balance between the advantages and limitations of the current approaches should be considered, as well as the most appropriate cells, materials and processing methods.

1.6.1 Cell sources

Several different types of cells were previously considered for the development of TEVGs. There are two main groups of cells sources to obtain functional TEVGs, autologous vascular cells and stem cells. Vascular cells possess several physiologic functions *in vivo*. ECs are important in maintaining a barrier between the blood and the vessel wall, and in regulating the inflammation and thrombosis [36]. Currently, ECs are isolated from human tissue, such as umbilical cord vein and human aortic, being in a differentiated and mature state [37,38]. However, the isolation of

large number of ECs for expansion is limited in this source, as well as their capacity of regeneration. Besides, the vascular endothelium is plastic in nature, but the phenotypic plasticity of ECs is limited, losing the phenotypic marker expression *in vitro* [36]. In addition, SMCs, isolated from human tissues, have been also applied in TEVGs to develop functional vascular grafts with mechanical integrity [14].

Endothelial progenitor cells (EPCs) were used to overcome the limitations of using ECs. These cells represent a less invasive cell source that can be isolated from peripheral blood or umbilical cord blood [38]. EPCs can be differentiated to an endothelial-like phenotype, promoting the vascularization in many pathophysiological situations [39,40]. Among EPCs, endothelial outgrowth cells (EOCs) have been studied due to their easy isolation from a patient blood sample, as well as their high proliferation capacity. These cells are expanded from circulating EPCs, providing a convenient source of autologous ECs. EOCs have been demonstrating an uniform expression of endothelial cell markers and a typical endothelial cell morphology [41].

Alternatively, stem cells were explored as a potential cell source for tissue engineering. Human embryonic stem cells (hESCs) are a population of cells that can be obtained from the inner cell mass of blastocyst-stage embryos, having the ability to proliferate indefinitely in culture [42]. Moreover, providing the right biochemical factors, it is possible to stimulate the hESCs differentiation into vascular ECs [42] and SMCs [43]. Despite their proliferative capacity and pluripotency, the source of this type of cells present many ethical concerns [42]. Alternatively, human induced pluripotent stem cells (hiPSCs) can be obtained from the patient's own somatic cells and differentiated into every cell type of the body. As such, it is possible to obtain ECs derived from hiPSCs [36], as well as vascular SMCs [44], displaying the characteristics of primary ECs and SMCs. This source has a similar potential to hESCs without the ethical constraints and in autologous context avoids the immunogenic issues of hESCs.

Adult mesenchymal stem cells (MSCs) can be isolated from the patient's own tissues, being also an alternative to hESCs. MSCs can be isolated from bone marrow, adipose tissue and they have the ability to self-renew indefinitely and to differentiate into mature cells in specific conditions [45]. The use of this type of cells is less invasive than harvesting vascular cells from autologous blood vessels. In many cases, patients may not have suitable blood vessels to harvest the cells due to a pre-existing vascular disease or the vessel use in previous procedures, which makes the stem cells a reliable and promisor cell source. These cells have the ability to differentiate into ECs and SMCs *in vitro* and *in vivo*, under specific stimulation. Additionally, MSCs present good

plasticity and play an important role in vascularization and angiogenesis [46]. However, the advanced patient age, the availability of cells from this source may be limited [47]. As an alternative to MSCs, adipose-derived stem cells (ASCs), obtained from the adipose tissue, can be easily isolated, representing a viable alternative to MSCs. ASCs can differentiate into vascular cells, acquiring several endothelial-like characteristics when exposed to mechanical stimuli and to a modified culture environment [47].

1.6.2 Cell-sheet approaches

Cell sheet self-assembly is a cell-based approach towards developing a TEVG, without the need of exogeneous materials. This strategy allows the production of an intact sheet of cells without enzymatic digestion, allowing the preservation of cell-to-cell junction proteins and ECM. Since the cell sheets must be detached from the culture flask without excessive mechanical stress, a temperature-responsive substrate can be used. Therefore, the cell layer is easily harvest from the substrate, depending on the temperature, which avoids the use of external excessive stresses [48].

L'Heureux *et al.*, [49] constructed vascular grafts based on cell-sheet self-assembly using fibroblasts isolated from patients who had undergone vascular bypass surgery. These cell sheets were produced, and, after their detachment, they were rolled around a tubular mandrel and cultured for an extended period to develop the tubular construct. These novel grafts were studied *in vivo* in short-term in canine model and in long-term in rats, presenting non-immunogenic properties and appropriate mechanical support. These encouraging findings resulted in early stage of clinical trials of these vascular grafts in six patients, demonstrating to be a feasible approach to use in vascular tissue engineering [50]. Despite the advantages achieved, this is considered a time-consuming strategy since it is required a long production time. Additionally, the ability to produce ECM *in vitro* differs between different cell types, as well as between different donors [51].

1.6.3 Scaffold-based approaches

The scaffold is one of the most critical components in tissue engineering because it must provide a temporary structure for tissue regeneration [15]. The development of scaffolds with suitable mechanical, structural and biological properties for vascular applications has been explored using different approaches.

1.6.3.1 Decellularized extracellular matrix

Decellularized extracellular matrix is an attractive approach for the creation of small-diameter vascular substitutes. The decellularization process consists of the removal of antigenic cellular material from the tissue, using a range of chemical agents. The use of decellularized natural matrices in tissue engineering takes advantage of the structure and mechanical performance of natural tissue ECM while avoiding any adverse immunological reactions due to its origin [52].

Olausson *et al.*, [53] conducted a clinical study in a child who presented a vein obstruction which was successfully treated with a tissue-engineered vascular graft. A vein segment, harvested from a donor, was decellularized and, subsequently, recellularized with endothelial and smooth muscle cells differentiated from stem cells. However, the decellularization process may compromise the structure of the vessel matrix and it may remove important ECM components such as elastin, leading to altered mechanical properties [54]. Although there are studies which combine the decellularization approach with other processing techniques to obtain more robust scaffolds [54], the time required to prepare these grafts, their cost and practicality limit their use in the health-care market.

1.6.3.2 Natural polymer-based scaffolds

The main natural polymers explored so far are collagen and elastin due to their presence in the native blood vessels. Tubular scaffolds prepared by blends of collagen and elastin have been produced, promoting a confluent monolayer of SMCs after 14 days [32,55]. These constructs may also benefit from suitable mechanical properties which may resemble those of native vascular tissues.

Chitosan is a natural polymer which presents structural similarity to glycosaminoglycans, the main component of the ECM. It has been used in TEVGs due to its biocompatibility and biodegradability [56,57]. Along with chitosan, gelatin, a natural polymer derived from collagen, was also explored due to its biological properties. Elsayed *et al.*, [58] developed a scaffold made of only gelatin to be used as tunica-media equivalent. This natural scaffold achieved values of suture retention strength close to the ones of saphenous vein. Also, it promoted SMCs adhesion, proliferation, elongation along the fibers and migration through the scaffold.

Hyaluronic acid, a polymer present in the natural ECM, has been also explored because it promotes the adhesion and proliferation of ECs [59]. In addition, silk-fibroin was investigated in TEVG because of its mechanical properties, biocompatibility and slow degradation *in vivo*. In

particular, Lovett *et al.*, [60] developed a biological construct made of silk fibroin cultured with both ECs and SMCs, resulting in enhanced non-thrombogenicity and mechanical properties compatible with those of rat aorta.

Hydrogels are also considered as valid substrates for the development of TEVG products due to the use of a natural origin polymers, inducing cell spreading and binding to ECM components. These structures aim to mimic the native vessel structure by embedding cells in gels with a solubilized protein matrix, such as fibrin and collagen [61,62]. Although some work has been developed on that direction, the scaffolds produced only by these natural polymers may not present the required mechanical properties needed for functional and patent vascular grafts.

1.6.3.3 Synthetic polymer-based scaffolds

Scaffolds made of synthetic biodegradable polymers have been commonly employed in the development of TEVGs owing to their easy processing, to control dimensions, degradation and mechanical properties. Furthermore, they may be biocompatible and can be easily processed by a number of different techniques [15,63].

Niklason *et al.*, [14] produced a tubular scaffold made of polyglycolic acid (PGA) sheets seeded with SMCs from bovine aorta. This construct was developed under conditions of pulsatile radial stress by a bioreactor for 8 weeks and, then, seeded with ECs in the luminal side. The results obtained demonstrated suitable biological response with enhanced collagen synthesis, burst pressure strength and mechanical integrity. However, this polymer exhibits rapid degradation which may compromise the stability of the construct for a sufficient time [64]. In contrast, polylactic acid (PLA) exhibits slower degradation times, but it is intrinsically very stiff with poor flexibility [23]. Particularly, it was reported that electrospun vascular scaffolds made of PLA collapsed when placed in a bioreactor system under physiological conditions [33].

Polycaprolactone (PCL) is often proposed for vascular applications since it has slow degradation rates and suitable mechanical properties as tensile and high elongation properties, crucial to withstand the physiological stress and elasticity [63]. Pektok *et al.*, [65] studied the *in vivo* performance of PCL tubular scaffolds in rats for 6 months, showing slow degradation times and better healing properties when compared to ePTFE grafts. Lately, Valence *et al.*, [66] performed a long-term *in vivo* experiment with these PCL scaffolds for up to 18 months, which demonstrated suitable patency and rapid endothelialization. Nevertheless, evidences of

calcification were reported after 6 months, suggesting that more long-term *in vivo* experiments of TEVGs should be conducted to give more information about their long-term responses.

Searching for an ideal scaffold, these polyesters are often combined with each other to provide the mechanical integrity and degradation rate similar to native blood vessels. For example, the copolymer composed of PLLA and poly(lactic-co-[glycolic acid]) (PLGA) presented an enhanced stability for vasculature formation [67]. Poly(L-lactide-co-ε-caprolactone) (PLCL) is another copolymer proposed in vascular applications due to its inherent elasticity and flexibility, and tailorable degradation properties [68]. Therefore, PLLA has been blended with PLCL to provide adequate elastic properties and structural integrity [23]. Shin'oka *et al.*, [69] produced a tubular scaffold made of PLCL reinforced with PGA that was pre-seeded with autologous bone marrow cells. These TEVGs were tested in clinical trials for larger-diameter blood vessels replacement in 23 patients, demonstrating no evidences of aneurysm formation or calcification after a follow-up time of 32 months. Other study conducted by Shalumon *et al.*, [70] produced a tubular scaffold with an inner layer of PLA aligned fibers for ECs adhesion and a randomly organized outer layer composed of a mixture of PLA-PCL for SMCs infiltration. This strategy resulted in a bilayered tubular scaffold with enhanced mechanical response, ECs organization and SMCs proliferation, mimicking the native morphology of blood vessels. A similar approach was explored by Vaz *et al.*, [71] where, in contrast, aligned PLA fibers were electrospun in the outer layer and random PCL fibers in the inner layer to construct a hierarchical scaffold with adequate mechanical and biological properties for blood vessel substitutes.

Elastic polymers were also explored in vascular tissue engineering such as polyurethanes (PUs) [11] and their derivatives, e.g. poly(ester-urethane)urea (PEUU) [15] due to their enhanced tensile properties, as well as their biocompatibility. Mi *et al.*, [72] developed a tubular scaffold made of a blend of PU and PCL to mimic the mechanical properties of elastin and collagen in the native vessels, respectively. This construct presented adequate compliance, suture retention strength and burst pressure strength, promoting ECs adhesion. In addition to PUs, it has been reported the use of fast-degrading polymers such as poly(glycerol sebacate) (PGS) and polydioxanone (PDS) to allow a rapid remodelling, reducing the time at which the tissue is exposed to the material [73,74]. Because PCL degrades slower, these polymers have been frequently combined with PCL to develop vascular grafts able to maintain the scaffold integrity with a sufficiently long degradation time [74,75].

1.6.3.4 Blends of natural and synthetic polymers

Aiming to provide enhanced mechanical properties and biological functionality, synthetic and natural polymers can be blended. Jin *et al.*, [33] developed a composite scaffold composed of PCL and collagen to provide sufficient biomechanical properties and to support ECs and SMCs adhesion and proliferation. The addition of collagen to PCL resulted in increased yield tensile strength and burst pressure strength, presenting biomechanical properties comparable to native vessels and long-term stability *in vitro*. Jeong *et al.*, [16] also reported the production of a scaffold composed of PLGA and collagen to provide a biomimetic environment to ECs and SMCs under pulsatile perfusion conditions. The results showed suitable mechanical properties and stability, inducing cellular alignment and the maintenance of the cell phenotype. Other examples of these blended scaffolds include PCL/chitosan [76] and PCL/tropoelastin [31]. In the latter, Wise *et al.*, [31] produced a vascular graft which comprised a luminal layer of only tropoelastin and an outer layer of a mixture of tropoelastin and PCL to mimic the mechanical properties of the human internal mammary artery. The addition of tropoelastin to the vascular graft resulted in reduced thrombogenicity due to lower platelets adhesion when compared to the constructs containing only PCL.

Multi-layered vascular grafts were also explored to mimic the native architecture of the blood vessels, combining different materials with different cells types [56,77]. A study conducted by McClure *et al.*, [78] focused on designing a three-layered scaffold composed of PCL, collagen and elastin to mimic as close as possible the native artery. These polymers were electrospun sequentially, using different polymer ratios and unique polymer blends, to develop the inner, media and outer layers. This preliminary study demonstrated that by tuning the different ratios of these blends, it was possible to obtain different fiber diameters, as well as suture retention and compliance values within the range of native vessels.

1.6.4 Processing techniques

Several processing techniques were used to fabricate 3D polymeric scaffolds such as freeze-drying [32], salt-leaching [73], phase separation [79] and electrospinning [33].

One of the most popular fabrication methods is freeze-drying with further cross-linking. The polymeric solutions are homogenized and the resulting suspension is frozen, and, then, freeze-dried [32]. This technique allows the production of porous three-dimensional scaffolds with high degree of porosity and interconnected porous network [32,59].

Salt-leaching is a manufacturing technique also used to fabricate 3D interconnected porous scaffolds [67]. This technique has been used along with solvent casting to produce scaffolds with tailored macroporosity. NaCl particles are mixed with the polymer solution for some time and transferred to the mold. After solvent evaporation, the scaffold is dried, and soaked in water to leach out the porogen particles, creating the porous structure [80].

Phase separation is a fabrication technique induced by temperature, being also known by thermally induced phase separation (TIPS). This method is commonly used to produce vascular grafts since it allows the fabrication of highly porous structures with a morphology that promotes cell adhesion and migration [15]. The molds are filled with a warm polymeric solution, followed by a rapid cooling, to reach -80°C . Afterwards, the scaffolds are immersed in ethanol for some time to allow the removal of the solvent, creating an interconnected pore structure [15,23].

Electrospinning is the most widely used processing techniques in TEVG strategies because of its ability to produce meshes of fibers with diameters in the nano to micrometer range. The polymer is dissolved in an organic solvent that is electrospun using a syringe pump at a constant flow rate and voltage. The fibers are electrospun and deposited in a conducting metallic collector which, in case of a tubular conduit, is a rotating mandrel, creating tubular scaffolds [33]. Soletti *et al.*, developed a tubular scaffold produced by TIPS and electrospinning. TIPS technique allows the production of highly porous scaffolds, but with poor mechanical properties. Therefore, it was combined with electrospinning to give mechanical properties more similar to those of native blood vessels. Additionally, co-electrospinning is an advanced form of electrospinning which has been applied to produce nanofibers with core-shell morphology by two different polymer solutions that flow separately through concentric nozzles to form a core-shell structure, combining different materials into one graft [74].

Wet and gel spinning are fabrication techniques that were also explored to produce tubular scaffolds. In the wet spinning technique the polymeric solution is spun into a non-solvent bath, forming fibers around a rotating mandrel [11]. In gel spinning, the polymeric solution is in a gel state that is deposited onto a cylindrical mandrel, followed by air-drying and lyophilization [60]. Additionally, dip coating was also used as a simple manufacturing technique where the mold is dipped into the polymeric solution [57].

The following Table 1. 2 contains a summary of the most processing techniques, materials and cell sources employed to fabricate TEVGs.

Table 1. 2 - Summary of some processing techniques, materials and cell sources explored to produce TEVGs

Processing technique	Scaffold material (s)	Cell source	Reference
Freeze-drying	Collagen/Elastin	SMCs	[32]
	Collagen/Hyaluronic acid	ECs	[59]
	PU	ECs	[81]
	PLCL	BMCs	[69]
Freeze-drying and Electrospinning	Collagen/PLGA	EC and SMCs	[16]
Salt-leaching and UV crosslinking	PTMC	-	[82]
Salt-leaching	PLLA/PLGA	ECs	[67]
	PLCL	-	[68]
	PGS	-	[73]
TIPS	PLLA/PLCL	ECs	[23]
	PEUU	Stem cells from skeletal muscle	[79]
TIPS and Electrospinning	PEUU	Stem cells from skeletal muscle	[15]
Solvent casting and phase separation	PLGA	SMCs	[83]
Electrospinning	PCL	-	[63,65,66]
	PCL/Tropoelastin	ECs	[31]
	PCL/Collagen	ECs and SMCs	[33]
	TPU/PCL	ECs	[72]
	Gelatin	SMCs	[58]
	PCL/PLA	ECs and SMCs	[70]
		Fibroblasts	[71]
	Gelatin	SMCs	[58]

Table I. 2 - Summary of some processing techniques, materials and cell sources explored to produce TEVGs (Continued)

Processing technique	Scaffold material (s)	Cell source	Reference
Electrospinning	PLGA/Gelatin PLGA/chitosan PCL/Gelatin	Fibroblasts (L-929) and ECs from a bovine pulmonary artery (CPAE)	[56]
	Collagen/Elastin	SMCs	[55]
	PCL/Collagen/Elastin	-	[78]
	PGS/PCL	-	[75]
	PCL/chitosan	EOCs	[76]
Electrospinning and UV crosslinking	PCL and PLA	MSCs	[84]
Co-electrospinning	PCL/PDS	-	[74]
Wet spinning and electrospinning	PCL/PU	ECs	[11]
Gel spinning	Silk fibroin	ECs and SMCs	[60]
Dip coating	Chitosan	SMCs	[57]
	PCL	SMCs	[77]

Abbreviations: BMCs – Bone Marrow Cells; PTMC - Poly (trimethylene carbonate); TPU - Thermoplastic polyurethane.

Scaffolds are used for co-culture systems and bioreactors. Co-culture systems have been employed to improve ECs adhesion and retention *in vitro* within the scaffold. By combining SMCs and fibroblasts with ECs, it is possible to increase the level of interactions with different cells, developing a scaffold with improved mechanical and biological performances [85,86]. The use of bioreactors in vascular graft fabrication was also investigated, aiming to reproduce the physiological conditions of native blood vessels such as pressure and blood flow rate. Pulsatile bioreactors provide a dynamic environment for cell culture and proliferation, allowing cell growth and maturation of the tissue-engineered vessels [14,77] or to promote the maturation of differentiated ECs [36].

1.6.5 Surface modification

The interaction between the scaffold and the biological environment takes place at the biomaterials' surface, where its physical and chemical characteristics are crucial to determine the biological response [28,87]. The commonly used synthetic polymers do not facilitate, in general, cell adhesion and proliferation due to their hydrophobicity or negative electrical charge [88]. This can lead to the detachment of poorly adhered cells when exposed to the blood flow, compromising its anti-thrombogenic behaviour [80]. Therefore, lack of cell-interactive properties and poor hemocompatibility may limit the use of these scaffolds as vascular grafts [28].

Surface modifications may improve either the hemocompatibility and the endothelialization of the luminal surface of vascular grafts, without affecting significantly their mechanical properties [21]. Physical and chemical methods were employed to introduce specific functional groups at the biomaterials' surface, such as plasma, wet chemical and photografting treatments [89].

Plasma treatments induce chemical reactions at the material surface, resulting in radical reactions between the chains of the polymer and the high energy gases in plasma [90]. Using different plasma sources, several functional groups can be inserted to modify the biomaterial surface chemistry, improving its surface properties [90,91]. Plasma treatments with oxygen, ammonia, nitrogen, argon and air are usually used to generate active and functional groups, allowing covalent immobilization of several bioactive molecules [90,92–95]. However, the penetration depth of plasma is a limitation of this method since it is not able to effectively modify deeply located fibers within the structure [89].

Wet chemical methods are based on the partial hydrolysis of the biomaterial surface, under acidic or basic conditions, to modify its wettability. This method involves the random chemical scission of ester linkages of the polymer backbones, leading to the generation of carboxylic and hydroxyl groups at the surface [89]. This results in surface degradation, as well as in increased roughness and hydrophilicity due to the presence of oxygen-containing functional groups [92,96]. These surface treatments provide a negatively charged and hydrophilic surface which may contribute to enhanced hemocompatibility of the scaffolds since this sort of surfaces do not allow the adhesion and activation of platelets [96]. Furthermore, the aminolysis method has been used to generate amine functionalised surfaces [89]. This method uses diamine molecules to insert amine groups at the biomaterial surface, aiming to achieve the immobilisation of biomolecules at the surface [87,97].

Photografting was also investigated as a method to functionalise the scaffolds surface. Using UV radiation or plasma, it is possible to generate free radicals to immobilise molecules to establish a stable coating with improved cell-material interaction [28].

Aiming to provide the required signals for cell survival and tissue maintenance, most of these approaches involve the immobilisation of bioactive molecules [88]. These strategies include the immobilisation of natural proteins, bioactive peptides, anti-coagulant drugs or growth factors.

The following Table 1. 3 summarizes the surface modification strategies employed in TEVGs.

Table 1. 3 - Summary of the surface modification strategies applied for TEVGs

Surface modification material	Scaffold material (s)	Surface modification method (s)	Reference
Gelatin	PET	Photografting	[28]
	PEEUU	Aminolysis	[80]
	PCU/PEGMA		[98]
	PCL		[87,99]
		Plasma treatment	[95]
Collagen	PEEUU	Aminolysis	[80]
	PCL		[87]
	PLLACL	Plasma treatment	[100]
Hyaluronic acid	PCL	Aminolysis	[101]
Tropoelastin	Metallic stent	Plasma treatment	[94]
	ePTFE		[102]
	PU		[93]
Fibrin	PCL	Coating	[103]
Fibronectin	Gelsoft™ and Polymaille*	Coating	[104]
	Decellularized scaffolds		[105]

Table I. 3 - Summary of the surface modification strategies applied for TEVGs (Continued)

Surface modification material	Scaffold material (s)	Surface modification method (s)	Reference
Biomimetic matrix	PCL	Coating	[106]
RGD peptide	PHBV/PCL	Coating	[107]
CAG peptide	PCL	Mix into PCL	[108]
ASA	PCL	Plasma treatment and wet chemical treatment	[92]
Heparin	PLLA/SPU	EDC/NHS coupling	[21]
	PLLA/PLCL		[23,109]
	Decellularized vessels		[110]
	Silk fibroin	Coating	[111]
	PLLA	Plasma treatment, followed by EDC/NHS coupling	[112]
VEGF	PCL	Plasma treatment and aminolysis	[92]
		Heparin binding	[113]
	PHBV/PCL	Coating	[107]
	PGLA/PGA/PCLLA	Heparin binding	[114]
SDF-1α	Gelsoft™ and Polymaille*	Coating with fibronectin	[104]
	PLLA/PCL	Heparin binding	[109]
CD34Ab	PGLA/PGA/PCLLA	Heparin binding	[114]
	ePTFE	Coating with Matrigel	[115]

Abbreviations: EDC/NHS - 1-(3-Dimethylaminopropyl)-3-ethylcarbodiimide hydrochloride/N hydroxysulfosuccinimide; PCU - polycarbonate urethane; PEGMA - poly(ethyleneglycol)methacrylate; PHBV - poly(3-hydroxybutyrate-co-3-hydroxyvalerate); SPU - Segmented polyurethane.

* Clinically available small-diameter vascular grafts.

Gelatin and collagen are natural proteins that have been immobilised at the surface of polymeric scaffolds by aminolysis, improving cells attachment and proliferation, as well as phenotype maintenance [80,87,100]. Hyaluronic acid was also considered in the modification of the materials' surface since it was demonstrated to play a crucial role on the regulation of ECs, namely in their adhesion, viability and proliferation [101].

Since elastin is present in the blood vessels, this protein is a candidate for scaffold coating because it regulates the ECs and the hemocompatibility [93,102]. Waterhouse *et al.*, [94] immobilized recombinant tropoelastin, the soluble building block of elastin, at the surface metallic stents by plasma treatment. This surface modification promoted a significant reduction in platelets adhesion and activation, contributing for the enhancement of hemocompatibility of these stents.

Fibrin is another protein investigated to promote an improved biological response. Zhu *et al.*, [103] coated PCL nanofibers with fibrin due to its important functions in blood clotting, and cellular matrix interactions. The fibrin-coated scaffolds promoted SMCs and ECs growth, activity and differentiation. Additionally, fibronectin, a ECM protein present in plasma and platelets, was immobilised onto decellularized aortic conduits to accelerate the recellularization *in vivo* [104,105]. Moreover, it has been employed the use of a biomimetic matrix composed of fibrin, fibronectin, gelatin, growth factors and GAGs to coat the scaffold surface [106]. This strategy aims to preserve a normal anti-thrombotic cell phenotype, as well as to improve the cell attachment, proliferation and survival.

The immobilisation of bioactive peptides was investigated as an alternative strategy for surface modification due to their high affinity to vascular cells [108]. The tripeptide sequence arginine–glycine–aspartic acid (RGD) is one of the peptides often proposed to improve the material biocompatibility, particularly the adhesive properties of the scaffold [107]. Along with RDG peptide, the cysteine-alanine-glycine (CAG) trimer peptide was also used due to its high affinity to ECs [108].

The surface modification with anti-coagulant drugs is a strategy extensively explored to improve the anti-thrombogenic properties of scaffolds [23,92]. The acetylsalicylic acid (ASA) is an anti-thrombogenic drug that has been studied to improve the hemocompatibility of vascular grafts, as well as to provide anti-inflammatory properties [92]. Heparin is another biomolecule which has been commonly used in vascular therapy as an anticoagulant agent to provide hemocompatibility and anti-coagulation properties to the scaffolds. Caracciolo *et al.*, [21] produced electrospun tubular scaffolds, which inner surface was, further, modified by the insertion of heparin. This surface modification approach resulted in the decrease of platelets attachment and the increase

in the hydrophilicity and water absorption, promoting the adhesion and proliferation of hASCs. These findings were also reported by Wang *et al.*, [23] where the immobilization of heparin at the surface resulted in an enhancement of hemocompatibility properties, cellular behaviour, as well as neovascularization after implantation in rabbits.

Heparin can be also used as a ligand of growth factors to protect them from proteolytic degradation and to allow them to be slowly released [114]. Singh *et al.*, [113] explored this approach by cross-linking heparin to PCL scaffolds to bind the vascular endothelial growth factor (VEGF). The results showed that the heparin-immobilized scaffolds presented lower burst release and higher retention of VEGF when compared to the scaffolds alone, being proportional to the heparin content. The *in vivo* analysis in mice demonstrated that these scaffolds loaded with VEGF increased the angiogenic response after 14 days. Besides these molecules, the chemokine stromal cell-derived factor-1a (SDF-1a) and the CD34 monoclonal antibody (CD34ab) were recently studied for biofunctionalization purposes owing to their high affinity and selectivity to endothelial progenitor cells. By cross-linked heparin, these molecules can be immobilised at the surface to promote the endothelialization of the scaffolds. [109,115]. In addition to the protein immobilisation, it is possible to modify the surface by loading growth factors into the scaffold, while it is processed. For instance, Han *et al.*, [12] developed a multilayered vascular scaffold with loaded VEGF in the inner layer and platelet-derived growth factor (PDGF) in the middle layer. The *in vivo* performance indicated that the dual release of growth factors promoted endothelialization and inhibited SMCs hyperproliferation, maintaining suitable patency in rabbit carotid artery for 8 weeks.

1.7 Purpose of the work

Currently, the synthetic vascular grafts used to replace small-diameter blood vessels fail in providing suitable mechanical support and anti-thrombogenic properties. Considering these limitations, the purpose of this work is to develop a synthetic vascular graft with appropriate mechanical properties and able to promote endothelialization. Tubular fibrous scaffolds made of PCL will be produced by electrospinning and their luminal surface will be functionalized by a wet chemical method to covalently bind tropoelastin. Therefore, tropoelastin will be immobilized onto activated (NaOH treatment) and aminolysed (HMD treatment) substrates by its $-NH_2$ and $-COOH$ groups, respectively, to study the effect of the exposed functional groups over the human ECs behaviour. These constructs will be characterized in terms of morphology, surface functionality and uniaxial tensile properties. The endothelialization of eTF scaffolds will be also assessed by culturing the HUVECs cell line EA.hy926. Endothelial cells will be cultured up to 7 days on the untreated,

functionalized (activated and aminolysed) and biofunctionalized (tropoelastin-immobilized on activated or on aminolysed) scaffolds. Metabolic activity, cell proliferation, total protein synthesis and VEGF secretion will be assessed, as well as cell morphology and phenotype.

1.8 References

- [1] M.H. Ross, W. Pawlina, Cardiovascular System, in: *Histol. A Text Atlas with Correl. Cell Mol. Biol.*, 2006: pp. 400–429.
- [2] H.-H. Greco Song, R.T. Rumma, C.K. Ozaki, E.R. Edelman, C.S. Chen, *Vascular Tissue Engineering: Progress, Challenges, and Clinical Promise*, *Cell Stem Cell*. 22 (2018) 340–354.
- [3] A. Hasan, A. Memic, N. Annabi, M. Hossain, A. Paul, M.R. Dokmeci, F. Dehghani, A. Khademhosseini, *Electrospun scaffolds for tissue engineering of vascular grafts*, *Acta Biomater.* 10 (2014) 11–25.
- [4] Y. Naito, T. Shinoka, D. Duncan, N. Hibino, D. Solomon, M. Cleary, A. Rathore, C. Fein, S. Church, C. Breuer, *Vascular tissue engineering: Towards the next generation vascular grafts*, *Adv. Drug Deliv. Rev.* 63 (2011) 312–323.
- [5] S. Mundi, M. Massaro, E. Scoditti, M.A. Carluccio, V.W.M. Van Hinsbergh, M.L. Iruela-Arispe, R. De Caterina, *Endothelial permeability, LDL deposition, and cardiovascular risk factors-A review*, *Cardiovasc. Res.* 114 (2018) 35–52.
- [6] P. Rajendran, T. Rengarajan, J. Thangavel, Y. Nishigaki, *The Vascular Endothelium and Human Diseases*, *Int. J. Biol. Sci.* 9 (2013) 1057–1069.
- [7] J.I. Rotmans, J.H. Campbell, *Tissue engineering for small-diameter vascular grafts*, in: C.P. Sharma (Ed.), *Biointegration Med. Implant Mater. Sci. Des.*, Woodhead Publishing Limited, 2010: pp. 116–146.
- [8] M.W. Majesky, X.R. Dong, V. Hoglund, W.M. Mahoney, G. Daum, *The Adventitia: a dynamic interface containing resident progenitor cells mark*, *Arterioscler. Thromb. Vasc. Biol.* 31 (2011) 1530–1539.
- [9] P. Libby, P.M. Ridker, G.K. Hansson, *Progress and challenges in translating the biology of atherosclerosis*, *Nature*. 473 (2011) 317–325.
- [10] C. Zhang, L. Zeng, C. Emanuelli, Q. Xu, *Blood flow and stem cells in vascular disease*, *Cardiovasc. Res.* 99 (2013) 251–259.
- [11] M. Richard, R. Black, C. Kielty, *PCL – PU composite vascular scaffold production for*

- vascular tissue engineering : Attachment , proliferation and bioactivity of human vascular endothelial cells, *Biomaterials*. 27 (2006) 3608–3616.
- [12] F. Han, X. Jia, D. Dai, X. Yang, J. Zhao, Y. Zhao, Y. Fan, X. Yuan, Performance of a multilayered small-diameter vascular scaffold dual-loaded with VEGF and PDGF, *Biomaterials*. 34 (2013) 7302–7313.
- [13] M. Ahmed, H. Ghanbari, B.G. Cousins, G. Hamilton, A.M. Seifalian, Small calibre polyhedral oligomeric silsesquioxane nanocomposite cardiovascular grafts: Influence of porosity on the structure, haemocompatibility and mechanical properties, *Acta Biomater*. 7 (2011) 3857–3867.
- [14] L.E. Niklason, R.L. J. Gao, W. M. Abbott, K. K. Hirschi, S. Houser, R. Marini, Functional Arteries Grown in Vitro, *Science*. 284 (1999) 489–494.
- [15] L. Soletti, Y. Hong, J. Guan, J.J. Stankus, M.S. El-kurdi, A bilayered elastomeric scaffold for tissue engineering of small diameter vascular grafts, *Acta Biomater*. 6 (2010) 110–122.
- [16] S. In Jeong, S.Y. Kim, S.K. Cho, M.S. Chong, K.S. Kim, H. Kim, S.B. Lee, Y.M. Lee, Tissue-engineered vascular grafts composed of marine collagen and PLGA fibers using pulsatile perfusion bioreactors, *Biomaterials*. 28 (2007) 1115–1122.
- [17] N.L. Heureux, N. Dusserre, A. Marini, S. Garrido, L. De Fuente, T. Mcallister, Technology Insight : the evolution of tissue- engineered vascular grafts – from research to clinical practice, *Nat. Rev. Cardiol*. 4 (2007) 389–395.
- [18] M. Weber, H. Steinle, S. Golombek, L. Hann, C. Schlensak, H.P. Wendel, M. Avci-Adali, Blood-Contacting Biomaterials: In Vitro Evaluation of the Hemocompatibility, *Front. Bioeng. Biotechnol*. 6 (2018) 99.
- [19] Y. Liu, D. Cai, J. Yang, Y. Wang, X. Zhang, S. Yin, In vitro hemocompatibility evaluation of poly (4-hydroxybutyrate) scaffold, *Int. J. Clin. Exp. Med*. 7 (2014) 1233–1243.
- [20] J. Hendriks, J. Riesle, C.A. van Blitterswijk, Vascular tissue engineering of small-diameter blood vessels: reviewing the electrospinning approach, *J. Tissue Eng. Regen. Med*. 9 (2015) 861–888.
- [21] P.C. Caracciolo, M.I. Rial-Hermida, F. Montini-Ballarín, G.A. Abraham, A. Concheiro, C.

- Alvarez-Lorenzo, Surface-modified bioresorbable electrospun scaffolds for improving hemocompatibility of vascular grafts, *Mater. Sci. Eng. C*. 75 (2017) 1115–1127.
- [22] S. Braune, M. Groß, M. Walter, S. Zhou, S. Dietze, S. Rutschow, A. Lendlein, C. Tschöpe, F. Jung, Adhesion and activation of platelets from subjects with coronary artery disease and apparently healthy individuals on biomaterials, *J. Biomed. Mater. Res. - Part B Appl. Biomater.* 104 (2016) 210–217.
- [23] W. Wang, J. Hu, C. He, W. Nie, W. Feng, K. Qiu, X. Zhou, Y. Gao, G. Wang, Heparinized PLLA/PLCL nanofibrous scaffold for potential engineering of small-diameter blood vessel: Tunable elasticity and anticoagulation property, *J. Biomed. Mater. Res. - Part A*. 103 (2015) 1784–1797.
- [24] M.B. Gorbet, M. V. Sefton, Biomaterial-associated thrombosis: Roles of coagulation factors, complement, platelets and leukocytes, *Biomaterials*. 25 (2006) 219–241.
- [25] A. Waterhouse, S.G. Wise, M.K.C. Ng, A.S. Weiss, Elastin as a Nonthrombogenic Biomaterial, *Tissue Eng. Part B Rev.* 17 (2011) 93–99.
- [26] S. Haghjooy Javanmard, J. Anari, A. Zargar Kharazi, E. Vatankhah, In vitro hemocompatibility and cytocompatibility of a three-layered vascular scaffold fabricated by sequential electrospinning of PCL, collagen, and PLLA nanofibers, *J. Biomater. Appl.* 31 (2016) 438–449.
- [27] B. Nilsson, K. Nilsson, T. Eirik, J.D. Lambris, The role of complement in biomaterial-induced inflammation, *Mol. Immunol.* 44 (2007) 82–94.
- [28] D.E. Giol, S. Van Vlierberghe, R.E. Unger, D. Schaubroeck, H. Ottevaere, H. Thienpont, C.J. Kirkpatrick, P. Dubruel, Endothelialisation And Anticoagulation Potential Of Surface-Modified PET Intended For Vascular Applications, *Macromol. Biosci.* 1800125 (2018) 1–11.
- [29] A. D. Michaels and K. Chatterjee, Angioplasty Versus Bypass Surgery for Coronary Artery Disease, *Circulation*. 106 (2002) 176–178.
- [30] D.G. Seifu, A. Purnama, K. Mequanint, D. Mantovani, Small-diameter vascular tissue engineering, *Nat. Rev. Cardiol.* 10 (2013) 410–421.
- [31] S.G. Wise, M.J. Byrom, A. Waterhouse, P.G. Bannon, M.K.C. Ng, A.S. Weiss, A multilayered

- synthetic human elastin / polycaprolactone hybrid vascular graft with tailored mechanical properties, *Acta Biomater.* 7 (2011) 295–303.
- [32] P. Buijtenhuijs, L. Buttafoco, A.A. Poot, W.F. Daamen, T.H. van Kuppevelt, P.J. Dijkstra, R.A.I. de Vos, L.M.T. Sterk, B.R.H. Geelkerken, J. Feijen, I. Vermes, Tissue engineering of blood vessels: Characterization of smooth-muscle cells for culturing on collagen-and-elastin-based scaffolds, *Biotechnol. Appl. Biochem.* 39 (2004) 141–149.
- [33] S. Jin, J. Liu, S. Heang, S. Soker, A. Atala, J.J. Yoo, Development of a composite vascular scaffolding system that withstands physiological vascular conditions, *Biomaterials.* 29 (2008) 2891–2898.
- [34] R. Langer, J.P. Vacanti, Tissue engineering, *Science* (80-). 260 (1993) 920–926.
- [35] S. Pashneh-tala, S. Macneil, F. Claeysens, The Tissue-Engineered Vascular Graft— Past, Present, and Future, *Tissue Eng. Part B.* 22 (2016). doi:10.1089/ten.teb.2015.0100.
- [36] A. Sivarapatna, M. Ghaedi, A. V. Le, J.J. Mendez, Y. Qyang, L.E. Niklason, Arterial specification of endothelial cells derived from human induced pluripotent stem cells in a biomimetic flow bioreactor, *Biomaterials.* 53 (2015) 621–633.
- [37] H. Inoguchi, T. Tanaka, Y. Maehara, T. Matsuda, The effect of gradually graded shear stress on the morphological integrity of a huvec-seeded compliant small-diameter vascular graft, *Biomaterials.* 28 (2007) 486–495.
- [38] D.A. Ingram, L.E. Mead, D.B. Moore, W. Woodard, A. Fenoglio, C. Mervin, W. Dc, M.C. Yoder, Vessel wall – derived endothelial cells rapidly proliferate because they contain a complete hierarchy of endothelial progenitor cells, *Blood.* 105 (2009) 2783–2786.
- [39] T. Shirota, H. He, H. Yasui, T. Matsuda, Human Endothelial Progenitor Cell-Seeded Hybrid Graft: Proliferative and Antithrombogenic Potentials in Vitro and Fabrication Processing, *Tissue Eng.* 9 (2003) 127–136.
- [40] H. Naito, H. Kidoya, S. Sakimoto, T. Wakabayashi, N. Takakura, Identification and characterization of a resident vascular stem/progenitor cell population in preexisting blood vessels, *EMBO J.* 31 (2012) 842–855.
- [41] K.A. Ahmann, S.L. Johnson, R.P. Hebbel, R.T. Tranquillo, Shear stress responses of adult blood outgrowth endothelial cells seeded on bioartificial tissue., *Tissue Eng. Part A.* 17

(2011) 2511–2521.

- [42] C.M. Metallo, M.A. Vodyanik, J.J. De Pablo, I.I. Slukvin, S.P. Palecek, The response of human embryonic stem cell-derived endothelial cells to shear stress, *Biotechnol. Bioeng.* 100 (2008) 830–837.
- [43] E. Vo, D. Hanjaya-Putra, Y. Zha, S. Kusuma, S. Gerecht, Smooth-muscle-like cells derived from human embryonic stem cells support and augment cord-like structures in vitro, *Stem Cell Rev. Reports.* 6 (2010) 237–247.
- [44] L. Gui, B.C. Dash, J. Luo, L. Qin, L. Zhao, K. Yamamoto, T. Hashimoto, H. Wu, A. Dardik, G. Tellides, L.E. Niklason, Y. Qyang, Implantable tissue-engineered blood vessels from human induced pluripotent stem cells, *Biomaterials.* 102 (2016) 120–129.
- [45] G. Matsumura, S. Miyagawa-Tomita, T. Shin'Okada, Y. Ikada, H. Kurosawa, First evidence that bone marrow cells contribute to the construction of tissue-engineered vascular autografts in vivo, *Circulation.* 108 (2003) 1729–1734.
- [46] Y. Zhao, S. Zhang, J. Zhou, J. Wang, M. Zhen, Y. Liu, J. Chen, Z. Qi, The development of a tissue-engineered artery using decellularized scaffold and autologous ovine mesenchymal stem cells, *Biomaterials.* 31 (2010) 296–307.
- [47] L.J. Fischer, S. McIlhenny, T. Tulenko, N. Golesorkhi, P. Zhang, R. Larson, J. Lombardi, I. Shapiro, P.J. DiMuzio, Endothelial Differentiation of Adipose-Derived Stem Cells: Effects of Endothelial Cell Growth Supplement and Shear Force, *J. Surg. Res.* 152 (2009) 157–166.
- [48] H. Ahn, Y.M. Ju, H. Takahashi, D.F. Williams, J.J. Yoo, S.J. Lee, T. Okano, A. Atala, Engineered small diameter vascular grafts by combining cell sheet engineering and electrospinning technology, *Acta Biomater.* 16 (2015) 14–22.
- [49] N. L'Heureux, N. Dusserre, G. Konig, B. Victor, P. Keire, T.N. Wight, N.A.F. Chronos, A.E. Kyles, C.R. Gregory, G. Hoyt, R.C. Robbins, T.N. McAllister, Human tissue-engineered blood vessels for adult arterial revascularization, *Nat. Med.* 12 (2006) 361–365.
- [50] N. L'Heureux, T.N. McAllister, L.M. De La Fuente, Tissue-Engineered Blood Vessel for Adult Arterial Revascularization, *N. Engl. J. Med.* 357 (2007) 1451–1453.
- [51] J.M. Bourget, R. Gauvin, D. Larouche, A. Lavoie, R. Labbé, F.A. Auger, L. Germain, Human fibroblast-derived ECM as a scaffold for vascular tissue engineering, *Biomaterials.* 33

- (2012) 9205–9213.
- [52] S.L.M. Dahl, A.P. Kypson, J.H. Lawson, J.L. Blum, J.T. Strader, Y. Li, R.J. Manson, W.E. Tente, L. DiBernardo, M.T. Hensley, R. Carter, T.P. Williams, H.L. Prichard, M.S. Dey, K.G. Begelman, L.E. Niklason, Readily available tissue-engineered vascular grafts., *Sci. Transl. Med.* 3 (2011) 68–79.
- [53] M. Olausson, P.B. Patil, V.K. Kuna, P. Chougule, N. Hernandez, K. Methe, C. Kullberg-lindh, H. Borg, Transplantation of an allogeneic vein bioengineered with autologous stem cells : a proof-of-concept study, *Lancet.* 380 (2012) 230–237.
- [54] W. Gong, D. Lei, S. Li, P. Huang, Q. Qi, Y. Sun, Y. Zhang, Hybrid small-diameter vascular grafts : Anti-expansion effect of electrospun poly ϵ -caprolactone on heparin-coated decellularized matrices, *Biomaterials.* 76 (2016) 359–370.
- [55] L. Buttafoco, N.G. Kolkman, P. Engbers-buijtenhuijs, Electrospinning of collagen and elastin for tissue engineering applications, *Biomaterials.* 27 (2006) 724–734.
- [56] T.-H. Nguyen, B.-T. Lee, The effect of cross-linking on the microstructure, mechanical properties and biocompatibility of electrospun polycaprolactone–gelatin/PLGA–gelatin/PLGA–chitosan hybrid composite, *Sci. Technol. Adv. Mater.* 13 (2012) 35002.
- [57] L. Zhang, Q. Ao, A. Wang, G. Lu, L. Kong, Y. Gong, N. Zhao, A sandwich tubular scaffold derived from chitosan for blood vessel tissue engineering, *J. Biomed. Mater. Res. - Part A.* 77 (2006) 277–284.
- [58] Y. Elsayed, C. Lekakou, F. Labeed, P. Tomlins, Fabrication and characterisation of biomimetic , electrospun gelatin fibre scaffolds for tunica media-equivalent , tissue engineered vascular grafts, *Mater. Sci. Eng. C.* 61 (2016) 473–483.
- [59] C. Zhu, D. Fan, Y. Wang, Human-like collagen/hyaluronic acid 3D scaffolds for vascular tissue engineering, *Mater. Sci. Eng. C.* 34 (2014) 393–401.
- [60] M. Lovett, G. Eng, J. Kluge, C. Cannizzaro, G. Vunjak-novakovic, D.L. Kaplan, Tubular silk scaffolds for small diameter vascular grafts, *Organogenesis.* 6 (2010) 217–224.
- [61] E.D. Grassl, T.R. Oegema, R.T. Tranquillo, A fibrin-based arterial media equivalent, *J. Biomed. Mater. Res. - Part A.* 66 (2002) 550–561.

- [62] D. Seliktar, R.A. Black, R.P. Vito, R.M. Nerem, Dynamic Mechanical Conditioning of Collagen-Gel Blood Vessel Constructs Induces Remodeling In Vitro, *Ann. Biomed. Eng.* 28 (2000) 351–362.
- [63] B. Nottelet, E. Pektok, D. Mandracchia, J.C. Tille, B. Walpoth, R. Gurny, M. Möller, Factorial design optimization and in vivo feasibility of poly(ϵ -caprolactone)-micro- and nanofiber-based small diameter vascular grafts, *J. Biomed. Mater. Res. - Part A.* 89 (2009) 865–875.
- [64] Y. Dong, B. Sc, T. Yong, D. Ph, S. Liao, C.K. Chan, Distinctive Degradation Behaviors of Electrospun Polyglycolide, Poly(dl-Lactide-co-Glycolide), and Poly(l-Lactide-co- ϵ -Caprolactone) Nanofibers Cultured With/Without Porcine Smooth Muscle Cells, *Tissue Eng. - Part A.* 16 (2010).
- [65] E. Pektok, B. Nottelet, J.-C. Tille, R. Gurny, A. Kalangos, M. Moeller, B.H. Walpoth, Degradation and Healing Characteristics of Small-Diameter Poly (ϵ -Caprolactone) Vascular Grafts in the Rat Systemic, Circulation. 118 (2008) 2563–2570.
- [66] S. de Valence, J.C. Tille, D. Mugnai, W. Mrowczynski, R. Gurny, M. Möller, B.H. Walpoth, Long term performance of polycaprolactone vascular grafts in a rat abdominal aorta replacement model, *Biomaterials.* 33 (2012) 38–47.
- [67] S. Landau, A.A. Szklanny, G.C. Yeo, Y. Shandalov, E. Kosobrodova, A.S. Weiss, S. Levenberg, Tropoelastin coated PLLA-PLGA scaffolds promote vascular network formation, *Biomaterials.* 122 (2017) 72–82.
- [68] S.H. Kim, C.H. Mun, Y. Jung, S.H. Kim, D.I. Kim, S.H. Kim, Mechanical properties of compliant double layered poly(L-lactide-co- ϵ - caprolactone) vascular graft, *Macromol. Res.* 21 (2013) 886–891.
- [69] T. Shin 'oka, G. Matsumura, N. Hibino, Y. Naito, M. Watanabe, T. Konuma, T. Sakamoto, M. Nagatsu, Midterm clinical result of tissue-engineered vascular autografts seeded with autologous bone marrow cells, *J. Thorac. Cardiovasc. Surg.* 129 (2005) 1330–1338.
- [70] K.T. Shalumon, P.R. Sreerexha, D. Sathish, H. Tamura, S. V. Nair, K.P. Chennazhi, R. Jayakumar, Hierarchically designed electrospun tubular scaffolds for cardiovascular applications, *J. Biomed. Nanotechnol.* 7 (2011) 609–620.
- [71] C.M. Vaz, S. van Tuijl, C.V.C. Bouten, F.P.T. Baaijens, Design of scaffolds for blood vessel

- tissue engineering using a multi-layering electrospinning technique, *Acta Biomater.* 1 (2005) 575–582.
- [72] H.Y. Mi, X. Jing, E. Yu, X. Wang, Q. Li, L.S. Turng, Manipulating the structure and mechanical properties of thermoplastic polyurethane/polycaprolactone hybrid small diameter vascular scaffolds fabricated via electrospinning using an assembled rotating collector, *J. Mech. Behav. Biomed. Mater.* 78 (2018) 433–441.
- [73] W. Wu, R.A. Allen, Y. Wang, Fast-degrading elastomer enables rapid remodeling of a cell-free synthetic graft into a neoartery, *Nat. Med.* 18 (2012) 1148–1153.
- [74] Y. Pan, X. Zhou, Y. Wei, Q. Zhang, T. Wang, M. Zhu, W. Li, R. Huang, R. Liu, J. Chen, G. Fan, K. Wang, D. Kong, Q. Zhao, Small-diameter hybrid vascular grafts composed of polycaprolactone and polydioxanone fibers, *Sci. Rep.* 7 (2017) 3615.
- [75] S. Sugama, K. Sekiyama, T. Kodama, Y. Takamatsu, M. Hashimoto, C. Bruno, Y. Kakinuma, M. Systems, C. Biology, L. Jolla, Long-term functional efficacy of a novel electrospun poly(glycerol sebacate)-based arterial graft in mice, *Ann. Biomed. Eng.* 44 (2017) 39–46.
- [76] M. Zhou, W. Qiao, Z. Liu, T. Shang, T. Qiao, C. Mao, C. Liu, Development and in vivo evaluation of small-diameter vascular grafts engineered by outgrowth endothelial cells and electrospun chitosan/poly(ϵ - caprolactone) Nanofibrous Scaffolds, *Tissue Eng. - Part A.* 20 (2014) 79–91.
- [77] K. Iwasaki, K. Kojima, S. Kodama, A.C. Paz, M. Chambers, M. Umezu, C.A. Vacanti, Bioengineered three-layered robust and elastic artery using hemodynamically-equivalent pulsatile bioreactor., *Circulation.* 118 (2008).
- [78] M.J. McClure, S.A. Sell, D.G. Simpson, B.H. Walpoth, G.L. Bowlin, A three-layered electrospun matrix to mimic native arterial architecture using polycaprolactone , elastin , and collagen : A preliminary study, *Acta Biomater.* 6 (2010) 2422–2433.
- [79] A. Nieponice, L. Soletti, J. Guan, B.M. Deasy, J. Huard, W.R. Wagner, D. a Vorp, Development of a tissue engineered vascular graft combining a biodegradable scaffold, muscle-derived stem cells and a rotational vacuum seeding technique, *Biomaterials.* 29 (2008) 825–833.
- [80] S. Asadpour, H. Yeganeh, J. Ai, H. Ghanbari, A novel polyurethane modified with

- biomacromolecules for small-diameter vascular graft applications, *J. Mater. Sci.* 53 (2018) 9913–9927.
- [81] X. Jiang, F. Yu, Z. Wang, J. Li, H. Tan, M. Ding, Q. Fu, Fabrication and characterization of waterborne biodegradable polyurethanes 3-dimensional porous scaffolds for vascular tissue engineering, *J. Biomater. Sci. Polym. Ed.* 21 (2010) 1637–1652.
- [82] Z. Guo, D.W. Grijpma, A.A. Poot, Preparation and characterization of flexible and elastic porous tubular PTMC scaffolds for vascular tissue engineering, *Polym. Adv. Technol.* 28 (2017) 1239–1244.
- [83] H. Shen, X. Hu, H. Cui, Y. Zhuang, D. Huang, F. Yang, X. Wang, S. Wang, D. Wu, Fabrication and effect on regulating vSMC phenotype of a biomimetic tunica media scaffold, *J. Mater. Chem. B.* 4 (2016) 7689–7696.
- [84] I. Stefani, J.J. Cooper-White, Development of an in-process UV-crosslinked, electrospun PCL/aPLA-co-TMC composite polymer for tubular tissue engineering applications, *Acta Biomater.* 36 (2016) 231–240.
- [85] I. Sukmana, P. Vermette, The effects of co-culture with fibroblasts and angiogenic growth factors on microvascular maturation and multi-cellular lumen formation in HUVEC-oriented polymer fibre constructs, *Biomaterials.* 31 (2010) 5091–5099.
- [86] S.T. Rashid, B. Fuller, G. Hamilton, A.M. Seifalian, Tissue engineering of a hybrid bypass graft for coronary and lower limb bypass surgery, *FASEB J.* 22 (2008) 2084–2089.
- [87] Y. Zhu, C. Gao, X. Liu, J. Shen, Surface modification of polycaprolactone membrane via aminolysis and biomacromolecule immobilization for promoting cytocompatibility of human endothelial cells, *Biomacromolecules.* 3 (2002) 1312–1319.
- [88] R. Ulijn, D. Woolfson, J.F. Almine, D. V Bax, S.M. Mithieux, L. Nivison-smith, J. Rnjak, A. Waterhouse, S.G. Wise, A.S. Weiss, Elastin-based materials, *Chem. Soc. Rev.* 39 (2010) 3371–3379.
- [89] H.S. Yoo, T.G. Kim, T.G. Park, Surface-functionalized electrospun nanofibers for tissue engineering and drug delivery, *Adv. Drug Deliv. Rev.* 61 (2009) 1033–1042.
- [90] A.M. Pappa, V. Karagkiozaki, S. Krol, S. Kassavetis, D. Konstantinou, C. Pitsalidis, L. Tzounis, N. Pliatsikas, S. Logothetidis, Oxygen-plasma-modified biomimetic nanofibrous

- scaffolds for enhanced compatibility of cardiovascular implants, *Beilstein J. Nanotechnol.* 6 (2015) 254–262.
- [91] A. Martins, E.D. Pinho, S. Faria, I. Pashkuleva, A.P. Marques, R.L. Reis, N.M. Neves, Surface modification of electrospun polycaprolactone nanofiber meshes by plasma treatment to enhance biological performance, *Small.* 5 (2009) 1195–1206.
- [92] K. Wulf, M. Teske, M. Löbler, F. Luderer, K.P. Schmitz, K. Sternberg, Surface functionalization of poly(ϵ -caprolactone) improves its biocompatibility as scaffold material for bioartificial vessel prostheses, *J. Biomed. Mater. Res. - Part B Appl. Biomater.* 98 B (2011) 89–100.
- [93] I. Kondyurina, S.G. Wise, A.K.Y. Ngo, E.C. Filipe, A. Kondyurin, A.S. Weiss, S. Bao, M.M.M. Bilek, Plasma mediated protein immobilisation enhances the vascular compatibility of polyurethane with tissue matched mechanical properties, *Biomed. Mater.* 12 (2017) 45002.
- [94] A. Waterhouse, Y. Yin, S.G. Wise, D. V. Bax, D.R. McKenzie, M.M.M. Bilek, A.S. Weiss, M.K.C. Ng, The immobilization of recombinant human tropoelastin on metals using a plasma-activated coating to improve the biocompatibility of coronary stents, *Biomaterials.* 31 (2010) 8332–8340.
- [95] Z. Ma, W. He, T. Yong, S. Ramakrishna, Grafting of gelatin on electrospun poly(caprolactone) nanofibers to improve endothelial cell spreading and proliferation and to control cell orientation, *Tissue Eng.* 11 (2005) 1149–58.
- [96] M.-C. Serrano, R. Pagani, J. Peña, M. Vallet-Regi, J.-V. Comas, M.-T. Portolés, Progenitor-derived endothelial cell response, platelet reactivity and haemocompatibility parameters indicate the potential of NaOH-treated polycaprolactone for vascular tissue engineering, *J. Tissue Eng. Regen. Med.* 5 (2011) 238–247.
- [97] M.R. Casanova, M. Alves da Silva, A.R. Costa-pinto, R.L. Reis, A. Martins, N.M. Neves, Chondrogenesis-inductive nanofibrous substrate using both biological fluids and mesenchymal stem cells from an autologous source, *Mater. Sci. Eng. C.* 98 (2019) 1169–1178.
- [98] C. Shi, W. Yuan, M. Khan, Q. Li, Y. Feng, F. Yao, W. Zhang, Hydrophilic PCU scaffolds

prepared by grafting PEGMA and immobilizing gelatin to enhance cell adhesion and proliferation, *Mater. Sci. Eng. C.* 50 (2015) 201–209.

- [99] G.M. Xiong, S. Yuan, C.K. Tan, J.K. Wang, Y. Liu, T.T. Yang, N.S. Tan, C. Choong, T.T. Yang Tan, Endothelial cell thrombogenicity is reduced by ATRP-mediated grafting of gelatin onto PCL surfaces, *J. Mater. Chem. B.* 2 (2014) 485.
- [100] W. He, Z. Ma, T. Yong, W.E. Teo, S. Ramakrishna, Fabrication of collagen-coated biodegradable polymer nanofiber mesh and its potential for endothelial cells growth, *Biomaterials.* 26 (2005) 7606–7615.
- [101] F. Du, W. Zhao, M. Zhang, H. Mao, D. Kong, J. Yang, The synergistic effect of aligned nanofibers and hyaluronic acid modification on endothelial cell behavior for vascular tissue engineering, *J Nanosci Nanotechnol.* 11 (2011) 6718–6725.
- [102] S.G. Wise, H. Liu, A. Kondyurin, M.J. Byrom, P.G. Bannon, G.A. Edwards, A.S. Weiss, S. Bao, M.M. Bilek, Plasma Ion Activated Expanded Polytetrafluoroethylene Vascular Grafts with a Covalently Immobilized Recombinant Human Tropoelastin Coating Reducing Neointimal Hyperplasia, *ACS Biomater. Sci. Eng.* 2 (2016) 1286–1297.
- [103] Y. Zhu, Y. Cao, J. Pan, Y. Liu, Macro-alignment of electrospun fibers for vascular tissue engineering, *J. Biomed. Mater. Res. - Part B Appl. Biomater.* 92 (2010) 508–516.
- [104] G. De Visscher, L. Mesure, B. Meuris, A. Ivanova, W. Flameng, Improved endothelialization and reduced thrombosis by coating a synthetic vascular graft with fibronectin and stem cell homing factor SDF-1 α , *Acta Biomater.* 8 (2012) 1330–1338.
- [105] A. Assmann, C. Delfs, H. Munakata, F. Schiffer, K. Horstkötter, K. Huynh, M. Barth, V.R. Stoldt, H. Kamiya, U. Boeken, A. Lichtenberg, P. Akhyari, Acceleration of autologous invivo recellularization of decellularized aortic conduits by fibronectin surface coating, *Biomaterials.* 34 (2013) 6015–6026.
- [106] D. Pankajakshan, K. Krishnan V, L.K. Krishnan, Functional stability of endothelial cells on a novel hybrid scaffold for vascular tissue engineering, *Biofabrication.* 2 (2010).
- [107] L. V. Antonova, A.M. Seifalian, A.G. Kutikhin, V. V. Sevostyanova, V.G. Matveeva, E.A. Velikanova, A. V. Mironov, A.R. Shabaev, T. V. Glushkova, E.A. Senokosova, G.Y. Vasyukov, E.O. Krivkina, A.Y. Burago, Y.A. Kudryavtseva, O.L. Barbarash, L.S. Barbarash, Conjugation

- with RGD peptides and incorporation of vascular endothelial growth factor are equally efficient for biofunctionalization of tissue-engineered vascular grafts, *Int. J. Mol. Sci.* 17 (2016).
- [108] F. Kuwabara, Y. Narita, A. Yamawaki-Ogata, K. Kanie, R. Kato, M. Satake, H. Kaneko, H. Oshima, A. Usui, Y. Ueda, Novel small-caliber vascular grafts with trimeric peptide for acceleration of endothelialization, *Ann. Thorac. Surg.* 93 (2012) 156–163.
- [109] J. Yu, A. Wang, Z. Tang, J. Henry, B. Li-Ping Lee, Y. Zhu, F. Yuan, F. Huang, S. Li, The effect of stromal cell-derived factor-1 α /heparin coating of biodegradable vascular grafts on the recruitment of both endothelial and smooth muscle progenitor cells for accelerated regeneration, *Biomaterials.* 33 (2012) 8062–8074.
- [110] M. Zhou, Z. Liu, C. Liu, X. Jiang, Z. Wei, W. Qiao, F. Ran, W. Wang, T. Qiao, C. Liu, Tissue engineering of small-diameter vascular grafts by endothelial progenitor cells seeding heparin-coated decellularized scaffolds, *J. Biomed. Mater. Res. - Part B Appl. Biomater.* 100 B (2012) 111–120.
- [111] M. Cestari, V. Muller, J.H.D.S. Rodrigues, C. V. Nakamura, A.F. Rubira, E.C. Muniz, Preparing silk fibroin nanofibers through electrospinning: Further heparin immobilization toward hemocompatibility improvement, *Biomacromolecules.* 15 (2014) 1762–1767.
- [112] Q. Cheng, K. Komvopoulos, S. Li, Plasma-assisted heparin conjugation on electrospun poly(L-lactide) fibrous scaffolds, *J. Biomed. Mater. Res. - Part A.* 102 (2014) 1408–1414.
- [113] S. Singh, B.M. Wu, J.C.Y. Dunn, The enhancement of VEGF-mediated angiogenesis by polycaprolactone scaffolds with surface cross-linked heparin, *Biomaterials.* 32 (2011) 2059–2069.
- [114] A.J. Melchiorri, N. Hibino, T. Yi, Y.U. Lee, T. Sugiura, S. Tara, T. Shinoka, C. Breuer, J.P. Fisher, Contrasting biofunctionalization strategies for the enhanced endothelialization of biodegradable vascular grafts, *Biomacromolecules.* 16 (2015) 437–446.
- [115] L. Chen, H. He, M. Wang, X. Li, H. Yin, Surface Coating of Polytetrafluoroethylene with Extracellular Matrix and Anti-CD34 Antibodies Facilitates Endothelialization and Inhibits Platelet Adhesion Under Shear Stress, *Tissue Eng. Regen. Med.* 14 (2017) 359–370.

CHAPTER II.

Materials and Methods

Chapter II. Materials and Methods

The aim of this chapter is to describe in detail the materials and the experimental procedures used, enabling the comprehension of the experimental results. Moreover, this chapter intends to justify properly the selection of materials and the experimental methods to achieve the main objectives of this experimental work.

2.1 Materials

2.1.1 Polycaprolactone

Polycaprolactone (PCL) is a biodegradable aliphatic polyester, which molecular structure consists of repeating five nonpolar methylene groups and a single relatively polar ester group (Figure 2. 1) [1]. It has a glass transition temperature of around -60°C and a melting point of $55-60^{\circ}\text{C}$, but these values may differ according to the molecular weight and the processing method used [2].

PCL is a biomaterial already Food and Drug Administration (FDA) approved in a variety of clinical applications such as drug delivery or suture material [3,4]. Owing to its low melting temperature, good blend-compatibility with other polymers and low cost production, this polymer can be processed by a wide range of fabrication techniques [2]. Additionally, this polymer has been extensively preferred in tissue engineering such as cartilage, bone and vascular applications [5–7].

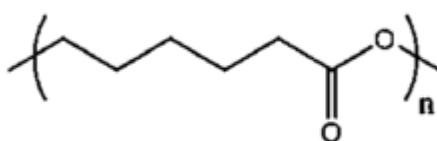


Figure 2. 1 - PCL chemical structure. Adapted from ref. [10].

The suitable mechanical properties of this polymer have been reported for vascular grafts as high strength and excellent compliance [7]. Several studies have investigated the mechanical properties of PCL tubular conduits, demonstrating the ability of this polymer to withstand the burst pressure and suture retention strength of native blood vessels both *in vitro* [8] and *in vivo* [9]. Moreover, it was demonstrated that PCL grafts presents faster endothelial coverage compared to ePTFE grafts [7].

Another important characteristic of PCL is its slow degradation rate due to its semi-crystalline and hydrophobic nature, which makes this polymer a potential candidate for vascular

applications [7,10]. For blood vessel replacements, degradation must be slow enough to avoid events of mechanical failure which can cause severe damages on the patient. As such, the vascular substitutes should provide structural resistance during the tissue regeneration process [11]. Typically, the *in vivo* degradation of PCL takes more than 2 years, resulting, sequentially, in loss of molecular weight by a slow nonenzymatic bulk activation, loss of mechanical strength by hydrolytic process and, finally, in loss of mass by phagocytosis [1,11]. The degradation mechanism of PCL nanofibers meshes is faster from those of bulk PCL due to the larger surface area-to-volume ratio, as well as changes in hydrophobicity and crystallinity induced by the electrospinning process [10].

Despite its excellent characteristics, the hydrophobic nature of PCL confers to the polymer a poor wettability [10]. Also, it has been reported that the hydrophobic PCL surface interacts with platelets, contributing to the thrombogenicity which could lead to thrombosis and intimal hyperplasia [9]. To overcome these drawbacks, several approaches have been explored to enhance the biological and mechanical properties of vascular grafts using PCL. Several bioactive molecules have been immobilised at the PCL surface such as gelatin [12], vascular endothelial growth factor (VEGF) [13] and fibrin to improve the cell-material interaction [14]. Blending PCL with other polymers as such polyurethane [15], collagen [8] and tropoelastin [9] was also considered to improve the mechanical properties of the vascular graft.

2.1.2 Tropoelastin

The ECM of the connective tissues is composed of proteins, proteoglycans and glycosaminoglycans which function is to provide a biologically and mechanically structural base that influences the cellular behaviour [16]. Elastin is a vital protein ECM component which provides elasticity and resilience to several biological tissues such as vasculature and skin. However, due to its insolubility and difficulty of handling, the use of elastin in biomaterials is limited [17]. This protein is formed by the cross-linking of its soluble precursor, the tropoelastin, which, in contrast, can be used in a range of elastin-related products [18].

Tropoelastin is secreted as a 60 kDa unglycosylated protein by several types of cells such as fibroblasts, endothelial and smooth muscle cells. Its molecular structure contains hydrophobic domains, responsible for the elasticity, alternated with hydrophilic domains with lysines residues crucial for cross-linking [19]. Structurally, in one end of the molecule structure, N-terminal is characterized by the presence of a 26-amino-acid signal peptide while the other end comprises the

C-terminal which terminates with a positively charged amino acid motif [19], responsible for cell-binding [20] (Figure 2. 2).



Figure 2. 2 - Tropoelastin structure which includes two functionally distinct regions, N and C terminal, separated by a bridge responsible for the mechanical coupling. Adapted from ref. [17].

Tropoelastin possesses high elasticity, being the most distensible monomer protein known in the human body. Tropoelastin participates in several cell interactions through its receptors, integrin $\alpha\text{v}\beta\text{3}$ and elastin binding protein (EBP), at the cell surface, influencing cell adhesion and proliferation [17].

Binding tropoelastin to biomaterial surfaces have been investigated to improve not only cell adhesion and proliferation but also to stimulate specific cellular responses, mimicking the natural cell environment [17,21,22]. Other ECM proteins such as collagen, fibronectin and laminin have been also coated onto polymer surfaces to improve and support ECs adhesion. Nevertheless, these proteins are often associated with fibrinogen deposition, platelet adhesion, activation and thrombus formation, which restricts their use as vascular conduits [23]. In contrast, it has been demonstrated the hemocompatibility of tropoelastin, presenting low thrombogenicity, minimal platelet adhesion and aggregation [24]. Over the past years, tropoelastin has been immobilised at the surface of several materials ranging from metallic surfaces, such as drug eluting stents (DES) [25], to polymeric surfaces such as PLLA-PLGA [18], polyethersulfone (PES) [21], polyurethane [26] and expanded polytetrafluoroethylene (ePTFE) [27].

2.2 Electrospinning

Electrospinning is an attractive and versatile approach for polymers processing which is based on the use of a high-voltage electrical field to generate fibers in a nano to micrometer

diameter range [28]. This technique is able to process a wide range of natural and synthetic polymers commonly proposed for tissue engineering applications such as PCL [7], PLA [29], PU [30], collagen [8] or gelatin [31].

The conventional electrospinning apparatus consists of a high voltage power source, a capillary where the polymer solution is extruded, and a grounded metal to collect the fibers [28]. When a high voltage is applied to the capillary, containing a polymeric solution dispensed by a syringe pump, a conical shape “Taylor cone” is generated at the tip of the capillary. A jet of fluid is ejected from the capillary tip with the increasing of the electrostatic field. While the jet progresses, it is stretched and the solvent evaporates, generating a polymeric fiber. This technique produces randomly oriented nanofiber meshes which can be collected on a stationary or rotating metallic collector to obtain flat meshes or tubular scaffolds, respectively [32].

Since most of the natural ECM of connective tissues is composed of randomly oriented fibers with nanometre scale diameters (50 to 500 nm), the electrospun meshes provide a biomimetic environment designed to resemble the natural ECM [33]. Additionally, using this technique enables the production of fibrous scaffolds with controllable pore size, porosity, composition and morphology [32,34]. Despite its interesting characteristics, one disadvantage of this technique is the production of thin scaffolds. In fact, the development of scaffolds with considerable thickness, higher than 0.5 mm is limited due to the small fiber diameter and pore size, influencing the possibility of cell infiltration into the scaffold [35].

2.2.1 Electrospinning parameters

The morphology of electrospun meshes is influenced by several factors such as solution, concentration and viscosity, processing and environmental parameters which may affect the electrospinning process. Thus, tuning these variables is crucial to control the fiber characteristics of the scaffold [28,36].

The type of polymer used, as well as its molecular weight, concentration, viscosity, surface tension and electrical conductivity, all affect the electrospinning process. The polymeric solution must have enough surface tension, charge density and viscosity to prevent the jet from coalescing into droplets before the solvent evaporation. Also, the properties of the solvent are of high importance since its volatility and polarity may influence the morphology and diameter of the fibers [32]. Increasing the concentration of the polymer, as well as its molecular weight and the solution viscosity, results in larger fiber diameters and, consequently, in higher pore sizes [28,36]. On the

other hand, an increase on the electrical conductivity of the polymeric solution decreases the fiber diameter [36]. Polymeric solutions with low conductivity may result in insufficient elongation of the jet to produce the fibers, leading to fibers with larger diameters [37].

The processing parameters comprise the applied voltage, the flow rate and the distance to the collector. When the applied voltage is increased, the fiber diameter tends to decrease, and vice-versa. The flow rate has influence on the jet velocity and material transfer rate. The higher the flow rate, the larger the fiber diameter and pore size [32]. However, it is commonly used lower flow rates to allow an efficient evaporation of the solvent from the fibers during the process [36]. Another important parameter is the distance between the needle tip and the collector which can equally affect the structure and morphology of the electrospun fibers. The distance influences the polymer deposition time and evaporation rate. Thus, shorter distances tend to produce wetter fibers since the fibers do not have sufficient time to dry before reaching the collector [32,37]. Equally important, the environmental conditions have a tremendous effect on the fiber morphology, determining the mesh properties. For instance, both temperature and humidity influence the solvent evaporation rate during the fiber formation process [10]. Increasing the temperature results in smaller fiber diameters which can be attributed to the decrease of viscosity of the polymeric solution [37].

2.2.2 Production of electrospun tubular fibrous (eTF) scaffolds

The production of eTF scaffolds by electrospinning was previously optimized considering different works from the literature [7,38]. As a result, several parameters were tested, as illustrated in Table 2. 1, in flat meshes and tubular structures.

Table 2. 1 - Electrospinning parameters tested for optimization of eTF scaffolds production

Electrospinning parameters	
PCL concentration	15% (v/v), 17% (v/v)
Organic solvent	Chloroform:ethanol (7:3), Chloroform: dimethylformamide (7:3)
Voltage	10 kV, 15 kV
Distance to collector	15 cm, 20 cm

Based on a morphological analysis, the most effective electrospinning condition was selected. The eTF scaffolds were produced using a customized electrospinning device. The Figure 2.3 illustrates the electrospinning setup used in this experimental work.

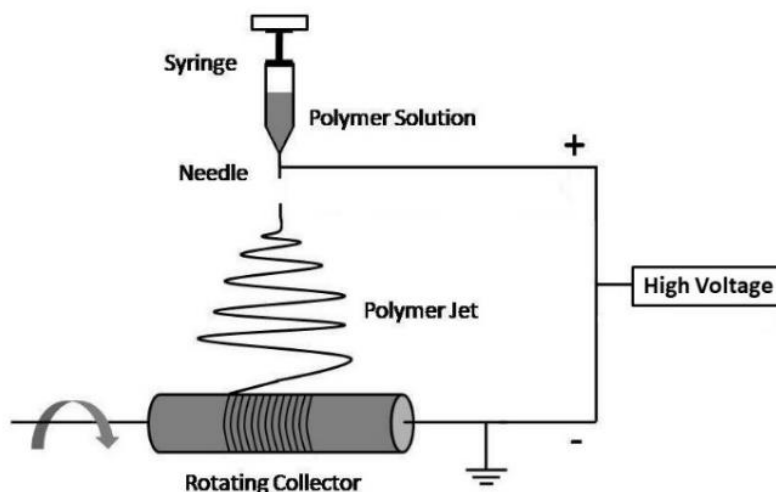


Figure 2.3 - Schematic representation of the electrospinning setup used to produce eTF scaffolds.

A polymeric solution was prepared by dissolving PCL ($M_w = 80,000$; Sigma-Aldrich, USA) at a concentration of 15% (v/v) into an organic solvent mixture of chloroform (Fisher Scientific, UK) and absolute ethanol (Fisher Scientific, UK) at a ratio of 7:3. Firstly, PCL was dissolved in chloroform under gentle stirring and, after total dissolution of the polymer, ethanol was added. The solution was kept in constantly stirring to avoid phase separation.

The PCL solution was placed into a 6 mL syringe (Braun, Germany) connected to a metallic 21G needle. The syringe was mounted in a syringe pump (model Alladin 220) to control the solution flow rate. A high-voltage power supply (0-25 kV) was applied to the needle to generate a continuous current with a voltage of 10 kV. The needle tip-to-collector distance and the flow rate were fixed at 15 cm and 1.0 mL h^{-1} , respectively. Fibers were electrospun onto a custom metallic rotating mandrel with 4 mm external diameter, rotating at 200 rpm for the manufacture of the conduit. The electrospinning process was conducted for 1 h. Both temperature and relative humidity were kept at $22^\circ\text{C} \pm 2$ and 35% - 42%, respectively. The eTF scaffolds were, then, extracted from the mandrel and cut into squares of $1 \times 1 \text{ cm}^2$ for further assays.

2.3 Functionalization of eTF scaffolds

The functionalization of eTF scaffolds aims at providing biochemical cues by the immobilization of tropoelastin at the surface to enhance the endothelial cells adhesion and proliferation. Since PCL does not have reactive functional groups, several strategies have been

implemented to achieve the immobilization of bioactive molecules at the nanofibers surface. Plasma treatment, UV-ozone irradiation and immersion in NaOH are common methods used to activate the surface of electrospun PCL nanofibers, following the incorporation of amine groups by aminolysis treatment and, consequently, the immobilization of biomolecules [39–42]. To accomplish the immobilization of tropoelastin at the luminal surface of the eTF scaffolds, a wet chemical method was selected. This method is based on the random chemical scission of ester linkages on the polymer backbones, allowing the modification in the inner layers of the meshes [43].

The surface functionalization was based on two reactions: activation, followed by the aminolysis reaction. Firstly, the surface eTF scaffolds was activated by sodium hydroxide solution (NaOH) (Fisher Scientific, UK). The ester groups (-COO-) of PCL were cleaved by NaOH solution, generating carboxylic (-COOH) and hydroxyl groups (-OH) at the nanofibers surface. After activation, eTF scaffolds were aminolysed using a diamine solution, hexamethylenediamine (HMD; Sigma-Aldrich, USA), resulting in a reaction between the amine groups (-NH₂) from the diamine solution and the carboxylic groups previously introduced. One -NH₂ reacts with the -COOH- group to form a covalent bond, -CONH-, the other one is unreacted and free [44]. The Figure 2. 4 illustrates the functionalization process onto eTF scaffolds surface.

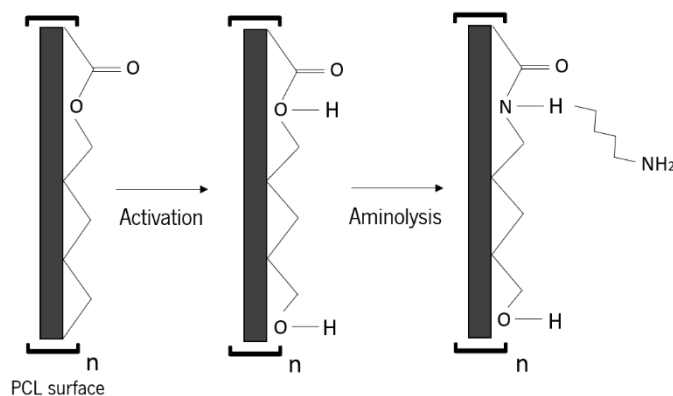


Figure 2. 4 - Schematic representation of activation (NaOH treatment) and aminolysis (HMD treatment) reactions on eTF scaffolds surface.

2.3.1 Optimisation of surface functionalisation

The duration of both reactions, as well as the concentration of the chemical agents, are important parameters that must be taken in attention in order to develop functional groups at the surface with minimal change in the bulk properties of the polymer [43]. Therefore, an optimisation process was conducted using flat electrospun PCL meshes (Table 2. 2).

Table 2. 2 - Concentrations and incubation times of both NaOH and HMD solutions tested for optimization of nanofibers surface functionalization

	NaOH solution			HMD solution	
Concentration	1M	2M	5M	1M	4M
Reaction time	3h	12h	3h	1h	24h
Ref.	[40]	[45]	[46]	[39]	[40]

Briefly, eTF scaffolds, placed in 24 well plates with the luminal surface faced up, were immersed in 1 mL of 1M NaOH solution. The 24 well plates were placed in a mechanical shaker (Model Mini shaker, VWR) to provide a homogeneous surface activation at room temperature. After this treatment, eTF scaffolds were washed with PBS three times. Then, eTF scaffolds were placed in new wells where 1 mL of HMD solution in isopropyl alcohol (VWR Chemicals, USA) was added. The plates were wrapped with aluminium foil to avoid degradation of the HMD reagent during the reaction time and, then, placed in an incubator (Model BE500, Memmert) at 37 °C. After this treatment, the washing process was repeated and the meshes were left to dry at room temperature for further analysis. The conditions which allowed the immobilization of a higher concentration of NH₂ groups without affecting the fibers morphology were 1M NaOH for 3h and, then, 4M HMD for 24h.

2.3.2 Amine groups (NH₂) quantification

The free amine groups (NH₂) introduced by the aminolysis reaction were quantified by the Ellman's reagent method [47]. Untreated, activated and aminolysed eTF scaffolds weighted, functionalized and, then, incubated with 300 µL of PBS at pH=7.27, containing 20 mM 2-Iminoethanol (2-IT; Sigma-Aldrich, USA) and 20 mM 4-dimethylaminopyridine (DMAP; Thermo Fisher Scientific, USA) for 1h at 37°C, protected from light. The incubation with 2-IT introduces sulfhydryl groups (-SH) at the surface by reacting specifically with the primary amines already present, generating one sulfhydryl group per one amine group reacted with the reagent [47]. Then, the samples were thoroughly washed with 400 µL of each of the following solutions, sequentially:

- a. PBS at pH = 7.27;
- b. Ultrapure water containing 1 mM dithiothreitol (DTT; abcr GmbH, Germany) and 10 mM Ethylenediaminetetraacetic acid (EDTA; Sigma-Aldrich, USA) at pH=7;

- c. Ultrapure water containing 1 M sodium chloride (NaCl; PANREAC QUIMICA, Spain) and 10 mM EDTA at pH=7;
- d. PBS containing 1mM EDTA at pH = 7.27.

The use of DTT in one of the washing solutions will ensure that the covalently bounded sulfhydryl groups remained in the reduced state [47]. After the washing procedure, samples were moved to new wells and incubated with 500 μ L of 0.1 mM 5,5'-dithiobis-(2-nitrobenzoic acid) (DTNB), Ellman 's reagent; Sigma-Aldrich, USA) solution in PBS at pH=7.27 for 1h at 37 °C, protected from light. The Ellman 's reagent is the detection reagent which allows the quantification of the sulfhydryl groups generated at the eTF scaffold surface. The reaction between the Ellman 's reagent and the -SH groups results in the cleavage of DTNB, producing 1 mol of 2-nitro-5-thiobenzoic acid (TNB) per mole of sulfhydryl groups. The quantification of free amine groups is carried out through the extinction coefficient of TNB at 412 nm [47]. After the Ellman 's reagent incubation, 150 μ L of each sample was transferred to a quartz 96 well plate in triplicate and the absorbance was read at 412 nm by a microplate reader (Synergy, HT, Bio-TEK) using DTNB solution alone as blank. Controls of each condition (untreated, activated and aminolysed) were used in triplicates, where only the first step (i.e. 2-IT incubation) was eliminated, using PBS instead. The quantification of free amine groups of each samples was calculated according to the equation 2.1.

$$NH_2 \text{ mol} = \frac{(OD_{sample} - OD_{blank}) \times 500 \times 10^{-6} \text{ L}}{14150 \text{ M}^{-1} \text{ cm}^{-1}} \quad (\text{Equation 2. 1})$$

The OD_{sample} refers to the absorbance of the sample incubated with 2-IT and the OD_{blank} refers to the absorbance of the sample without the first incubation. The absorbances were corrected for the volume of DTNB solution that reacted with the samples and divided by the TNB² molar absorption coefficient value of 14,150 $M^{-1} \text{ cm}^{-1}$.

2.4 eTF scaffolds characterization

2.4.1. Scanning Electron Microscopy (SEM)

SEM is a technique which allows the morphological characterization of a sample. This technique is based on the interaction between the electrons and the sample, producing several signals at the sample surface [48]. When a sample is scanned by a focused beam of electrons, these signals can be collected to give information about the morphology and surface topography.

Additionally, SEM is a suitable method to analyze the material surface due to its high resolution, less than 1 nm [49]. Since the scaffolds are composed of nanofibers, SEM is an appropriate technique to analyze their surface. However, this microscopy method can only analyze conductive samples and, thus, the nonconductive samples must be coated with a thin layer of conductive material [48].

To analyse the eTF scaffolds by SEM, the following procedure was applied: frozen in liquid nitrogen for 15 min and, then, cut with a scalpel to obtain a clean cross-section surface. 10 images of the cross-section surface at x150 magnification were used and at least 3 measures were performed to assess the scaffold thickness using the software ImageJ (National Institute of Health, USA). Along with the cross-section surface, both inner and outer surfaces, before and after the functionalization process, were sputter-coated with gold (Cressington, model 108A) for 2 min at 15 mA. The samples were further analyzed by SEM (JSM-6010 LV, JEOL, Japan) with an acceleration voltage of 5-10 kV. The magnifications used were x150, x500 and x1000.

The diameters of the nanofibers characterization was assessed using the DiameterJ plugin created for ImageJ. DiameterJ is an open-access and simple-to-use image analysis tool which enables a rapid and efficient measurement of nanofiber diameters from SEM micrographs [50]. At least 6 images of luminal surfaces at x1000 magnification (before and after surface treatments) were used to perform the DiameterJ analysis, according to Hotaling, *et al.* [50]. Overall, this analysis is based on, firstly, the segmentation of the original image into a binary image, where fibers are white and the background is black; secondly, the analysis of the segmented image. As outputs, the algorithm produces histograms of fiber diameters and orientation, as well as gives information of pore area, pore size and the amount of the porosity. The outputs displayed correspond to a representative frequency distribution of each fiber properties.

2.4.2. Uniaxial tensile testing

The evaluation of the mechanical properties of biomaterials for vascular use is an important aspect that should be considered when designing vascular grafts. Hence, uniaxial tensile testing was performed to characterize the material's response to loading [51].

In a uniaxial tensile test, a strip of the material is placed between the grips which are connected to a movable cross-head that can be moved up and down by a hydraulic piston. The specimen is strained at a constant speed and the load gives the load supported by the specimen

over time. The mechanical test ends when the specimen fractures. For a correct determination of the failure properties, failure must not occur in the grips [51,52].

A typical tensile specimen is illustrated in Figure 2. 5. It has enlarged ends for gripping and a reduced gage section to localize the deformation and failure within this region. The gage length is the region over which measurements are made and it is centered within the area of more reduced cross-section [53].

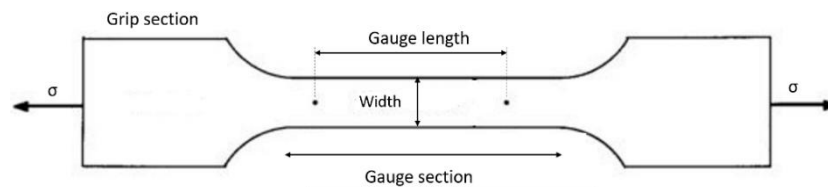


Figure 2. 5 - Typical tensile specimen with an enlarged ends and reduced gage section. Adapted from ref. [53].

The *tensile stress* (σ) is defined as the *load* (P), expressed in newtons (N) per *cross-sectional area* (A) of the *gage section* (equation 2. 2). Thus, *tensile stress* is expressed in units of force per unit area (N/m^2 or Pa) [52].

$$\sigma = \frac{P}{A} \quad (\text{Equation 2. 2})$$

The *tensile strain* (ε) is defined as the change in *gage length* (Δl) relatively to the *initial gage length* (l_0) of the specimen (equation 2. 3). *Tensile strain* can be expressed in millimeter per millimeter or as unit of percentage ($\text{mm}/\text{mm} \times 100$) [52].

$$\varepsilon = \frac{\Delta l}{l_0} = \frac{L - l_0}{l_0} \quad (\text{Equation 2. 3})$$

From the tensile stress and tensile strain values, a stress-strain curve can be obtained, which gives information about the mechanical properties of the material. A typical stress-strain curve for a ductile material is shown in Figure 2. 6.

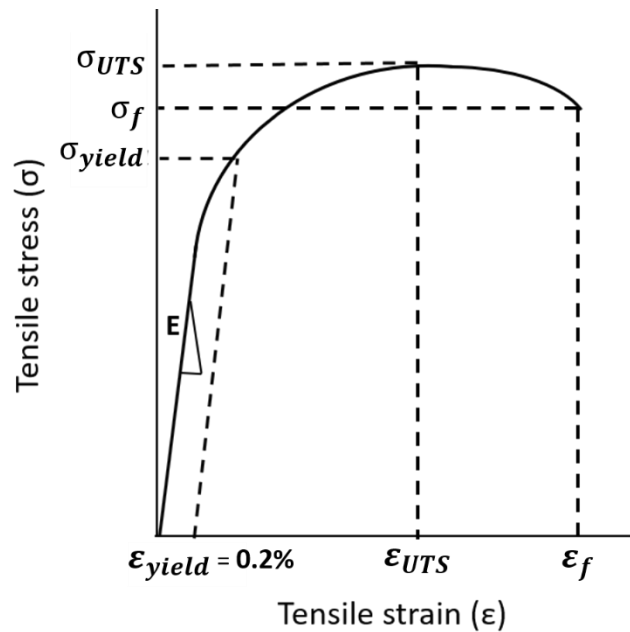


Figure 2. 6 - Stress-strain curve for a ductile material. Adapted from ref. [52].

In the early portion of the stress-strain curve (low strain), the material behaves in an elastic manner. Thus, the material obeys Hooke's Law where the stress is proportional to strain, being the deformation elastically recoverable [52]. The slope of the straight-line portion of the stress-strain diagram ($\Delta\sigma/\Delta\epsilon$) is called *Elastic Modulus* or *Young's Modulus*, denoted by E , expressed in units of force per unit area (N/m^2 or Pa) (equation 2. 4). *Young's modulus* is a basic physical property of each biomaterial [51].

$$E = \frac{\sigma}{\epsilon} \quad (\text{Equation 2. 4})$$

After a certain stress level is reached, the material enters in a plastic deformation regime before failure. Once the plastic deformation occurs, the strain is no longer proportional to the stress and it is not recovered when the stress is removed due to the irreversibly rearrangement of its internal molecular structure [52]. The transition from elastic to plastic deformation is not frequently easy to identify. As such, the yield strength can be obtained by constructing a straight line parallel to the initial linear portion of the stress-strain curve, but offset by 0.02%, 0.2% or 2%. The yield strength is the stress needed to induce plastic deformation which can be 0.02%, 0.2% or 2% of permanent strain, depending on the mechanical behaviour of each material. Other property that is often reported from the stress-strain curve is the *ultimate tensile stress* (σ_{UTS}) or *tensile strength*. The *tensile strength* is the stress calculated from the maximum load experienced during the tensile

test, giving information about the maximum load that a material can support in an uniaxial loading. The *fracture strength* (σ_f) is the stress at the point of fracture [51,52].

Since a dimension of 18 mm in length of the specimens was required, the 4 mm diameter scaffolds did not present enough perimeter along radial direction (~12 mm). Therefore, 6 mm internal diameter tubular scaffolds were produced using a custom rotating collector with 6 mm external diameter. The 6 mm diameter scaffolds were cut into strips (18x5 mm) along their radial or axial directions (Figure 2. 7A), using a scalpel. The thickness of the specimens was measured at three different points using a digital micrometer (Mitutoyo, Japan). The average of the three measurements was obtained for each specimen and their dimensions were used in the tensile test. At least 6 specimens in each radial and axial direction were tested before and after the activation and aminolysis reactions. As such, the specimens were activated or aminolysed and left to dry over a teflon foil to avoid attachment to the plate. All specimens were mounted in paper frames using double-side tape on both edges to ensure a firm retention of the eTF scaffold within the tensile system grips (Figure 2. 7B). Immediately, before the mechanical test, the lateral sides of the paper frames were cut.

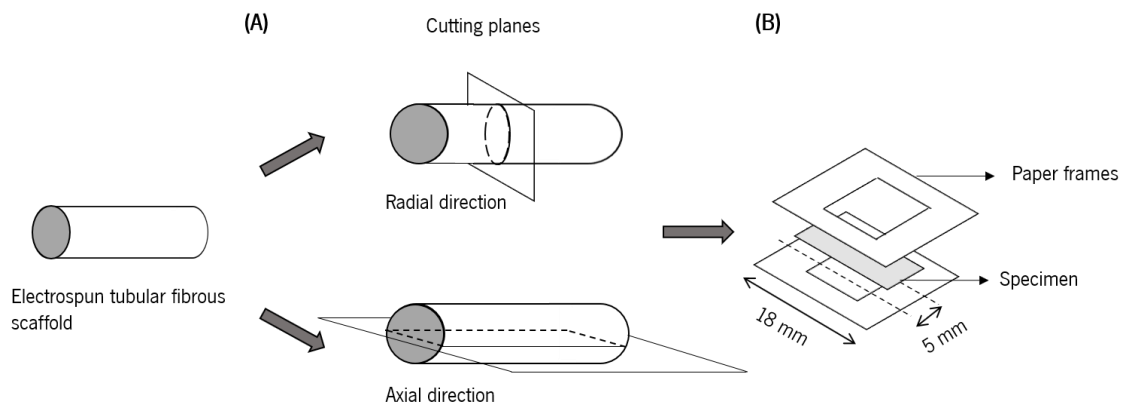


Figure 2. 7 - Specimens preparation (A) and specimens mounting (B) for uniaxial tensile testing.

Uniaxial tensile properties were measured using a universal mechanical testing equipment (Model 5543, INSTRON, UK) equipped with a 1kN load cell. A cross-head speed of 2 mm/min and a 10 mm gauge length were used. Untreated, activated and aminolysed specimens from each direction were tested under dry and wet conditions at room temperature. In the latter, the mounted specimens were rehydrated by spraying PBS on the specimens prior to testing. The mechanical tests were performed until specimen fracture. Load and displacement measurements were acquired by the software Bluehill 2, and tensile stress and strain were calculated and plotted, according to the initial length and cross-sectional area of the specimens. A linear regression of the maximum linear region from stress-strain curves was used to calculate the Young's modulus.

Maximum stress and *strain at maximum stress* were considered, respectively, as the maximum stress value before failure and its corresponding strain value.

2.5 Tropoelastin immobilization

After selecting the best condition for the functionalization of eTF scaffolds, tropoelastin can be further immobilized at their surface using two pathways: (i) the immobilization can be performed by the reaction between its -NH₂ groups and the -COOH groups introduced at the fibers surface, after the activation step (Figure 2. 8A); (ii) or the tropoelastin can be immobilized by the reaction between its -COOH groups and the -NH₂ groups introduced at the fibers surface, after the aminolysis step (Figure 2. 8B). In both cases, it is established a covalent bond between the protein and the polymeric substrate.

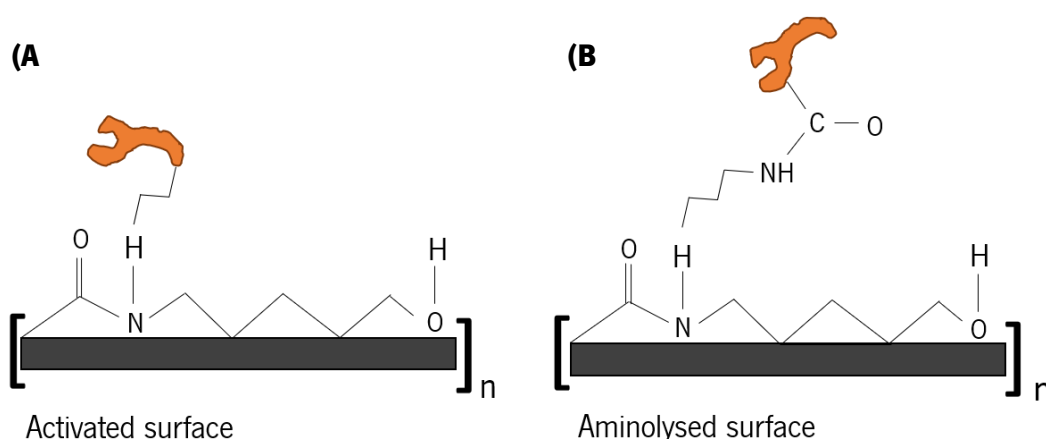


Figure 2. 8 - Schematic representation of tropoelastin immobilization on activated (A) and aminolysed (B) eTF scaffolds surface.

Human recombinant tropoelastin was produced at Weiss Lab (The University of Sydney, Australia) by an *Escherichia coli* expression system [54].

To achieve a more stable and strong immobilization, 1-Ethyl-3-[3-dimethylaminopropyl]carbodiimide hydrochloride/Nhydroxysuccinimide (EDC/NHS; Sigma-Aldrich Aldrich, USA) was used as a linker to enhance the efficiency of the binding. EDC reacts with the carboxylic groups (from protein or substrate) generating an unstable reactive ester, O-acylisourea. In combination of NHS, a semi-stable amine-reactive NHS-ester is formed. These species can interact with the amine groups (from the protein or substrate) establishing a covalent bond between the protein and the substrate. Combining the EDC with the NHS, the efficiency of the coupling is enhanced, resulting in the chemical reaction illustrated in the Figure 2. 9 [55].

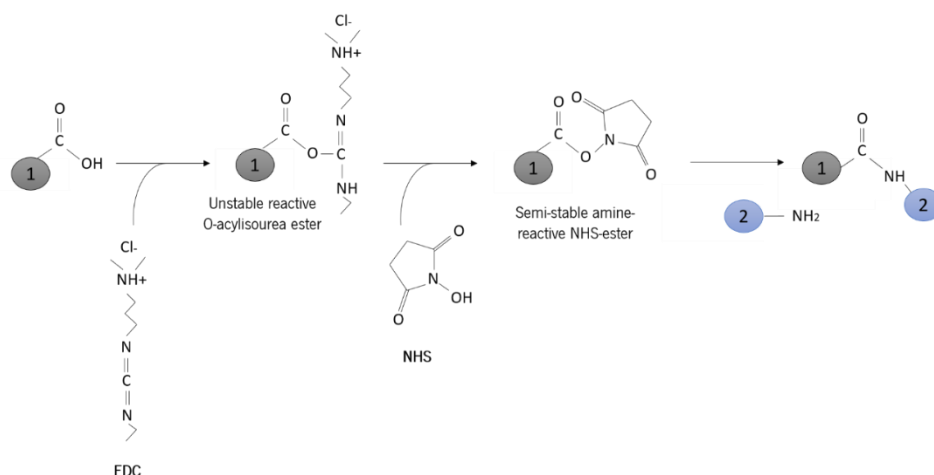


Figure 2. 9 - Chemical reaction for the EDC/NHS coupling. Adapted from ref. [55].

The parameters of the EDC/NHS solution, as concentration and ratio, were previously optimized [39]. Briefly, 50 mM EDC and 200 mM NHS (1:4) was dissolved in 0.1 M 2-N-morpholino (ethanesulfonic acid hydrate) buffer (MES; Sigma-Aldrich-Aldrich, USA) with 0.9% (w/w) NaCl (Panreac Quimica, Spain), following pH adjustment to 4.7. Tropoelastin solution was then mixed with 1% (v/v) EDC/NHS solution for 15 min, at room temperature, prior the incubation with eTF scaffolds. After the incubation with EDC/NHS solution, the activated and aminolysed eTF scaffolds were placed in non-adherent 24 well-plates and 500 μ L of tropoelastin solution was added to each sample for 2h, at room temperature, under gentle stirring.

2.6 Chemical characterization of the biofunctionalized eTF scaffolds

2.6.1. Quantification of immobilized tropoelastin

To ensure that eTF scaffolds were used at their maximum immobilization capacity, an optimization of the tropoelastin concentration at the activated and aminolysed surfaces was conducted, using the MicroBCA™ Protein Assay Kit (Pierce, Thermo Scientific). MicroBCA assay is a common method to measure proteins in solution. When a protein is placed in an alkaline environment containing Cu^{2+} , the peptide bonds of the protein react with Cu^{2+} atoms, leading to the reduction of Cu^{2+} to Cu^{1+} , within the complexation sites of the protein. Bicinchoninic acid (BCA), the detection reagent, is a sensitive, stable, water-soluble compound and highly specific for Cu^{1+} , establishing a 2:1 complex with Cu^{1+} . This results in a stable and highly colored complex with an absorbance at 562 nm, which is directly proportional to the protein concentration [56].

The microBCA assay was performed with some modifications from the manufacturer's protocol. Several concentrations of tropoelastin (0, 5, 10, 15 and 20 μ g/mL) were used to assess the amount of retained tropoelastin at the eTF scaffold surface, in duplicate. After the

immobilization of tropoelastin solutions, the scaffolds were washed three times with PBS, 5 min each. Afterwards, PBS was completely removed and 150 μL of working reagent was added along with 150 μL of PBS directly on the eTF scaffolds for 2h at 37 $^{\circ}\text{C}$. The preparation of the working reagent was done according to the manufacture's instructions and a standard curve with values ranging from 0 $\mu\text{g}/\text{mL}$ to 20 $\mu\text{g}/\text{mL}$ was prepared in PBS. After the incubation time, 300 μL of the solution that reacted with the eTF scaffold was transferred to a 96-well plate and the absorbance was read at 562 nm, using a microplate reader (Synergy, HT, Bio-TEK). The concentration of immobilized tropoelastin was interpolated from the standard curve. The assay was performed five independent times.

2.6.2. Surface charge properties

The surface properties of biomaterials such as surface chemistry, charge and topography influence the biological performance and response of materials to the surrounding environment [57]. *Zeta potential*, denoted as ζ , is a parameter which gives information about the charge at the solid/liquid interfacial layer of a material in an aqueous solution [58]. This parameter is an useful indicator of surface charges and, therefore, can be used to characterize surface functionality of biomaterials.

When a material is immersed in an electrolyte solution, the functional groups on its surface react with the surrounding medium, attracting oppositely charged ions (counterions) onto the surface (Figure 2. 10). This leads to the formation of an electrical double layer at the interfacial boundary by attractive forces between a surface-charged material and counterions. The layer that is generated where the counterions are strongly attached to the surface charge is called Stern layer. Outside this layer, a diffuse layer is present containing a low concentration of counterions that are not firmly bound to the material surface. Between these two layers, a boundary, called shear plane, is formed. The electric potential of the shear plane is called zeta potential [58].

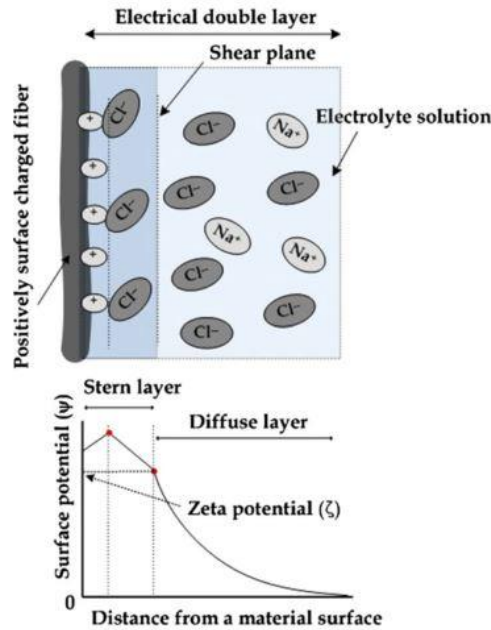


Figure 2. 10 - Schematic representation of charge distribution in the zeta potential measurement. Adapted from ref. [58].

The formation of surface charge is dependent on the pH value of the aqueous electrolyte solution. Zeta potential can be determined with different measurement techniques, being the streaming potential the most commonly used method [58]. This method is based on the generation of an electric field when a liquid is forced to flow through a stationary charged surface. The sample is enclosed into a measuring cell, where an aqueous electrolyte solution flows, causing an electrical charge separation in the flow direction. The resulting differential potential (streaming potential) or electrical current (streaming current) is detected by electrodes that are connected to the measuring cell. During the measurement, the pressure increases continuously in both flow directions, and *pressure difference* across the measuring cell (dp) and *streaming potential* (dU) or *streaming current* (I) are recorded. The measured values of dp and dU or I are used to calculate the zeta potential [58].

The zeta potential of eTF scaffolds was determined using the SurPASS electrokinetic analyzer (Anton Paar GmbH, Austria). Untreated, activated, aminolysed and tropoelastin immobilized eTF scaffolds were cut in 12 cm² disks and placed in an adjustable disk gap cell (14mm), with an adjusted gap of 115 μ m. The streaming currents were detected by the Ag/AgCl electrodes at different pH values within the range 6.0 to 10. An electrolyte solution of 1 mM KCl was flushed through the cell with a pressure of 400 mbar and the pH was automatically adjusted by adding 0.05 M NaOH to the electrolyte solution. The data was recorded and analyzed using the Attract 2.0 software.

2.7 Cell biology assays

A biological assessment of the proposed material is crucial to understand how the scaffold behaves in the presence of cells. This analysis aims to study if the eTF scaffolds are suitable to support endothelialization by assessing the metabolic activity, proliferation, protein synthesis, morphology and phenotype maintenance.

2.7.1. Cell source

A cell line is an immortalized population of cells that proliferate indefinitely due to a genetically induced mutation. Since primary cells have limited lifespan and display different features due to their different donor origin, immortalized cell lines have been commonly used instead of primary cells [59,60]. Cell lines are cost effective, easy to use and offer a pure population of cells which provide consistent sample and reproducible results. Additionally, the use of these cells avoid ethical issues related to the use of animal or human tissue [59]. Despite this, special attention should be taken when using cell lines. These cells should exhibit and maintain functional characteristics, similar to those of primary cells which can be difficult since the immortalization process may interfere with their phenotype and native functions [59].

In endothelialization research, Human Umbilical Vein Endothelial Cells (HUVECs) are widely used to study the function of endothelial cells in several physiological and pathological studies. As they are primary cells, HUVECs have an average life span of 10 serial passages before entering in the senescence stage, when they stop proliferating. Moreover, they lose their primary features and responsiveness to several stimuli. Therefore, several endothelial cell lines were established, characterized and used for various research purposes [60]. The human umbilical vein endothelial cell line EA.hy926 is well characterized and frequently used. This cell line was generated by a genetic mutation of HUVEC [60]. EA.hy926 have been previously studied for endothelialization purposes within vascular tissue engineering [61–63]. As such, EA.hy926 (LGC Standards, Spain) was used to assess the endothelialization of the developed biofunctionalized eTF scaffolds.

2.7.2. Cell culture and seeding

EA.hy926 cells were cultured in Dulbecco's Modified Eagle Medium (DMEM; Sigma-Aldrich, USA) low glucose supplemented with sodium bicarbonate (Sigma-Aldrich, USA), 10% Fetal Bovine Serum (FBS; Life Technologies, USA) and 1% antibiotic/antimycotic (A/A; Life Technologies,

USA) and incubated at 37°C in a humidified 5% CO₂ atmosphere. EA.hy926 cells were used within 10-18 passages. Medium was changed every 2-3 days until a 90% confluency was reached.

The eTF scaffolds were sterilized by UV light for 30 min, on each side, inside a laminar flow chamber (PV-100, Telstar). Both functionalization and tropoelastin immobilization were further performed under sterile conditions by filtering each solution with 0.22 µm filters. The cell seeding was performed by dropping a cell suspension containing 100 000 cells on top of each untreated, activated, aminolysed and tropoelastin immobilized eTF scaffolds. After 4h of cell adhesion, culture medium was added to each well and the plate was maintained in an incubator. After 1, 3 and 7 days, the seeded constructs and the culture medium were collected to perform the biological assays described below. As controls, untreated, activated, aminolysed and tropoelastin immobilized eTF scaffolds were prepared, as described before, and used throughout the cell culture without cells.

2.7.3. Metabolic activity

The MTS assay is a colorimetric method widely used to assess the metabolic activity. 3-(4,5-dimethylthiazol-2-yl)-5-(3-carboxymethoxyphenyl)-2-(4-sulfophenyl)-2H-tetrazolium (MTS) is a tetrazolium compound that is reduced by nicotinamide adenine dinucleotide (NADH) and nicotinamide adenine dinucleotide phosphate (NADPH) enzymes present in metabolically active cells. This reduction leads to the production of a brown formazan product, which is soluble in cell culture medium. The amount of formazan produced can be assayed colorimetrically, at 490 nm absorbance, which is directly proportional to the amount of living cells in culture [64].

At the defined time points, the metabolic activity of the endothelial cells seeded on untreated, activated, aminolysed and tropoelastin-immobilized eTF scaffolds was analyzed by the MTS assay (CellTiter 96® Aqueous One solution, Promega). Briefly, at each time point, the culture medium was removed and the samples were washed three times with Dulbecco's Phosphate Buffered Saline (DPBS; Life Technologies, USA). A mixture of culture medium, without phenol red and FBS, and MTS reagent (5:1 ratio) was prepared and added to each sample, as well as to the negative control with no cells or samples, in triplicate for 3h at 37°C in a humidified 5% CO₂ atmosphere. Afterwards, the absorbance of the MTS medium of each sample was read in triplicate at 490 nm in a microplate reader (Synergy, HT, Bio-TEK). The absorbance of each sample was subtracted to the absorbance of its corresponding negative control.

2.7.4. Cell proliferation

The assessment of the cell proliferation is essential in several biological studies, being an important indicator of the cells health. Fluorochromes that interact with DNA are commonly used to measure the amount of cells by quantifying their DNA [65]. The cell proliferation was assessed using a fluorimetric quantification Kit (Quant-iT™, PicoGreen®, Molecular Probes, Invitrogen, USA). PicoGreen is a fluorescence dye that binds specifically to double-stranded DNA (dsDNA). When bound to dsDNA, the dye is excited at 480 nm and emits at 520 nm [65].

After each time point, the samples were washed three times with DPBS and the adhered cells were lysed by thermal and osmotic shock. As such, these samples were transferred to eppendorfs tubes containing 1 mL of ultrapure water (Milli-Q Direct 16, Millipore) which were further placed inside a water bath at 37°C for 1h and, then, stored at -80°C until further use. Before starting the DNA quantification, the samples were left to thaw at room temperature and placed in an ultrasound bath for 15 min to remove all cell content.

The reagents from the kit were prepared according to the manufacturer's instructions. The DNA standards, provided by the kit, were prepared in ultrapure water at concentrations ranging from 0 to 2 µg/mL for the standard curve. In each well of a white opaque 96-wells plate, 28.7 µL of sample or standard (n=3), 71.3 µL of PicoGreen solution and 100 µL of TE buffer were added. Additionally, 28.7 µL of controls (samples with no cells) were used as negative control for DNA quantification. The plates were incubated in the dark for 10 min and, then, the fluorescence was read in a microplate reader (Synergy, HT, Bio-TEK) with an excitation wavelength of 485/20 nm and emission wavelength of 528/20 nm. The DNA concentration of each sample was calculated from the standard curve, which relates the DNA concentration with the fluorescence intensity. The results from controls with no cells of each testing condition were further subtracted to the ones with cells. Also, the samples were diluted accordingly to fit within the standard curve.

2.7.5. Total Protein synthesis

The amount of protein synthesized by the cells was assessed using the same lysates prepared for the cell proliferation assay. For the quantification of total protein, the MicroBCA™ Protein Assay Kit (Pierce, Thermo Scientific) was used. The assay was performed according to the manufacturer's protocol. Briefly, the standards were prepared at concentrations ranging from 0 to 40 µg/mL in ultrapure water. In each well of a 96-well plate, 150 µL of samples or standards, and 150 µL of working reagent were added. The plate was sealed and incubated for 2h at 37°C. After

the incubation time, the plate was left to cool at room temperature and, then, the absorbance was measured at 562 nm in a microplate reader (Synergy HT, Bio-Tek). The protein concentration of each sample was calculated from the standard curve which relates the protein (Bovine Serum Albumin) concentration with the absorbance intensity. Since there is already protein immobilized in certain conditions and knowing that proteins from cell culture medium may adhere to the activated and aminolysed substrates, the negative controls were also assayed as for the other samples. As a result, the amount of protein detected in each negative control was subtracted to the amount of protein of its corresponding testing condition.

2.7.6. Soluble VEGF quantification

Vascular Endothelial Growth factor (VEGF) is a protein produced by endothelial cells which regulates the angiogenesis [66]. As such, the production of this protein by endothelial cells was quantified by performing an enzyme-linked immunosorbent assay (ELISA) on the culture medium collected at each time point for each condition. For this purpose, a Human VEGF DuoSet ELISA kit (R&D Systems, USA) was used. The assay was performed according to the manufacturer's indications as well as the preparation of the reagents. The washing buffer was prepared by dissolving 0,05% Tween 20 (Sigma-Aldrich, USA) in DPBS solution previously filtered. The washing steps were performed manually three times. The blocking buffer was prepared by diluting a reagent diluent concentrate (R&D Systems, USA) in filtered ultrapure water. The stop solution was 2N sulfuric acid (Sigma-Aldrich, USA) in ultrapure water.

Briefly, the wells of Nunc MaxiSorp 96-well plate (Thermo-Fisher, USA) were coated with 100 μ L of capture antibody, overnight at room temperature. The wells were washed three times with 400 μ L of wash buffer and, then, 300 μ L of blocking buffer was incubated for 1h. The wells were again washed three times and 100 μ L of standards diluted in cell culture medium, at concentrations ranging from 0 to 2000 pg/mL, and samples with unknown VEGF concentration were added to the coated wells, in duplicate for 2h, at room temperature. This time allowed for the antigen from the samples bind to the immobilized antibody at the bottom of the wells. After the incubation, a washing step was performed and 100 μ L of detection antibody was added to the wells for 2 hours more to bind to the captured antigen. Afterwards, the wells were again washed and Streptavidin-HRP was added for 20 min, protected from light. After this washing step, 100 μ L of substrate solution composed of a 1:1 mix of color reagent A and color reagent B from the kit was added to each well and incubated for 20 min. To complete the procedure, 50 μ L of stop

solution was added to each well and the absorbance was immediately read on a microplate reader at 450nm and 540nm. Then, the 540nm absorbance was subtracted to 450nm for correction of optical imperfections in the plate.

2.7.7. Cells morphology

At the defined time points, the samples were washed three times with DPBS and 1mL of 2.5% glutaraldehyde (VWR, USA) solution in PBS was added to each well, to fix the cells. The samples were left in the fixation solution at 4°C, until further use. The specimens were then dehydrated with an increasing concentration series of ethanol solutions (10, 20, 30, 40, 50, 60, 70, 80, 90 and 100%). Briefly, 1 mL of each solution was added to the samples for 30 min at room temperature. After the last ethanol solution, the sample was left to dry overnight. Afterwards, the samples were mounted in copper stubs and sputter-coated with gold for SEM analysis. SEM was used to assess the cell distribution and morphology at 250x and 1000x magnifications.

2.7.8. Immunocytochemistry

To assess the maintenance of endothelial cell phenotype, the expression of CD31 by endothelial cells seeded on the scaffolds was analyzed. CD31 is a transmembrane glycoprotein, belonging to the immunoglobulin family, which is also designed as PECAM-1 (Platelet Endothelial Cell Adhesion Molecule). This protein is present at the surface of platelets, monocytes and macrophages, and it is a component of the endothelial intercellular junction. CD31 plays an important role in the adhesion between endothelial cells during angiogenesis and, thus, it is recognized for its angiogenic role [67].

After each time point, the samples were washed three times with PBS and fixed with 1mL of 10% formalin (Thermo Fisher Scientific, USA) for 20 min at room temperature. After the fixation time, the samples were washed three times with PBS and left in PBS solution at 4°C, until further analysis. The seeded constructs were permeabilized with 0.01% Triton (Fisher Scientific, USA) in PBS for 5 min. Afterwards, the specimens were washed three times with PBS, 5 min each. Then, 3% BSA (Sigma-Aldrich, USA) in PBS was used to block unspecific binding sites and incubated for 30 min at room temperature. After this, the samples were incubated overnight with primary antibody against human CD31 in PBS (1:100) (Abcam, UK), in a humid environment at 4°C. After the incubation time, the constructs were washed with PBS, as described before. A secondary antibody was used to bind to the anti-CD31 antibody, alexa fluor 488 in PBS (1:200)

(ThermoFisher, USA) was incubated for 1h at room temperature, protected from light. The washing step was performed again and DAPI in PBS (1:5000) was incubated for 1 min, protected from light, to stain the cell nuclei. The samples were analyzed by fluorescent microscopy (Zeiss, Germany) at 20x magnification.

2.8 Statistical analysis

Statistical analysis was performed using the SPSS statistic software (release 24.0.0.0 for Mac). First, a Shapiro-Wilk test was used to ascertain the data normality and Levene test for the homogeneity of variances. For all quantitative data, except for NH₂ groups quantification, the normality and variance homogeneity were rejected and non-parametric tests were used (Kruskal-Wallis test followed by Tukey's HSD test). P values lower than 0.01 were considered statistically significant and the results were expressed as median \pm interquartile range. NH₂ groups quantification data followed a normal distribution and the comparison of the mean values was performed by one-way ANOVA tests followed by Tukey's HSD test for multiple comparisons. P values lower than 0.05 were considered statistically significant and the results were expressed as mean \pm standard deviation.

2.9 References

- [1] D.E. Perrin, J.P. English, Polycaprolactone, in: A. Domb, J. Kost, D. Wiseman (Eds.), *Handb. Biodegrad. Polym.*, CRC Press, Amsterdam, Netherlands, 1997: pp. 63–77.
- [2] I. Engelberg, J. Kohn, Physico-mechanical properties of degradable polymers used in medical applications : a comparative study, *Biomaterials*. 12 (1991) 292–304.
- [3] M.S. Roby, J. Kennedy, Application of Materials in Medicine, Biology, and Artificial Organs, in: R. Buddy, H. Allan, F. Schoen, J. Lemons (Eds.), *Biomater. Sci. An Introd. to Mater. Med.*, 2004: pp. 615–629.
- [4] C.G. Pitt, Poly- ϵ -Caprolactone and Its Copolymers, in: M. Chasin, R. Langer (Eds.), *Biodegrad. Polym. as Drug Deliv. Syst.*, Marcel Dekker, Inc., 1990: pp. 71–121.
- [5] J.F. Piai, M.A. da Silva, A. Martins, A.B. Torres, S. Faria, R.L. Reis, E.C. Muniz, N.M. Neves, Chondroitin sulfate immobilization at the surface of electrospun nanofiber meshes for cartilage tissue regeneration approaches, *Appl. Surf. Sci.* 403 (2017) 112–125.
- [6] J. V. Araujo, A. Martins, I.B. Leonor, E.D. Pinho, R.L. Reis, N.M. Neves, Surface controlled biomimetic coating of polycaprolactone nanofiber meshes to be used as bone extracellular matrix analogues, *J. Biomater. Sci. Polym. Ed.* 19 (2008) 1261–1278.
- [7] B. Nottelet, E. Pektok, D. Mandracchia, J.C. Tille, B. Walpoth, R. Gurny, M. Möller, Factorial design optimization and in vivo feasibility of poly(ϵ -caprolactone)-micro- and nanofiber-based small diameter vascular grafts, *J. Biomed. Mater. Res. - Part A*. 89 (2009) 865–875.
- [8] S. Jin, J. Liu, S. Heang, S. Soker, A. Atala, J.J. Yoo, Development of a composite vascular scaffolding system that withstands physiological vascular conditions, *Biomaterials*. 29 (2008) 2891–2898.
- [9] S.G. Wise, M.J. Byrom, A. Waterhouse, P.G. Bannon, M.K.C. Ng, A.S. Weiss, A multilayered synthetic human elastin / polycaprolactone hybrid vascular graft with tailored mechanical properties, *Acta Biomater.* 7 (2011) 295–303.
- [10] A. Cipitria, A. Skelton, T.R. Dargaville, P.D. Dalton, D.W. Hutmacher, Design, fabrication and characterization of PCL electrospun scaffolds—a review, *J. Mater. Chem.* 21 (2011) 9419.

- [11] S. de Valence, J.C. Tille, D. Mugnai, W. Mrowczynski, R. Gurny, M. Möller, B.H. Walpoth, Long term performance of polycaprolactone vascular grafts in a rat abdominal aorta replacement model, *Biomaterials*. 33 (2012) 38–47.
- [12] Z. Ma, W. He, T. Yong, S. Ramakrishna, Grafting of gelatin on electrospun poly(caprolactone) nanofibers to improve endothelial cell spreading and proliferation and to control cell orientation, *Tissue Eng.* 11 (2005) 1149–58.
- [13] S. Singh, B.M. Wu, J.C.Y. Dunn, The enhancement of VEGF-mediated angiogenesis by polycaprolactone scaffolds with surface cross-linked heparin, *Biomaterials*. 32 (2011) 2059–2069.
- [14] Y. Zhu, Y. Cao, J. Pan, Y. Liu, Macro-alignment of electrospun fibers for vascular tissue engineering, *J. Biomed. Mater. Res. - Part B Appl. Biomater.* 92 (2010) 508–516.
- [15] M. Richard, R. Black, C. Kielty, PCL – PU composite vascular scaffold production for vascular tissue engineering : Attachment , proliferation and bioactivity of human vascular endothelial cells, *Biomaterials*. 27 (2006) 3608–3616.
- [16] R.O. Hynes, Extracellular matrix: not just pretty fibrils, *Science*. 326 (2009) 1216–1219.
- [17] S.M. Mithieux, S.G. Wise, A.S. Weiss, Tropoelastin – A multifaceted naturally smart material, *Adv. Drug Deliv. Rev.* 65 (2013) 421–428.
- [18] S. Landau, A.A. Szklanny, G.C. Yeo, Y. Shandalov, E. Kosobrodova, A.S. Weiss, S. Levenberg, Tropoelastin coated PLLA-PLGA scaffolds promote vascular network formation, *Biomaterials*. 122 (2017) 72–82.
- [19] B. Vrhovski, A.S. Weiss, Biochemistry of tropoelastin, *Eur. J. Biochem.* 8 (1998) 1–18.
- [20] D. V Bax, U.R. Rodgers, M.M.M. Bilek, A.S. Weiss, Cell Adhesion to Tropoelastin Is Mediated via the C-terminal GRKRK Motif and Integrin $\alpha\beta_3$, *J. Biol. Chem.* 284 (2009) 28616–28623.
- [21] G.C. Yeo, A. Kondyurin, E. Kosobrodova, S. Weiss, M.M.M. Bilek, A sterilizable , biocompatible , tropoelastin surface coating immobilized by energetic ion activation, *J. R. Soc. Interface.* 14 (2017).
- [22] R. Ulijn, D. Woolfson, J.F. Almine, D. V Bax, S.M. Mithieux, L. Nivison-smith, J. Rnjak, A.

- Waterhouse, S.G. Wise, A.S. Weiss, Elastin-based materials, *Chem. Soc. Rev.* 39 (2010) 3371–3379.
- [23] S.P. Vyas, B. Vaidya, Targeted delivery of thrombolytic agents: role of integrin receptors, *Expert Opin. Drug Deliv.* 6 (2009) 499–508.
- [24] D. V. Bax, A. Kondyurin, A. Waterhouse, D.R. McKenzie, A.S. Weiss, M.M.M. Bilek, Surface plasma modification and tropoelastin coating of a polyurethane co-polymer for enhanced cell attachment and reduced thrombogenicity, *Biomaterials.* 35 (2014) 6797–6809.
- [25] A. Waterhouse, Y. Yin, S.G. Wise, D. V. Bax, D.R. McKenzie, M.M.M. Bilek, A.S. Weiss, M.K.C. Ng, The immobilization of recombinant human tropoelastin on metals using a plasma-activated coating to improve the biocompatibility of coronary stents, *Biomaterials.* 31 (2010) 8332–8340.
- [26] I. Kondyurina, S.G. Wise, A.K.Y. Ngo, E.C. Filipe, A. Kondyurin, A.S. Weiss, S. Bao, M.M.M. Bilek, Plasma mediated protein immobilisation enhances the vascular compatibility of polyurethane with tissue matched mechanical properties, *Biomed. Mater.* 12 (2017) 45002.
- [27] S.G. Wise, H. Liu, A. Kondyurin, M.J. Byrom, P.G. Bannon, G.A. Edwards, A.S. Weiss, S. Bao, M.M. Bilek, Plasma Ion Activated Expanded Polytetrafluoroethylene Vascular Grafts with a Covalently Immobilized Recombinant Human Tropoelastin Coating Reducing Neointimal Hyperplasia, *ACS Biomater. Sci. Eng.* 2 (2016) 1286–1297.
- [28] A. Martins, J. V Araújo, R.L. Reis, N.M. Neves, Electrospun nanostructured scaffolds for tissue engineering applications, *Nanomedicine (Lond).* 2 (2007) 929–942.
- [29] K.T. Shalumon, P.R. Sreerekha, D. Sathish, H. Tamura, S. V. Nair, K.P. Chennazhi, R. Jayakumar, Hierarchically designed electrospun tubular scaffolds for cardiovascular applications, *J. Biomed. Nanotechnol.* 7 (2011) 609–620.
- [30] H.Y. Mi, X. Jing, E. Yu, X. Wang, Q. Li, L.S. Turng, Manipulating the structure and mechanical properties of thermoplastic polyurethane/polycaprolactone hybrid small diameter vascular scaffolds fabricated via electrospinning using an assembled rotating collector, *J. Mech. Behav. Biomed. Mater.* 78 (2018) 433–441.
- [31] Y. Elsayed, C. Lekakou, F. Labeed, P. Tomlins, Fabrication and characterisation of

- biomimetic , electrospun gelatin fibre scaffolds for tunica media-equivalent , tissue engineered vascular grafts, *Mater. Sci. Eng. C.* 61 (2016) 473–483.
- [32] A. Martins, R.L. Reis, N.M. Neves, Electrospinning: processing technique for tissue engineering scaffolding, *Int. Mater. Rev.* 53 (2008) 257–274.
- [33] R.G. Flemming, C.J. Murphy, G.A. Abrams, S.L. Goodman, P.F. Nealey, Effects of synthetic micro- and nano-structured surfaces on cell behavior, *Biomaterials.* 20 (1999) 573–588.
- [34] J. Hendriks, J. Riesle, C.A. van Blitterswijk, Vascular tissue engineering of small-diameter blood vessels: reviewing the electrospinning approach, *J. Tissue Eng. Regen. Med.* 9 (2015) 861–888.
- [35] A. Martins, N.M. Neves, R.L. Reis, Critical Aspects of Electrospun Meshes for Biomedical Applications, in: N.M. Neves (Ed.), *Electrospinning Adv. Biomed. Appl. Ther., Ltd, Smith, UK, 2012: pp. 69–87.*
- [36] A. Hasan, A. Memic, N. Annabi, M. Hossain, A. Paul, M.R. Dokmeci, F. Dehghani, A. Khademhosseini, Electrospun scaffolds for tissue engineering of vascular grafts, *Acta Biomater.* 10 (2014) 11–25.
- [37] N. Bhardwaj, S.C. Kundu, Electrospinning: A fascinating fiber fabrication technique, *Biotechnol. Adv.* 28 (2010) 325–347.
- [38] A. Martins, E.D. Pinho, S. Faria, I. Pashkuleva, A.P. Marques, R.L. Reis, N.M. Neves, Surface modification of electrospun polycaprolactone nanofiber meshes by plasma treatment to enhance biological performance, *Small.* 5 (2009) 1195–1206.
- [39] C. Oliveira, A.R. Costa-pinto, R.L. Reis, A. Martins, N.M. Neves, Biofunctional Nanofibrous Substrate Comprising Immobilized 2 Antibodies and Selective Binding of Autologous Growth Factors, *Biomacromolecules.* 15 (2014) 2196–205.
- [40] S. Regis, S. Youssefian, M. Jassal, M.D. Phaneuf, N. Rahbar, S. Bhowmick, Fibronectin adsorption on functionalized electrospun polycaprolactone scaffolds: Experimental and molecular dynamics studies, *J. Biomed. Mater. Res. - Part A.* 102 (2014) 1697–1706.
- [41] N. Monteiro, A. Martins, R. Pires, S. Faria, N.A. Fonseca, J. Moreira, R.L. Reis, N.M. Neves, Immobilization of bioactive factor-loaded liposomes on the surface of electrospun nanofibers targeting tissue engineering, *Biomater. Sci.* 2 (2014) 1195–1209.

- [42] K. Wulf, M. Teske, M. Löbler, F. Luderer, K.P. Schmitz, K. Sternberg, Surface functionalization of poly(ϵ -caprolactone) improves its biocompatibility as scaffold material for bioartificial vessel prostheses, *J. Biomed. Mater. Res. - Part B Appl. Biomater.* 98 B (2011) 89–100.
- [43] H.S. Yoo, T.G. Kim, T.G. Park, Surface-functionalized electrospun nanofibers for tissue engineering and drug delivery, *Adv. Drug Deliv. Rev.* 61 (2009) 1033–1042.
- [44] Y. Zhu, C. Gao, X. Liu, J. Shen, Surface modification of polycaprolactone membrane via aminolysis and biomacromolecule immobilization for promoting cytocompatibility of human endothelial cells, *Biomacromolecules.* 3 (2002) 1312–1319.
- [45] H.S. Yu, J.H. Jang, T. Il Kim, H.H. Lee, H.W. Kim, Apatite-mineralized polycaprolactone nanofibrous web as a bone tissue regeneration substrate, *J. Biomed. Mater. Res. - Part A.* 88 (2009) 747–754.
- [46] F. Chen, C.N. Lee, S.H. Teoh, Nanofibrous modification on ultra-thin poly(ϵ -caprolactone) membrane via electrospinning, *Mater. Sci. Eng. C.* 27 (2007) 325–332.
- [47] P.E. Tyllianakis, S.E. Kakabakos, G.P. Evangelatos, Colorimetric Determination of Reactive Primary Amino Groups of Macro- and Microsolid Supports, *Appl. Biochem. Biotechnol.* 38 (1993) 15–25.
- [48] B. Gu, D.J. Burgess, *Polymeric Materials in Drug Delivery*, in: S.G. Kumbar, C.T. Laurencin, M. Deng (Eds.), *Nat. Synth. Biomed. Polym.*, Elsevier Inc., 2014: pp. 333–349.
- [49] A. Polini, F. Yang, *Physicochemical characterization of nanofiber composites*, in: M. Ramalingam, S. Ramakrishna (Eds.), *Nanofiber Compos. Biomed. Appl.*, Elsevier Ltd, 2017: pp. 97–115.
- [50] N.A. Hotaling, K. Bharti, H. Kriel, C.G. Simon, DiameterJ: A Validated Open Source Nanofiber Diameter Measurement Tool, *Biomaterials.* 61 (2015) 327–338.
- [51] D. Roylance, *Uniaxial Mechanical Response*, in: *Mech. Prop. Mater.*, 2008: pp. 5–23.
- [52] E. Carew, F. Cooke, J. Lemons, B. Ratner, I. Vesely, E. Vogler, *Properties of Materials*, in: R. Buddy, H. Allan, F. Schoen, J. Lemons (Eds.), *Biomater. Sci. An Introd. to Mater. Med.*, 2004: pp. 26–30.

- [53] A. International, Introduction to Tensile Testing, in: J.R. Davis (Ed.), Tensile Test., 2004: pp. 1–12.
- [54] S.L. Martin, B. Vrhovski, A.S. Weiss, Total synthesis and expression in *Escherichia coli* of a gene encoding human tropoelastin, *Gene*. 154 (1995) 159–166.
- [55] M.J.E. Fischer, Amine Coupling Through EDC / NHS : A Practical Approach, in: Surf. Plasmon Reson. Methods Mol. Biol. (Methods Protoc., 2010: pp. 55–73.
- [56] A.K. Mallia, M.D. Frovenzano, E.K. Fujimoto, B.J. Olson, D.C. Klenk, P.C. Company, Measurement of Protein Using Bicinchoninic Acid, *Anal. Biochem.* 85 (1985) 76–85.
- [57] K. Cai, M. Frant, G. Hildebrand, K. Liefeth, K.D. Jandt, Surface functionalized titanium thin films : Zeta-potential , protein adsorption and cell proliferation, *Colloids Surfaces B Interfaces*. 50 (2006) 1–8.
- [58] D. Cho, S. Lee, M.W. Frey, Characterizing zeta potential of functional nanofibers in a microfluidic device, *J. Colloid Interface Sci.* 372 (2012) 252–260.
- [59] G. Kaur, J.M. Dufour, Cell lines, *Spermatogenesis*. 5562 (2012) 1–5.
- [60] G.A.P. Hospers, C. Meijer, G. Molema, N.H. Mulder, Endothelium in vitro : A review of human vascular endothelial cell lines for blood vessel-related research, *Angiogenesis*. 4 (2001) 91–102.
- [61] A. Abdal-hay, A. Memic, K.H. Hussein, Y. Seul, M. Fouad, F.F. Al-jassir, H. Woo, Y. Morsi, Rapid fabrication of highly porous and biocompatible composite textile tubular scaffold for vascular tissue engineering, *Eur. Polym. J.* 96 (2017) 27–43.
- [62] M. Neufurth, X. Wang, E. Tolba, B. Dorweiler, Modular Small Diameter Vascular Grafts with Bioactive Functionalities, *PLoS One*. 10 (2015) 1–24.
- [63] D. Palmieri, M. Mura, S. Mambrini, D. Palombo, Effects of Pleiotrophin on endothelial and inflammatory cells : Pro-angiogenic and anti-inflammatory properties and potential role for vascular bio-prosthesis endothelialization, *Adv. Med. Sci.* 60 (2015) 287–293.
- [64] D.D. Dunigan, S.B. Waters, T.C. Owen, S. Florida, E.F. Avenue, Aqueous soluble tetrazolium / formazan MTS as an indicator of NADH- and NADPH-dependent dehydrogenase activity, *Biotechniques*. 19 (1995) 640–649.

- [65] S.J. Ahn, J. Costa, J.R. Emanuel, PicoGreen quantitation of DNA : effective evaluation of samples pre- or post-PCR, *Nucleic Acids Res.* 24 (1996) 2623–2625.
- [66] J. Vernes, Y.G. Meng, Detection and Quantification of VEGF Isoforms by ELISA, *Methods Mol. Biol.* 1332 (2015) 25–37.
- [67] M.P. Pusztaszeri, W. Seelentag, F.T. Bosman, Immunohistochemical Expression of Endothelial Markers CD31 , CD34 , von Willebrand Factor , and Fli-1 in Normal Human Tissues, *J. Histochem. Cytochem.* 54 (2006) 385–395.

CHAPTER III.

Tubular fibrous scaffold functionalized
with tropoelastin as a small-diameter
vascular graft

Chapter III. Tubular fibrous scaffold functionalized with tropoelastin as a small-diameter vascular graft

3.1 Abstract

Cardiovascular disorders, such as coronary artery diseases, are one of the major healthcare problems in today's society. The clinically available synthetic vascular grafts exhibit thrombogenic behaviour and could induce intimal hyperplasia when used to restore small-diameter blood vessels ($\varnothing < 6\text{mm}$). Rapid endothelialization and matched mechanical properties are two major requirements that should be considered when designing functional vascular grafts.

Herein, an electrospun tubular fibrous (eTF) scaffold made of polycaprolactone was functionalized to immobilize tropoelastin at the luminal surface, providing a biomimetic environment of a small-diameter blood vessel. The luminal surface comprised a mix of micro to submicro fibers and its functionalization was confirmed by an increase of the zeta potential and by the insertion of NH_2 groups. Tropoelastin was immobilized at $20 \mu\text{g/mL}$ via its $-\text{NH}_2$ and $-\text{COOH}$ groups at the activated or aminolysed eTF scaffolds, respectively, to study the effect of exposed functional groups over human endothelial cells (ECs) behaviour. Tensile properties demonstrated that functionalized eTF scaffolds presented strength and stiffness within the range of those of native blood vessels. Tropoelastin immobilized on activated eTF scaffolds promoted higher metabolic activity and proliferation of ECs, whereas when immobilized on aminolysed eTF scaffolds a significantly higher protein synthesis was observed. The developed biofunctional eTF scaffolds are a promising small-diameter vascular graft which is able to promote a rapid endothelialization and have mechanical properties compatible with this demanding application.

Keywords: Electrospinning, Tissue-engineered vascular graft, Biofunctionalization, Tropoelastin, Mechanical properties, Endothelialization.

3.2 Introduction

Diseases of the cardiovascular system are the major causes of morbidity and mortality worldwide. Coronary heart disease is mainly caused by atherosclerotic changes in the walls of coronary arteries which can narrow the vessel enough to impair the blood flow and the oxygen supply to cardiac muscle [1]. In severe cases, a coronary artery bypass graft (CABG) surgery is performed, using a portion of a healthy vessel such as the saphenous vein and the internal mammary artery [2]. These autologous substitutes are considered the gold standard in CABG surgery since they are viable, non-thrombogenic, biocompatible and have adequate patency. Nevertheless, the lack of non-affected autologous grafts in patients with vascular diseases and the need for an additional surgery, limit their use [1]. There are commercially available alternatives, namely, synthetic vascular grafts made of polyethylene terephthalate (PET) and expanded polytetrafluoroethylene (ePTFE). However, they tend to fail when applied in small-diameter blood vessels ($\varnothing < 6$ mm) due to their thrombogenic behaviour and mechanical mismatch, producing low patency [3]. Therefore, an ideal small-diameter vascular graft for these clinical situations is needed.

Tissue engineering is a multidisciplinary field, which principles have been applied to develop functional substitutes for blood vessels [4]. Most strategies are focused on the biological performance of these constructs, attempting to mimic the native structure and ECM composition. Examples of these grafts can be a vascular graft made of cell sheets wrapped around a tubular mandrel [5], obtained by decellularization of ECM synthesized by smooth muscle cells (SMCs) [6], or based on hydrogels with cells embedded in a matrix of biological proteins [7]. These approaches are quite complex and lack appropriate mechanical response.

Scaffolds composed of synthetic polymers are promising alternatives, owing to the ability to control their degradation and mechanical properties [8]. In fact, a durable biomaterial is required to withstand the physiological conditions without the risk of collapse or premature degradation until the formation of a new tissue *in vivo* [9,10]. Mechanical properties of human healthy blood vessels have been extensively reported in the literature, as illustrated in the Table 3. 1, which resumes the young 's modulus and maximum stress values measured for some native blood vessels. Therefore, these values can be used as target properties for the development of new and functional vascular grafts.

Table 3. 1 - Uniaxial tensile mechanical properties: Young 's modulus and maximum stress of some native human blood vessels

Native blood vessels	Young 's modulus (MPa)		Maximum stress (MPa)		Refs
	Axial	Radial	Axial	Radial	
Saphenous vein	23.7 ± 15	4.2 ± 3.3	6.3 ± 4.0	1.8 ± 0.8	[11]
	—	2.25	—	4	[8]
Left internal mammary artery	16.8 ± 7.1	8 ± 3.0	4.3 ± 1.8	4.1 ± 0.9	[11]
Coronary arteries	1.48 ± 0.24		1.44 ± 0.87		[12]
	1.4 ± 0.72		—		[13]
Ascending aortas	2.61 ± 0.26	3.25 ± 0.63	1.71 ± 0.14	1.80 ± 0.24	[14]

Electrospinning is frequently used to produce scaffolds with fiber diameters in the nano to micrometer range [15]. Since the natural ECM is composed of nanofibers, the electrospun scaffolds provide an ideal biomimetic substrate for the development of blood vessel substitutes [16]. Single or multilayer vascular grafts have been electrospun to mimic the native architecture of blood vessels, combining different materials [17–20]. Polycaprolactone (PCL) is a synthetic biodegradable polymer widely used to produce vascular conduits by electrospinning due to its suitable mechanical properties as strength and high elongation, and slow degradation kinetics [10,21]. The mechanical and biological response of electrospun PCL tubular scaffolds were investigated *in vivo*, demonstrating appropriate patency and faster endothelialization compared to ePTFE grafts [22]. Although PCL is well tolerated *in vivo*, its hydrophobicity may lead to platelet adhesion and, consequently, failure of the grafts [20].

The surface properties of scaffolds has been tailored to improve the hemocompatibility and the endothelialization of vascular grafts, without affecting their mechanical properties [23]. Binding ECM proteins to the surface of the scaffolds gained special interest since they mimic the natural cell environment, particularly, when using tropoelastin [24]. Tropoelastin, the soluble precursor of elastin, is a protein present in the vascular ECM which is secreted by the endothelial cells. Structurally, tropoelastin is asymmetric with two functional regions, C-terminal and N-terminal, which mediate several interactions at the cell surface, influencing their adhesion and proliferation [25]. Furthermore, tropoelastin presents lower thrombogenicity, minimal platelet adhesion and aggregation compared to other ECM proteins such as collagen and fibronectin [26,27]. Therefore, tropoelastin has been used as a coating on polymeric [28] and metallic [29] surfaces.

The present study aims at developing a biofunctional electrospun tubular fibrous (eTF) scaffold with adequate mechanical properties and capable of supporting endothelialization for

blood vessel grafts. Hence, tubular scaffolds will be produced by electrospinning and, further, biofunctionalized with tropoelastin to provide biochemical cues at their luminal surface. The mechanical response of eTF scaffolds, before and after surface treatments, will be assessed. Finally, by culturing an endothelial cell line (EA.hy926), the potential of these constructs to support endothelialization will be validated *in vitro*.

3.3 Materials and methods

3.3.1. Production of electrospun tubular fibrous scaffolds

A 15% PCL ($M_w = 80,000$; Sigma-Aldrich, USA) solution was prepared in a solvent mixture of chloroform and absolute ethanol (Fisher Scientific, UK) at a ratio of 7:3. The polymeric solution was loaded into a syringe connected to a metallic 21G needle. Fibers were electrospun at a voltage of 10 kV, using a needle tip-to-collector distance of 15 cm and a flow rate of 1.0 mL h^{-1} . A customized metallic rotating mandrel with 4 mm external diameter was used to collect the fibers, rotating at 200 rpm for the manufacture of the conduit. The electrospinning process was conducted for 1 h. The range of temperature and relative humidity used was $22^\circ\text{C} \pm 2$ and 35% - 42%, respectively. The electrospun tubular fibrous (eTF) scaffolds were, then, extracted from the mandrel and cut into squares of $1 \times 1 \text{ cm}^2$ for further assays.

3.3.2. Surface functionalization

The eTF scaffolds were, firstly, activated with 1M sodium hydroxide (NaOH; Fisher Scientific, UK) solution for 3h at room temperature. Afterwards, the activated substrates were washed with PBS and immersed in 4M hexamethylenediamine (HMD; Sigma-Aldrich, USA) solution in isopropyl alcohol (VWR Chemicals, USA) for 24h at 37°C to insert NH_2 groups at the surface.

3.3.2.1. Amine groups quantification

The amine groups (NH_2) inserted by the aminolysis reaction were quantified by the Ellman's reagent method [30]. Untreated, activated and aminolysed eTF scaffolds were incubated with PBS at $\text{pH}=7.27$, containing 20 mM 2-Iminoethanol (2-IT, Sigma-Aldrich, USA) and 20 mM 4-dimethylaminopyridine (DMAP, Thermo Fisher Scientific, USA) for 1h at 37°C , protected from light. Then, the scaffolds were thoroughly washed with each one of the following solutions, sequentially: (1) PBS at $\text{pH} = 7.27$; (2) ultrapure water containing 1 mM dithiothreitol (DTT, abcr GmbH, Germany) and 10 mM Ethylenediaminetetraacetic acid (EDTA; Sigma-Aldrich, USA) at $\text{pH}=7$; (3) ultrapure water containing 1 M sodium chloride (NaCl; Panreac Quimica, Spain) and 10 mM EDTA at $\text{pH}=7$; (4) PBS containing 1mM EDTA at $\text{pH} = 7.27$. Afterwards, the constructs were incubated with 0.1 mM 5,5'-dithiobis-2-nitrobenzoic acid (DTNB, Ellman's reagent; Sigma-Aldrich, USA) solution in PBS at $\text{pH}=7.27$ for 1h at 37°C , protected from light. After the Ellman's reagent incubation, 150 μL of each sample was transferred to a quartz 96 well plate in triplicate and the

absorbance was read at 412 nm in a microplate reader (Synergy, HT, Bio-TEK) using DTNB solution alone as blank. Controls of each condition (untreated, activated and aminolysed) were used in triplicates where only the first step (i.e. 2-IT incubation) was eliminated, using PBS instead. The quantification of amine groups of each sample was calculated using the TNB² molar absorption coefficient value of 14,150 M⁻¹ cm⁻¹ [30].

3.3.3. Scaffolds characterization

3.3.3.1. Scanning Electron Microscopy

The eTF scaffolds were frozen in liquid nitrogen and cut to obtain a clean cross-section surface. Also, the luminal surfaces, before and after the activation and aminolysis, were sputter-coated with gold (Cressington, model 108A) for 2 min at 15 mA and analysed by SEM (JSM-6010 LV, JEOL, Japan) with an acceleration voltage of 5-10 kV. The magnification used was 500x and 1000x.

SEM micrographs (10 images) of the cross-section surface at x150 magnification were used and at least 3 measures were performed to assess the scaffold thickness. Also, at least 6 images of luminal surfaces at 1000x magnification (before and after surface treatments) were used to assess the fiber features. This characterization was performed using the plug-in DiameterJ created for the software ImageJ (National Institute of Health, USA), according to the literature [31]. As outputs, the algorithm produces histograms of fiber diameters and orientation, as well as information about pore area, pore size and porosity.

3.3.3.2. Uniaxial tensile properties

Since a dimension of 18 mm in length of the specimens was required, the 4 mm diameter scaffolds did not present enough perimeter along radial direction (~12 mm). Therefore, 6 mm internal diameter tubular scaffolds were produced using a custom rotating collector with 6 mm external diameter. The 6 mm internal diameter tubular scaffolds were cut into strips (18x5 mm) along their radial or axial directions. The thickness of the specimens was measured at three different points using a digital micrometer (Mitutoyo, Japan). At least 7 specimens in each radial and axial direction were tested before and after the activation and aminolysis reaction, under dry and hydrated conditions, at room temperature. Uniaxial tensile properties were measured using a universal mechanical testing equipment (Model 5543, INSTRON, UK) equipped with a 1kN load cell. A cross-head speed of 2 mm/min and a 10 mm gauge length were used. The mechanical

tests were performed until complete fracture of the specimen. Load and displacement measurements were acquired, and tensile stress and strain were calculated from the raw data. A linear regression of the maximum linear region from stress-strain curves was used to calculate the Young's modulus. Maximum stress and strain at maximum stress were considered as the maximum stress value and its corresponding strain value before failure.

3.3.4. Tropoelastin immobilization at luminal surface

Human recombinant tropoelastin was produced at the Weiss Lab (The University of Sydney, Australia) by an *Escherichia coli* expression system [32]. Briefly, tropoelastin was immobilized at the luminal surface of activated and aminolysed eTF scaffolds by a covalent bond mediated by a coupling agent, 1-Ethyl-3-[3-dimethylaminopropyl]carbodiimide hydrochloride (EDC)/hydroxysuccinimide (NHS) (Sigma-Aldrich Aldrich, USA). Specifically, 50 mM EDC and 200 mM NHS mixture (1:4 ratio) was prepared in 0.1 M 2-N-morpholino (ethanesulfonic acid hydrate) buffer (MES; Sigma-Aldrich-Aldrich, USA) with 0.9% (w/w) NaCl at pH=4.7. Next, 500 μ L of tropoelastin solution in PBS (Sigma-Aldrich, USA) was mixed with 1% (v/v) of EDC/NHS solution 15 min for protein activation and, further, incubated with activated and aminolysed substrates for 2h at room temperature, under gentle stirring.

3.3.5. Chemical characterization of biofunctionalized scaffolds

3.3.5.1. Optimization of tropoelastin immobilization

To ensure that eTF scaffolds were used at their maximum immobilization capacity, several tropoelastin concentrations ranging from 5 to 20 μ g/mL were used and incubated with activated and aminolysed eTF scaffolds. The MicroBCA™ Protein Assay Kit (Pierce, Thermo Scientific) was used to detect the amount of immobilized tropoelastin at the eTF scaffolds surface, in duplicate. After tropoelastin immobilization, activated and aminolysed eTF scaffolds were washed three times with PBS, 5 min each. Then, 150 μ L of working reagent was added with 150 μ L of PBS directly to the eTF scaffolds for 2h at 37°C. The working reagent was prepared according to the manufacture's instructions. After the incubation time, 300 μ L of the solution that reacted with the eTF scaffolds was transferred to a 96-well plate and the absorbance was read at 562 nm, using a microplate reader (Synergy, HT, Bio-TEK). The concentration of immobilized tropoelastin was

interpolated from the standard curve with values ranging from 0 $\mu\text{g}/\text{mL}$ to 20 $\mu\text{g}/\text{mL}$. The assay was performed independently five times.

3.3.5.2. Surface charge properties

Zeta potential, denoted as ζ , of eTF scaffolds was measured using the SurPASS electrokinetic analyser (Anton Paar GmbH, Austria). Untreated, activated, aminolysed and tropoelastin immobilized eTF scaffolds were cut in 12 cm^2 disks and placed in an adjustable disk gap cell (14mm), with an adjusted gap of 115 μm . The streaming currents were detected by the Ag/AgCl electrodes at different pH values within the range of 6.0 to 10. An electrolyte solution of 1 mM potassium chloride (KCl; VWR, USA) was flushed through the cell with a pressure of 400 mbar and the pH was automatically adjusted by adding 0.05 M NaOH to the electrolyte solution. The data was recorded and analysed using the software Attract 2.0.

3.3.6. Cell biology assays

3.3.6.1. Cell culture and seeding

A human umbilical vein endothelial cell line (EA.hy926; LGC Standards, Spain) was used to assess the endothelialization of the developed eTF scaffolds, as reported by other authors [33,34]. ECs were cultured in Dulbecco 's Modified Eagle Medium (DMEM; Sigma-Aldrich-Aldrich, USA) low glucose supplemented with 10% Fetal Bovine Serum (FBS; Life Technologies, USA) and 1% antibiotic/antimycotic (A/A; Life Technologies, USA) and incubated at 37°C in a humidified 5% CO_2 atmosphere. ECs cells were used within passages 10-18. Medium was changed every 2-3 days until a 90% confluency was reached.

The eTF scaffolds were sterilized by UV light for 30 min, on each side, inside a laminar flow chamber (PV-100, Telstar). Activation, aminolysis and tropoelastin immobilization were further performed under sterile conditions. The cell seeding was performed by dropping a cell suspension containing 100,000 cells on top of each substrate. After 4h of cell adhesion, culture medium was added to each sample and kept in the incubator. After 1, 3 and 7 days, the seeded constructs and the culture medium were collected for metabolic activity, cell proliferation, total protein synthesis, soluble VEGF production as well as for cell morphology and phenotype analysis. As negative controls of quantitative data, untreated, activated, aminolysed and tropoelastin immobilized eTF scaffolds were prepared, as described before, and tested throughout the cell culture experiment

without cells. All experiments were conducted in triplicates and repeated at least three times independently.

3.3.6.2. Metabolic activity

At the defined time points, the metabolic activity of the endothelial cells seeded on untreated, activated, aminolysed and tropoelastin-immobilized eTF scaffolds was analysed by the MTS assay (CellTiter 96® Aqueous One solution, Promega, USA). At each time point, the culture medium was removed and the samples were washed three times with sterile Dulbecco's Phosphate Buffered Saline (DPBS; Life Technologies, USA). A mixture of culture medium, without phenol red and FBS, and MTS reagent (5:1 ratio) was prepared and added to each sample, as well as to the negative controls and blank, in triplicate, for 3h at 37°C in a humidified 5% CO₂ atmosphere. Thereafter, the absorbance of the MTS medium of each sample was read in triplicate at 490 nm in a microplate reader (Synergy, HT, Bio-TEK). The absorbance of each sample was subtracted to the absorbance of its corresponding negative control.

3.3.6.3. Cell proliferation

After each time point, the samples were washed three times with sterile DPBS and transferred to eppendorf tubes containing 1 mL of ultrapure water (Milli-Q Direct 16, Millipore) which were further placed inside a water bath at 37°C for 1h and, then, stored at -80°C. Before starting the DNA quantification, the samples were left to thaw at room temperature and placed in an ultrasound bath for 15 min to remove all cell content from the scaffolds. The reagents from the kit were prepared according to the manufacturer's instructions. The DNA standards, provided by the Quant-iT™ PicoGreen® dsDNA assay Kit (Invitrogen, USA) were prepared in ultrapure water at concentrations ranging from 0 to 2 µg/mL for the standard curve. In each well of a white opaque 96-wells plate, 28.7 µL of samples, negative controls or standards (in triplicate), 71.3 µL of PicoGreen solution and 100 µL of TE buffer were added. The plates were incubated in the dark for 10 min and, then, the fluorescence was read in a microplate reader (Synergy, HT, Bio-TEK) with an excitation wavelength of 485/20 nm and emission wavelength of 528/20 nm. The results from negative controls of each testing condition were further subtracted to the ones with cells.

3.3.6.4. Total protein synthesis

The amount of synthesized protein by the cells was assessed using the same lysates prepared as described for the cell proliferation assay. For the quantification of total protein synthesis, the MicroBCA™ Protein Assay Kit was used. The assay was performed according to the manufacturer's protocol, using a standard curve ranging from 0 to 40 µg/mL in ultrapure water. The plate was incubated for 2h at 37°C and, then, the absorbance was measured at 562 nm in a microplate reader (Synergy HT, Bio-Tek). The negative controls were also assayed for a correct measure of total protein synthesis. Accordingly, the amount of protein detected in each negative control was subtracted to the amount of protein of its corresponding testing condition.

3.3.6.5. Soluble VEGF quantification

The expression of vascular endothelial growth factor (VEGF) by endothelial cells was quantified by performing an enzyme-linked immunosorbent assay (ELISA) on the cell culture medium collected at each time point for each condition. For this purpose, a Human VEGF DuoSet ELISA kit (R&D Systems, USA) was used. The assay was performed according to the manufacturer's indications, as well as the preparation of the reagents. All steps were performed at room temperature. The wash buffer was 0.05% Tween 20 (Sigma-Aldrich, USA) in filtered DPBS solution. The washing steps were performed manually three times. The blocking buffer (R&D Systems, USA) was diluted in filtered ultrapure water. The stop solution was 2N sulfuric acid (Sigma-Aldrich, USA) prepared in ultrapure water. The ELISA 96-well plate (Thermo-Fisher, USA) was coated with capture antibody, overnight, followed by the addition of blocking buffer for 1h. The standards and samples were then incubated, in duplicate, for 2h. After the incubation, the detection antibody was added to the wells for 2 hours. Afterwards, the Streptavidin-HRP was added for 20 min, protected from light and, then, substrate solution was incubated for 20 min. To complete the procedure, stop solution was added to each well and the absorbance was immediately read on a microplate reader at 450nm and 540nm. Then, the 540nm absorbance was subtracted to 450nm for correction of optical imperfections in the plate.

3.3.6.6. Cells morphology

At the defined time points, the samples were washed three times with sterile DPBS and fixed with a 2.5% glutaraldehyde (VWR, USA) solution in PBS. The constructs were then dehydrated with an increasing concentration series of ethanol solutions (10, 20, 30, 40, 50, 60, 70, 80, 90

and 100%) each for 30 min. After the last ethanol solution, the sample was left to dry overnight. Afterwards, the samples were mounted in copper stubs and sputter-coated with gold for SEM analysis. SEM was used to assess cell distribution and morphology at 250x and 1000x magnifications.

3.3.6.7. Immunocytochemistry

The expression of CD31 endothelial cell marker was analysed to assess the maintenance of the endothelial cell phenotype. After each time point, the samples were washed three times with PBS and fixed with 10% formalin (Thermo Fisher Scientific, USA) for 20 min. The seeded constructs were permeabilized with 0.01% Triton (Fisher Scientific, USA) in PBS for 5 min. Thereafter, the samples were washed three times with PBS, 5 min each, and blocked with 3% BSA (Sigma-Aldrich, USA) in PBS for 30 min at room temperature. Then, the samples were incubated with primary antibody against human CD31 in PBS (1:100) (Abcam, UK) overnight at 4°C. After the incubation, the constructs were washed with PBS and the secondary antibody, alexa fluor 488 in PBS (1:200) (Thermo Fisher, USA), was incubated for 1h at room temperature, protected from light. DAPI in PBS (1:5000) was incubated for 1 min, protected from light, to stain the cell nuclei. The samples were analyzed by fluorescent microscopy (Zeiss, Germany) at 20x magnification.

3.3.7. Statistical analysis

Statistical analysis was performed using the SPSS statistic software (release 24.0.0.0 for Mac). First, a Shapiro-Wilk test was used to ascertain about the data normality and Levene test for the homogeneity of variances. For all quantitative data, except for NH₂ groups quantification, the normality and variance homogeneity were rejected and non-parametric tests were used (Kruskal-Wallis test followed by Tukey's HSD test). P values lower than 0.01 were considered statistically significant and the results were expressed as median ± interquartile range. NH₂ groups quantification data followed a normal distribution and the comparison of the mean values was performed by one-way ANOVA tests followed by Tukey's HSD test for multiple comparisons. P values lower than 0.05 were considered statistically significant and the results were expressed as mean ± standard deviation.

3.4 Results

3.4.1. Scaffolds characterization

The tubular scaffolds produced by electrospinning had 10-15 cm in length with about 4 mm internal diameter (Figure 3. 1A and Figure 3. 1B). The SEM micrographs show the cross-section of the eTF scaffolds, having an average wall thickness of $240.85 \pm 46.91 \mu\text{m}$ (Figure 3. 1C and Figure 3. 1D).

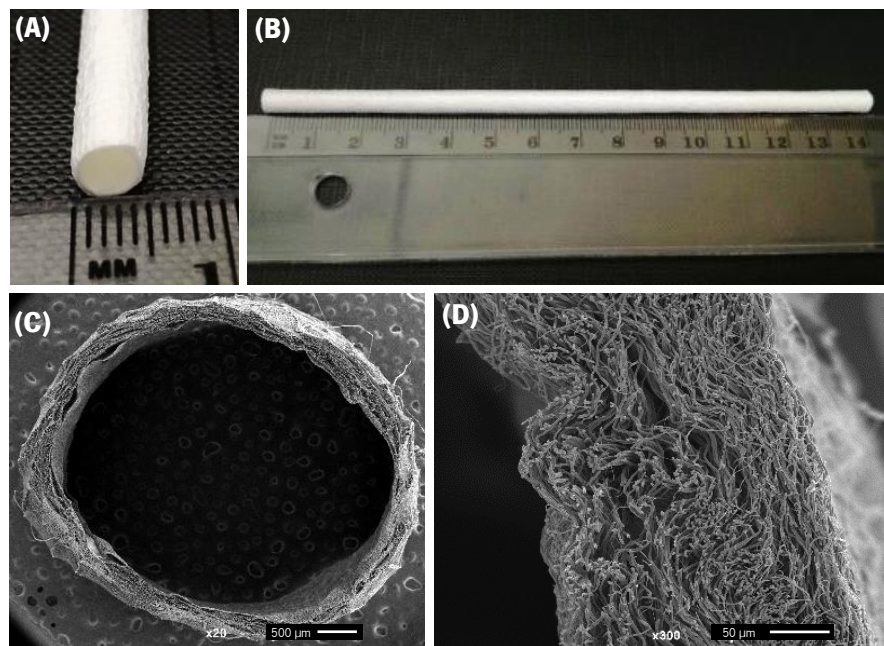


Figure 3. 1- Electrospun tubular fibrous (eTF) scaffolds. Macrostructure (A and B) and SEM micrographs of the cross-section (C and D).

SEM micrographs of the luminal surface were taken along axial (x axis) (Figure 3. 2A) and radial (y axis) directions (Figure 3. 2B), showing that the first layers of fibers were randomly organized, but with a tendency to present some orientation along the axial direction. This is supported by the fiber orientation analysis (Figure 3. 2C) showing one single peak at approximately 0° . The eTF scaffolds' inner surface displayed fiber diameters ranging from submicron to several microns (Figure 3. 2D): 19% of diameters are below $1 \mu\text{m}$, diameters ranging between 1 and $3 \mu\text{m}$ accounted for 66% of total fiber diameter; and 15% are larger than $3 \mu\text{m}$ and up to $7 \mu\text{m}$. The porosity obtained was about $33.55 \pm 4.05 \%$. The pore size and area were also analysed. About 90% of total pore lengths (major and minor) are below $10 \mu\text{m}$ and $5 \mu\text{m}$, respectively (Figure 3. 2E). The remaining 10% accounted for major pore lengths higher than $10 \mu\text{m}$ and up to $23 \mu\text{m}$ and minor pore lengths higher than $5 \mu\text{m}$ and up to $11 \mu\text{m}$ (Figure 3. 2E). Concerning the pore

area, 85% of pores have an area lower than $20 \mu\text{m}^2$ while pores with areas up to $70 \mu\text{m}^2$ represented 15% of the total pores (Figure 3. 2F).

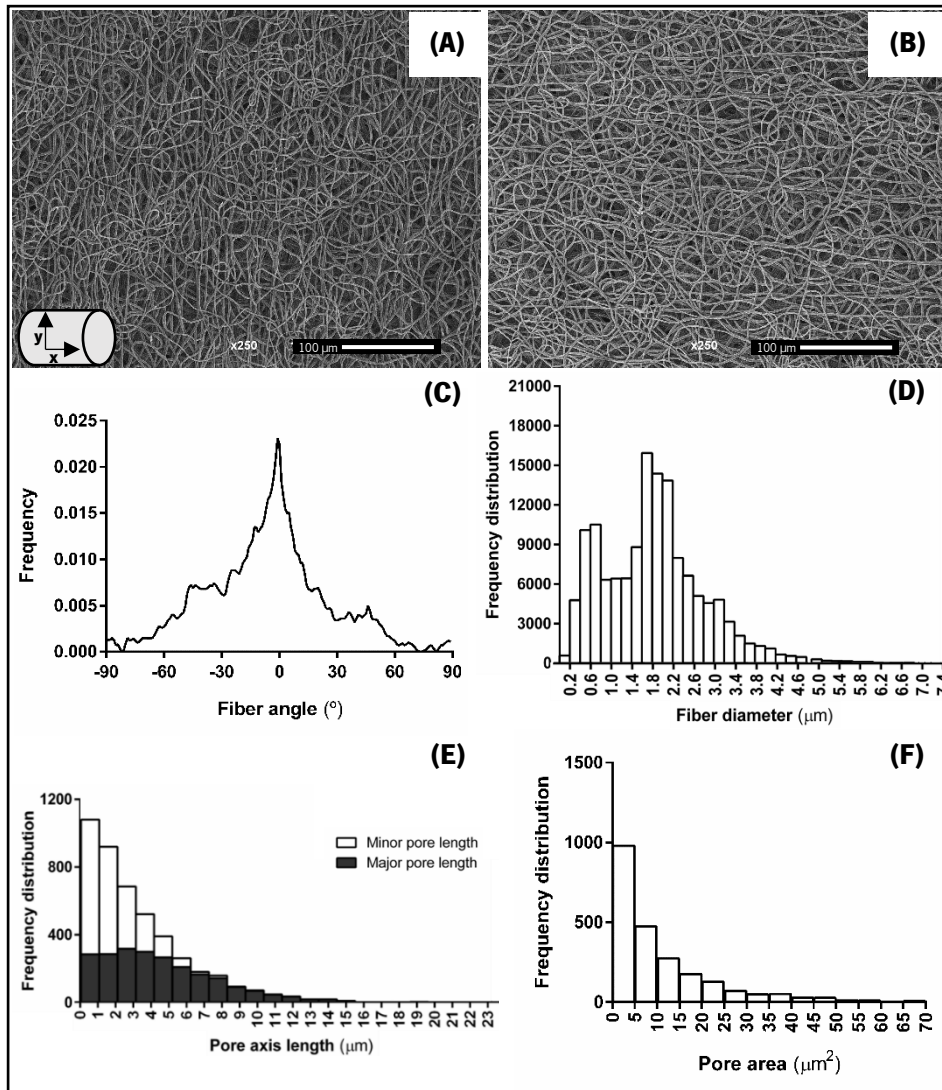


Figure 3. 2 - SEM micrographs of eTF scaffolds along axial (A) and radial (B) directions. Fibers morphology analysis: fiber orientation of axial and radial directions (C), fiber diameter frequency (D), pore size frequency (E) and pore area frequency (F).

3.4.2. Characterization of functionalized scaffolds

The morphology and fiber diameter distribution of the eTF scaffolds after activation and aminolysis, as well as the amount of NH_2 groups inserted at their surface are shown in Figure 3. 3. Both activation (Figure 3. 3A) and aminolysis (Figure 3. 3B) did not induce changes in fiber morphology. The fiber diameter distributions remained comparable between surface treatments, also comprising two main groups of fibers: less than $1 \mu\text{m}$ and between 1 and $3 \mu\text{m}$. However, a decrease in the amount of fibers with diameters less than $1 \mu\text{m}$ was observed after NaOH (Figure 3. 3C) and aminolysis (Figure 3. 3D) treatments, corresponding to about 10% and 13% of total fiber

diameters, respectively. Diameters ranging from 1 to 3 μm accounted for 70% and 74% of total fiber diameter for activated and aminolysed scaffolds, respectively.

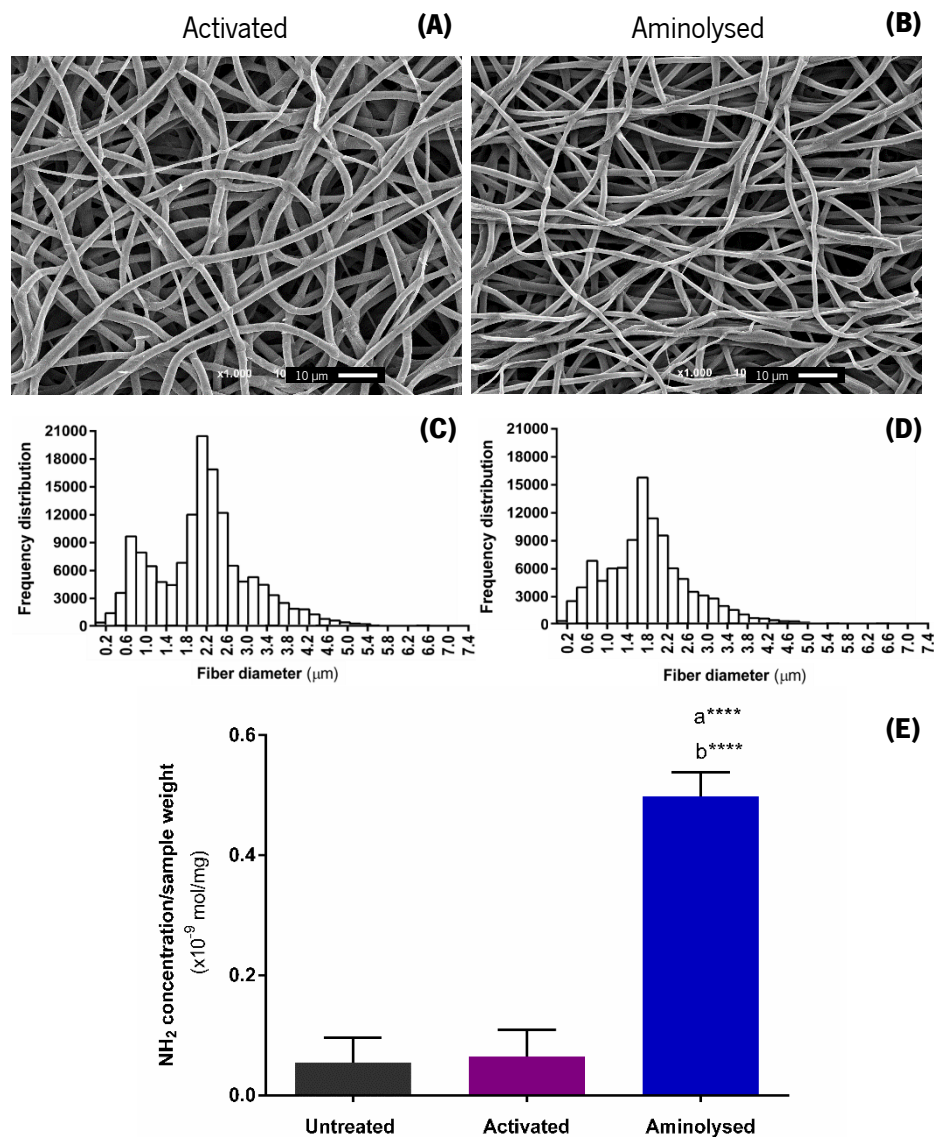


Figure 3. 3 - SEM micrographs of the activated (A) and aminolysed (B) surfaces. Frequency distribution of fibers diameter of activated (C) and aminolysed (D) surfaces. NH_2 groups quantification on untreated, activated and aminolysed eTF scaffolds (E). Data were analyzed by the one-way ANOVA test, followed by the Tukey's HSD test ($p < 0.05$): **a** denotes significant differences compared to untreated condition and **b** denotes significant differences compared to activated condition. The data is expressed as the mean \pm standard deviation.

Untreated and activated conditions presented a residual amount of NH_2 groups at the eTF scaffolds surface. In contrast, after aminolysis, eTF scaffolds presented on average 0.5 ± 0.04 nmol/mg of NH_2 groups ($p < 0.0001$) (Figure 3. 3E).

3.4.3. Uniaxial tensile properties

The stress-strain curves for untreated, activated and aminolysed eTF scaffolds, for both axial and radial orientations, in dry and hydrated states, are presented in Figure 3. 4. The curves were similar before and after the surface functionalization, but slightly different between axial and radial directions. The radial properties were generally characterized by a lower maximum stress and its corresponding strain (Figure 3. 4B) when compared to those obtained for the properties in the axial direction (Figure 3. 4A).

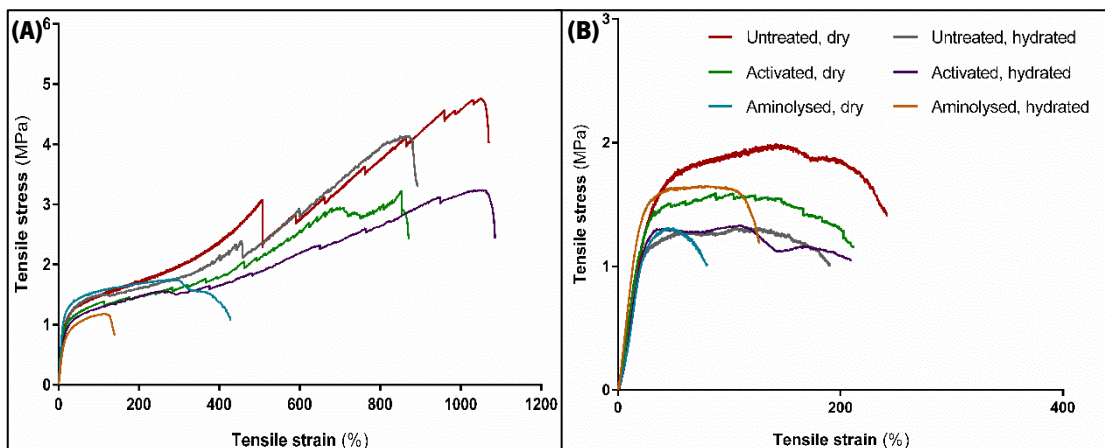


Figure 3. 4 - Stress-Strain curves of untreated, activated and aminolysed eTF scaffolds, tested in dry and hydrated conditions: axial direction (A) and radial direction (B).

The surface functionalization did not affect the stiffness of the eTF scaffolds along axial and radial direction (Figure 3. 5A1 and Figure 3. 5A2). Under dry conditions, the Young 's modulus of untreated samples was 8.16 (6.10 – 8.63) MPa. After NaOH and aminolysis treatments, it increased to 9.80 (7.62 – 10.27) MPa and to 11.21 (8.73 – 13.10) MPa, respectively, although no statistical differences were observed. In radial direction, the Young 's modulus values were also not significantly different among conditions, being 6.78 (5.07 – 8.09) MPa for the untreated, 6.41 (5.52 – 10.41) MPa for the activated and 6.63 (6.43 – 7.13) MPa for the aminolysed specimens. After hydration, the stiffness was equivalent under both axial and radial directions among conditions.

In the axial direction, the aminolysis treatment induced a decrease in the maximum stress values to 1.59 (1.51 – 1.77) MPa comparing to the untreated (4.82 (3.53 – 6.84) MPa; $p < 0.0001$) and activated (3.23 (2.59 – 3.50) MPa; $p < 0.001$) in dry condition (Figure 3. 5B1 and Figure 3. 5B2). After hydration, the same trend was observed in comparison to the untreated ($p < 0.0001$)

and activated samples ($p < 0.0001$). When tested radially, these differences were not observed in both dry and hydrated states, being the maximum stress values similar for all conditions.

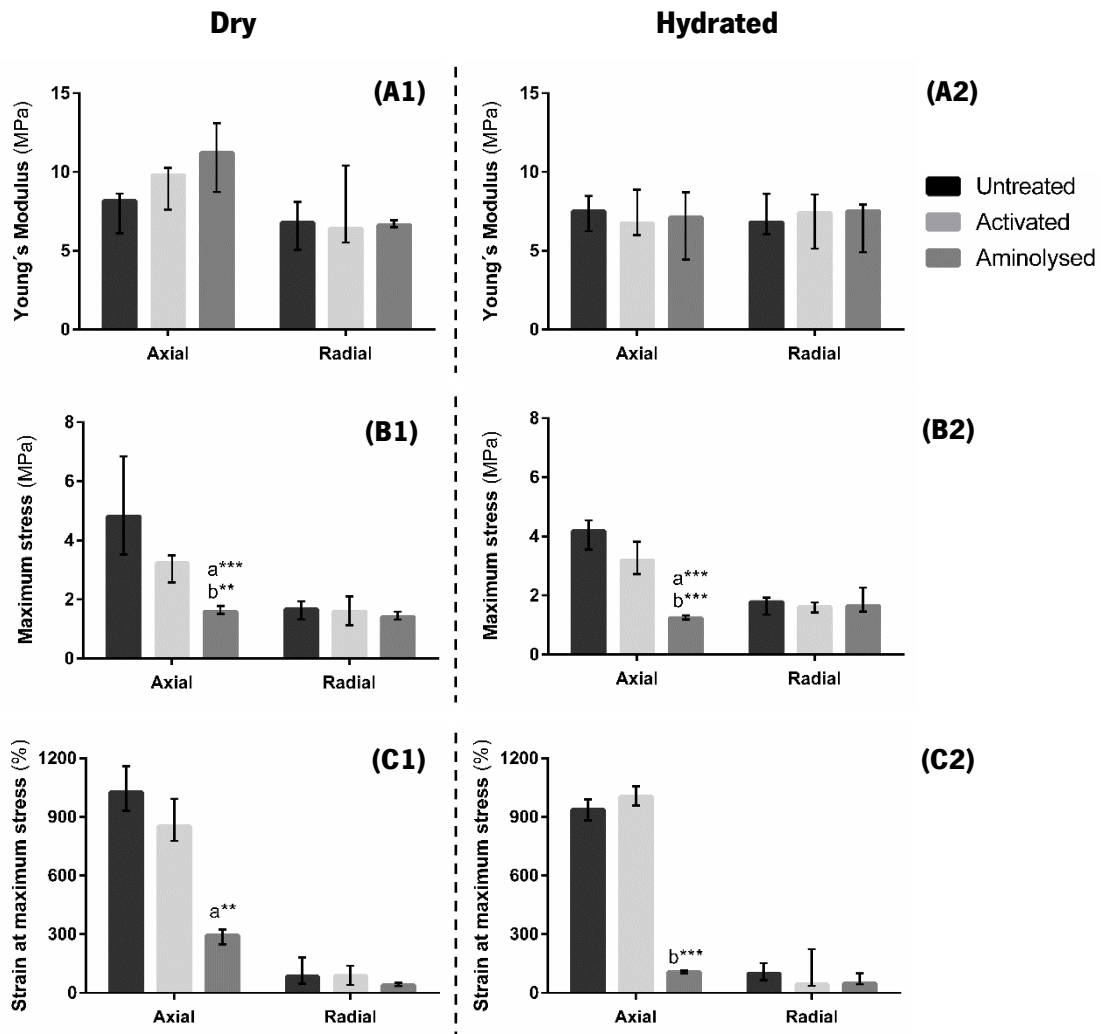


Figure 3. 5 - Uniaxial tensile properties of untreated, activated and aminolysed eTF scaffolds under axial and radial directions, tested in dry (1) and hydrated (2) conditions: Young 's modulus (A), maximum stress (B) and strain at maximum stress (C). Data were analysed by the Krustal-Wallis tes Wallis test, followed by the Tukey's HSD test ($p < 0.01$): *a* denotes significant differences compared to untreated and *b* denotes significant differences compared to activated condition. The data is expressed as median \pm interquartile range.

Specimens tested under axial direction were able to experience larger strain compared to the specimens tested under radial direction (Figure 3. 5C1 and Figure 3. 5C2). Untreated specimens were significantly more compliant (1026 (930.3 – 1158) %) than the aminolysed ones ($p < 0.001$) which presented strain values of 300.6 (250.8 – 381.4) %, in dry state. After hydration, this value decreased to 106.1 (99.64 – 113.2) %, being lower than activated ($p < 0.0001$) condition.

Interestingly, in radial direction, the strain experienced at maximum stress was comparable among conditions, tested under dry and hydration conditions.

3.4.4. Characterization of biofunctionalized scaffolds

3.4.4.1. Quantification of immobilized tropoelastin

Tropoelastin was immobilized at the luminal surface of activated and aminolysed eTF scaffolds, in concentrations ranging from 0 to 20 $\mu\text{g}/\text{mL}$, aiming to determine the maximum immobilization capacity (Figure 3. 6).

The activated eTF scaffolds (*OH-TE*) presented a higher immobilization capacity of tropoelastin in comparison to the aminolysed substrate (*NH₂-TE*). Activated eTF scaffolds allowed the immobilization of $82 \pm 16 \%$ when incubated with 5 $\mu\text{g}/\text{mL}$ of tropoelastin, while for 20 $\mu\text{g}/\text{mL}$ of tropoelastin this binding capacity decreased to $71 \pm 14 \%$. The same tendency was observed for the aminolysed substrates which promoted an immobilization of $61 \pm 20 \%$ and $43 \pm 17 \%$ after the incubation with 5 $\mu\text{g}/\text{mL}$ and 20 $\mu\text{g}/\text{mL}$ of tropoelastin, respectively.

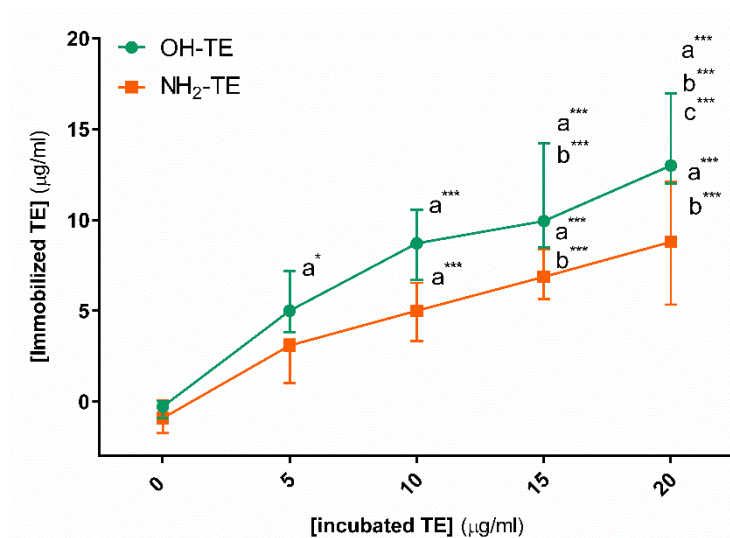


Figure 3. 6 - Maximum immobilization capacity of tropoelastin at the surface of activated (*OH-TE*) and aminolysed (*NH₂-TE*) eTF scaffolds. Data were analysed by the Kruskal-Wallis test, followed by the Tukey's HSD test ($p < 0.01$): **a** denotes significant differences compared to concentration 0 $\mu\text{g}/\text{mL}$; **b** denotes significant differences compared to concentration 5 $\mu\text{g}/\text{mL}$; **c** denotes significant differences compared to concentration 10 $\mu\text{g}/\text{mL}$. The data is expressed as median \pm interquartile range.

Concerning the activated surfaces, the incubation with 20 $\mu\text{g}/\text{mL}$ of tropoelastin was statistically different from the incubation with 10 $\mu\text{g}/\text{mL}$ ($p < 0.0001$). In contrast, for aminolysed substrates, incubation with 20 $\mu\text{g}/\text{mL}$ of tropoelastin was significantly different from incubation

with 5 $\mu\text{g}/\text{mL}$ ($p < 0.0001$). Thus, the tropoelastin immobilization capacity reached its maximum at 20 $\mu\text{g}/\text{mL}$ from which no statistically differences were observed. Taking these results into consideration, 20 $\mu\text{g}/\text{mL}$ of tropoelastin concentration was selected for further studies, using both surface functionalities.

3.4.4.2. Surface charge properties

The zeta potential (ζ), an indicator of surface electric charge, was measured on untreated, functionalized and biofunctionalized eTF scaffolds. The Figure 3. 7 shows the behaviour of zeta potential along pH for each testing condition. The untreated eTF scaffold presents a negative surface charge at pH from 6.5 to 9.5. At physiological values (pH = 7.4), it presents a zeta potential around -100 mV. After activation with NaOH, the zeta potential became more negative, approximately -300 mV, at pH = 7.4. Following the aminolysis treatment, the surface charge shifted from negative to positive, roughly +30 mV, within physiological conditions, presenting an isoelectric point (IEP) at pH = 8. The biofunctionalized surfaces were also analysed to understand the effect of tropoelastin orientation on the surface charge. The activated eTF scaffolds that were further immobilized with tropoelastin (*OH-TE*) presented a zeta potential of -240 mV at pH = 7.4. This charge is less negative comparing to the activated eTF scaffold. Moreover, tropoelastin-immobilized on aminolysed scaffolds (*NH₂-TE*) showed a potential of +20 mV at physiological pH. However, this condition presented a higher IEP = 8.8.

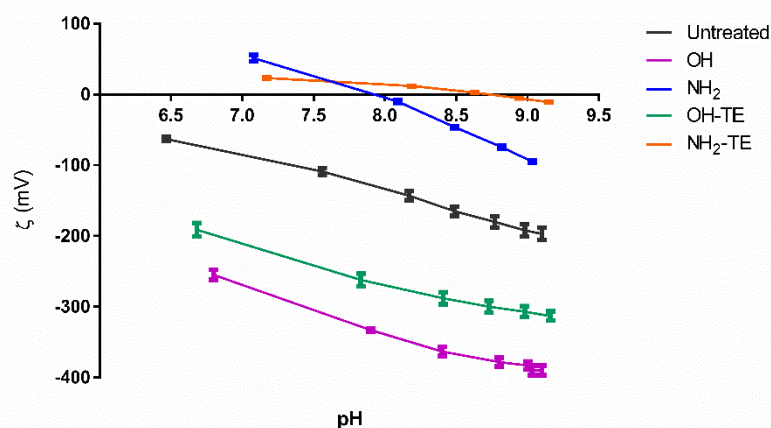


Figure 3. 7 - Surface zeta potential of untreated, activated (OH), aminolysed (NH₂) and tropoelastin-immobilized on activated (OH-TE) or on aminolysed (NH₂-TE) eTF scaffolds along pH.

3.4.5. Biological performance

Different biological assays were performed to assess the endothelialization of the eTF scaffolds. A HUVEC cell line (EA.hy926) was cultured at the surface of five different substrate

conditions: (i) untreated eTF scaffolds (*Untreated*), (ii) activated eTF scaffolds (*OH*), (iii) aminolysed eTF scaffolds (*NH₂*), (iv) tropoelastin immobilized on activated eTF scaffolds (*OH-TE*) and (v) tropoelastin immobilized on aminolysed eTF scaffolds (*NH₂-TE*).

3.4.5.1. *Metabolic activity and cell proliferation*

The metabolic activity results shown an increased cell metabolic activity during the time-course of the experiment for every group (Figure 3. 8A). The activated eTF scaffolds presented a higher metabolic activity in comparison to the untreated eTF scaffolds at 1 day of culture ($p < 0.01$). Particularly, at the *OH-TE* condition, the endothelial cells were significantly more metabolically active when compared with the untreated condition, after 1 ($p < 0.0001$) and 3 ($p < 0.01$) days of culture. Also, the *NH₂-TE* condition presented higher metabolic activity than the untreated condition after 1 day ($p < 0.01$).

Concerning the cell proliferation, the DNA content of endothelial cells significantly increased for all time points, being more noticeable from day 3 to 7 (Figure 3. 8B). Activated surface, as well as tropoelastin-immobilized substrates do promote higher cell proliferation compared to the untreated condition, even if not statistically significant different.

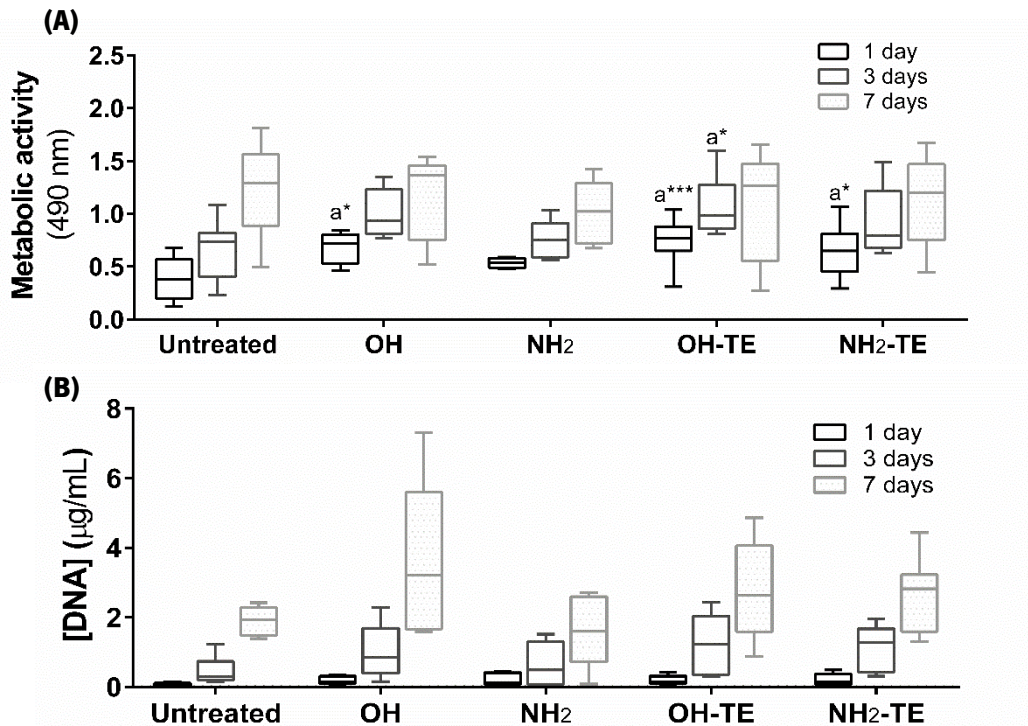


Figure 3. 8 - Metabolic activity (A) and DNA quantification (B) of human endothelial cells seeded on untreated, activated (OH), aminolysed (NH₂) and tropoelastin-immobilized on activated (OH-TE) or on aminolysed (NH₂-TE) eTF scaffolds after 1, 3 and 7 days of culture. Data were analysed by the Kruskal-Wallis test, followed by the Tukey's HSD test ($p < 0.01$): **a** denotes significant differences compared to the untreated condition.

3.4.5.2. Total protein synthesis and soluble VEGF production

An increase in total protein synthesis was observed for all conditions along the time-course of the experiment (Figure 3. 9A). In particular, statistically significant differences can be seen for both conditions comprising immobilized tropoelastin. After 1 day of culture, endothelial cells produced a higher amount of protein on *OH-TE* condition compared to the untreated one ($p < 0.01$). Furthermore, the tropoelastin immobilization onto aminolysed eTF scaffolds (*NH₂-TE*) promoted a higher protein production throughout the entire experiment. The protein synthesis was significantly higher than the untreated ($p < 0.0001$) and activated ($p < 0.01$) conditions and when compared with the untreated ($p < 0.01$) and aminolysed ($p < 0.01$) conditions after 1 and 3 days of culture, respectively. After 7 days of culture, the protein production was even higher in comparison to the untreated ($p < 0.0001$), activated ($p < 0.0001$), aminolysed ($p < 0.0001$) and the *OH-TE* ($p < 0.01$) conditions.

By performing an enzyme-linked immunosorbent assay (ELISA), it was possible to quantify the production of soluble VEGF present in the cell culture medium (Figure 3. 9B). A slight increase

in VEGF production was observed from day 1 to 7. Despite no statistical differences were observed, OH-TE condition seems to induce a higher expression of soluble VEGF compared to the NH₂-TE condition, after 7 days of culture.

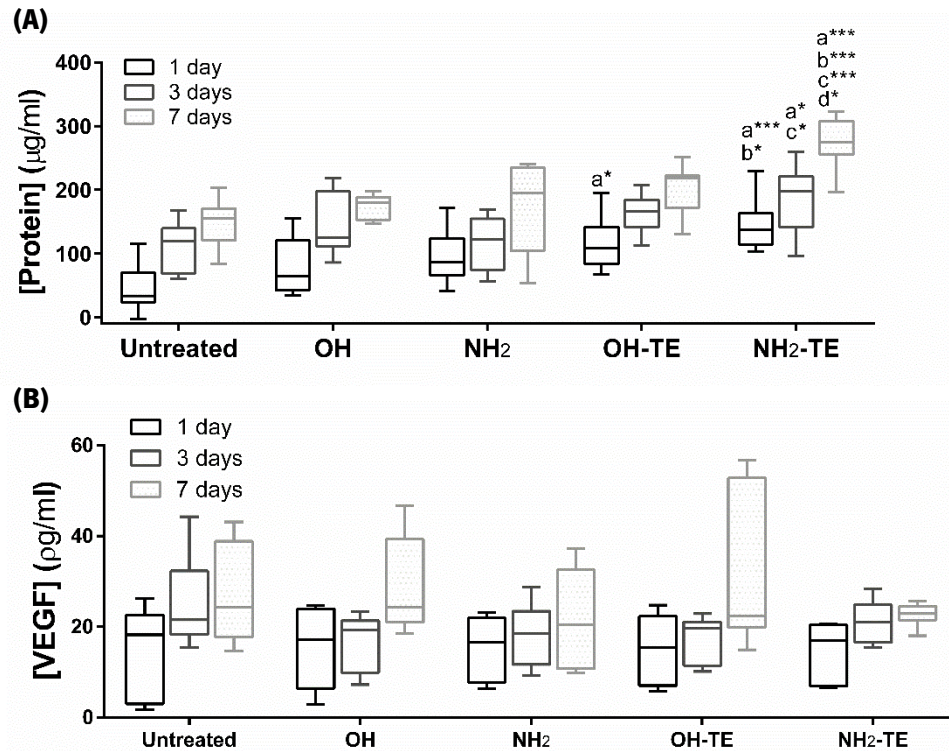


Figure 3. 9 - Total protein synthesis (A) and soluble VEGF production (B) human endothelial cells seeded on untreated, activated (OH), aminolysed (NH₂) and tropoelastin-immobilized on activated (OH-TE) or on aminolysed (NH₂-TE) eTF scaffolds after 1, 3 and 7 days of culture. Data were analysed by the Kruskal-Wallis test, followed by the Tukey 's HSD test ($p < 0.01$): **a** denotes significant differences compared to the untreated condition; **b** denotes significant differences compared to the activated condition; **c** denotes significant differences compared to the aminolysed condition and **d** denotes significant differences compared to the OH-TE condition.

3.4.5.3. Endothelial cells morphology

After 1, 3 and 7 days, the morphology of adhered endothelial cells to the eTF scaffolds was investigated by SEM (Figure 3. 10). Along the time-course of the experiment, it was possible to observe in the SEM micrographs an increase on cell number, in agreement with the DNA content results. In particular, at day 7, the presence of a confluent endothelial cell monolayer was observed, covering most of the scaffolds surface.

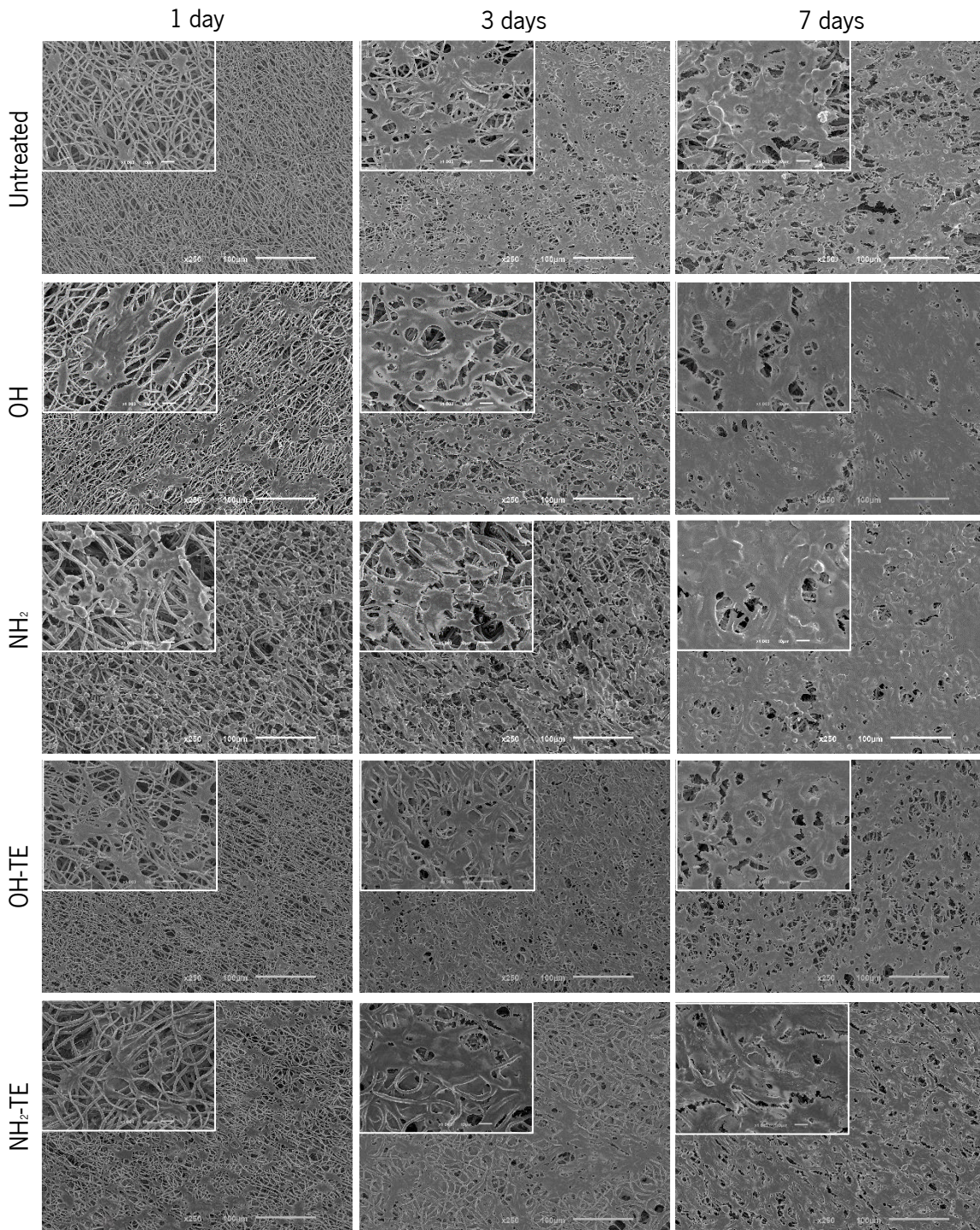


Figure 3. 10 - Morphological analysis by SEM of human endothelial cells cultured on untreated, activated (OH), aminolysed (NH₂) and tropoelastin-immobilized on activated (OH-TE) or on aminolysed (NH₂-TE) eTF scaffolds surface after 1, 3 and 7 days of culture. Scale bar: 100 μm (250x magnification) and 10 μm (1000x magnification).

3.4.5.4. *Immunoexpression of CD31 surface marker*

The analysis of the fluorescence images showed that CD31 at the cell-cell interface was synthesized for all conditions throughout the experiment (Figure 3. 11). At day 1 and 3, a well-

marked expression of CD31 on the endothelial cells membrane was visible due to their low confluent stage. Nevertheless, this endothelial cell marker at the cell-cell interface was more noticeable after 7 days, particularly on NH_2 -TE constructs, demonstrating its role in stimulating the formation of endothelial intercellular junctions.

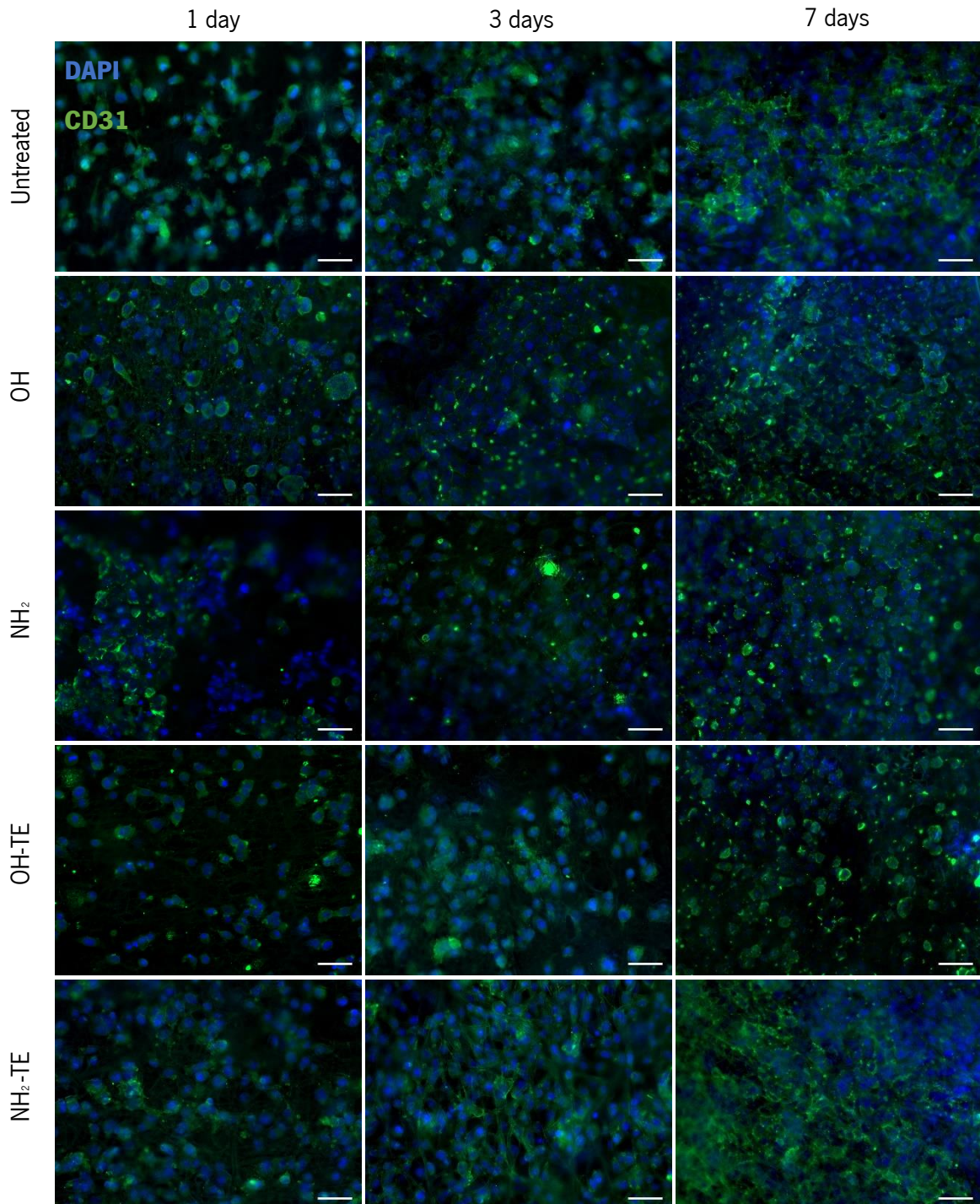


Figure 3. 11 - Fluorescent images of human endothelial cells seeded on untreated, activated (OH), aminolysed (NH₂) and tropoelastin immobilized on activated (OH-TE) or on aminolysed (NH₂-TE) eTF scaffolds surface after 1, 3 and 7 days of culture. Cell nuclei are stained in blue by DAPI and the CD31 endothelial cell marker is stained in green. Scale bar: 50 μ m.

3.5 Discussion

There is a demand to develop vascular grafts with biomechanical properties compatible to those of blood vessels, whilst supporting endothelial cell attachment and proliferation, as well as having non-thrombogenic properties [35,36]. The present study reports the development of a tubular fibrous scaffold functionalized with tropoelastin as a biomimetic approach for vascular tissue engineering. The immobilization of tropoelastin at its luminal surface is proposed to provide biochemical cues that endothelial cells recognize from the native ECM. Taking advantage of the low thrombogenicity of tropoelastin [37], this approach aims at improving the endothelialization and hemocompatibility without affecting the mechanical properties.

An ideal vascular graft should mimic the native ECM and the electrospinning is able to produce tubular fibrous structures that mimic its structure. Porous and fibrous tubular scaffolds were fabricated with a thickness of $240.85 \pm 46.91 \mu\text{m}$, comprising a mix of micro to submicrometer fibers. They present a porous luminal surface composed of randomly oriented fibers at the first layers, showing evidences of a transition to more oriented fibers along the axial direction due to the low rotation speed of the mandrel. The eTF scaffolds presented pore sizes that vary significantly, ranging from $1 \mu\text{m}$ to $23 \mu\text{m}$, and pore areas up to $70 \mu\text{m}^2$. In fact, it was reported an ideal pore size between 10 and $45 \mu\text{m}$ that do not induce fibrous tissue infiltration and blood leakage [38]. Therefore, the morphology of the obtained eTF scaffolds luminal surface will allow the endothelial cells adhesion and proliferation.

To favour the biofunctionalization of eTF scaffolds, a surface modification was performed to allow the covalent binding of tropoelastin to the inner surface of the PCL fibers. Firstly, given the long-term application of these constructs, a wet chemical method was selected which promotes a random chemical scission of PCL ester linkages. Then, aminolysis was successfully achieved by inserting $0.5 \pm 0.04 \text{ nmol/mg NH}_2$ groups to the eTF scaffolds surface without affecting the fibers morphology, as reported previously in the literature by our group [39,40]. Concerning the fiber diameter distribution, the surface treatment promoted a decrease of the group of fibers with diameters less than $1 \mu\text{m}$, maintaining a similar distribution for the larger fibers, also reported by other authors [41,42]. Zeta potential measurement has been carried out to identify chemical modifications of materials [43,44]. Untreated PCL fibers presented a negative surface charge at physiological values which can be explained by the preferential orientation of the carbonyl groups at the surface [45]. The NaOH treatment introduced polar groups such as carboxyl ($-\text{COOH}$) and hydroxyl (OH), at the surface of the fibers, as confirmed by the decrease on the surface zeta

potential values, along the pH. After the aminolysis reaction, NH_2 groups were inserted at the fibers surface and their protonation led to an increase on surface charge, confirming the effectiveness of this functionalization procedure.

Since surface functionalization may induce changes in the bulk properties of eTF scaffolds, the impact of NaOH and aminolysis treatments over the mechanical properties was also assessed. In addition to the dry condition, the specimens were also analyzed after hydration since it closely reflects the *in vivo* environment. Healthy arteries are relatively deformable with linear elastic behaviour under stress-strain cycles [12]. The stress-strain curves of eTF scaffolds on axial and radial directions, before and after functionalization, exhibited an initial elastic behaviour, followed by stiffening, which is similar to the tensile behaviour of native vessels. The uniaxial tensile properties, on axial and radial directions, for every condition were found to be relatively different. Generally, the axial direction presented higher values of maximum stress and its corresponding strain in comparison to the radial direction. Since the axial direction presents some fibers aligned with the tensile test direction, these fibers were able to stretch more and support higher stresses, providing higher mechanical properties. After the aminolysis treatment, the strength and elongation of the constructs decreased in the axial direction, which indicates that the treatment slightly affected the bulk properties of the polymer. Considering the mechanical properties obtained after the surface functionalization, the functionalized eTF scaffolds showed sufficient strength and stiffness for vascular applications. The reported Young's modulus and maximum stress were found to be within the range of those obtained for various native vessels (Table 3. 1). Moreover, these scaffolds were able to elongate in a higher extent compared to, for instance, the strain of human coronary arteries reported in the literature, which was less than 100% [12].

Tropoelastin is the monomer of elastin which possesses hydrophobic domains responsible for the elasticity, alternated with hydrophilic domains containing lysine residues involved in the cross-linking [46]. The N-terminal of the molecule is characterized by the presence of a 26-amino-acid signal peptide, while the other end comprises the C-terminal which terminates with a positively charged amino acid motif [46], responsible for cell-binding [47]. It has been extensively described the effect of the C-terminal in cell adhesion, mainly, for fibroblasts [48] and endothelial cells [37], promoting their adhesion, spreading and proliferation. Additionally, endothelial cells were reported to strongly interact with the N-terminal, influencing their attachment and proliferation [49]. In this sense, both interactions and their effect over endothelial cell behaviour was herein investigated.

Tropoelastin was immobilized on activated and aminolysed substrates, which allowed its immobilization at two different orientations, exploring different exposed moieties of the molecule. In one hand, the activated surface presented -COOH and -OH groups which mediated the immobilization of tropoelastin by its -NH₂ groups and, probably, would expose the C-terminal for cell recognition. Alternatively, the -NH₂ groups from the aminolysed surface reacted with -COOH groups from the tropoelastin to expose the N-terminal for cell binding. Herein, tropoelastin was successfully immobilized on activated and aminolysed surfaces with reasonable efficiency, about $14.11 \pm 2.89 \mu\text{g/mL}$ and $8.57 \pm 3.36 \mu\text{g/mL}$, respectively. From the surface charge analysis, the immobilization of tropoelastin by its -NH₂ (*OH-TE*) and -COOH (*NH₂-TE*) groups promoted a more positive and stable surface charge of the eTF scaffolds.

A rapid endothelialization of a vascular graft is crucial for its anti-thrombogenic properties and to keep long-term patency [36]. Therefore, the interaction between HUVECs cell line and the eTF scaffolds was studied. The surface functionalization did not negatively affect the endothelial cells behaviour when compared with untreated eTF scaffolds. Indeed, endothelial cells were metabolically active and were able to adhere and proliferate *in vitro*, as demonstrated by the MTS assay and DNA quantification. The eTF scaffolds modified with tropoelastin showed a trend to have enhanced biological performance. Specifically, when immobilized on activated eTF scaffolds (*OH-TE*), the tropoelastin improved cell viability and protein synthesis. Additionally, enhanced VEGF production in its soluble form, at day 7, was observed which may indicate that tropoelastin immobilized in this manner may have a positive influence over the endothelial cell activity, but no statistical significant differences were observed. Alternatively, when exposing its NH₂ groups (*NH₂-TE*), tropoelastin significantly induced endothelial cells to synthesise their own proteins, showing clear differences compared to all other conditions after 7 days. Overall, tropoelastin, when covalently immobilized, demonstrated to have an impact on endothelial cells-biomaterial interaction, as reported by other authors [50,51], using both conformations. Endothelial cells expressed the endothelial cell adhesion molecule CD31 at cell-cell junctions along the time-course of the experiment, being also more evident for *NH₂-TE* condition at day 7. Regardless the presence of the tropoelastin, the CD31 staining confirmed that eTF scaffolds supported cell adhesion and proliferation, as well as phenotype maintenance. After 7 days, the presence of an endothelial layer on the luminal surface, fully covering the eTF scaffolds, was confirmed by SEM analysis. These findings suggest that endothelial cells were able to form an anti-thrombogenic luminal surface at

early stages of cell culture. Hence, this feasible approach is attractive to produce blood vessel substitutes with demonstrated and enhanced cell-material interactions towards endothelialization.

3.6 Conclusions

We have successfully developed a biofunctional eTF scaffold for vascular applications with appropriate uniaxial tensile properties within the same range of those of native blood vessels. By tailoring the surface functionality, different interactions between the biofunctional substrate and endothelial cells can be achieved. Indeed, exposing tropoelastin -COOH groups to cells seemed to influence the endothelial cells behaviour towards enhancing its viability and activity. Otherwise, exposing its -NH₂ groups stimulated endothelial cells to produce higher amounts of protein. After 7 days of culture, a confluent endothelial cell monolayer was present on the eTF scaffolds surface which promoted a rapid endothelialization. This study suggests that by combining the fibrous and porous structure, and the mechanical properties obtained from eTF scaffolds with biochemical cues provided by tropoelastin, it is possible to design a biofunctional and bioactive tubular scaffold as a valid alternative to functional engineered vascular grafts.

3.7 References

- [1] D.G. Seifu, A. Purnama, K. Mequanint, D. Mantovani, Small-diameter vascular tissue engineering, *Nat. Rev. Cardiol.* 10 (2013) 410–421.
- [2] A. D. Michaels and K. Chatterjee, Angioplasty Versus Bypass Surgery for Coronary Artery Disease, *Circulation.* 106 (2002) 176–178.
- [3] R.Y. Kannan, H.J. Salacinski, P.E. Butler, G. Hamilton, A.M. Seifalian, Current status of prosthetic bypass grafts: A review, *J. Biomed. Mater. Res. - Part B Appl. Biomater.* 74 (2005) 570–581.
- [4] R. Langer, J.P. Vacanti, *Tissue Engineering, Science.* 260 (1993) 920–926.
- [5] N. L'Heureux, N. Dusserre, G. Konig, B. Victor, P. Keire, T.N. Wight, N.A.F. Chronos, A.E. Kyles, C.R. Gregory, G. Hoyt, R.C. Robbins, T.N. McAllister, Human tissue-engineered blood vessels for adult arterial revascularization, *Nat. Med.* 12 (2006) 361–365.
- [6] S.L.M. Dahl, A.P. Kypson, J.H. Lawson, J.L. Blum, J.T. Strader, Y. Li, R.J. Manson, W.E.

- Tente, L. DiBernardo, M.T. Hensley, R. Carter, T.P. Williams, H.L. Prichard, M.S. Dey, K.G. Begelman, L.E. Niklason, Readily available tissue-engineered vascular grafts., *Sci. Transl. Med.* 3 (2011) 68–79.
- [7] D. Seliktar, R.A. Black, R.P. Vito, R.M. Nerem, Dynamic Mechanical Conditioning of Collagen-Gel Blood Vessel Constructs Induces Remodeling In Vitro, *Ann. Biomed. Eng.* 28 (2000) 351–362.
- [8] L. Soletti, Y. Hong, J. Guan, J.J. Stankus, M.S. El-kurdi, A bilayered elastomeric scaffold for tissue engineering of small diameter vascular grafts, *Acta Biomater.* 6 (2010) 110–122.
- [9] S. Jin, J. Liu, S. Heang, S. Soker, A. Atala, J.J. Yoo, Development of a composite vascular scaffolding system that withstands physiological vascular conditions, *Biomaterials.* 29 (2008) 2891–2898.
- [10] B. Nottelet, E. Pektok, D. Mandracchia, J.C. Tille, B. Walpoth, R. Gurny, M. Möller, Factorial design optimization and in vivo feasibility of poly(ϵ -caprolactone)-micro- and nanofiber-based small diameter vascular grafts, *J. Biomed. Mater. Res. - Part A.* 89 (2009) 865–875.
- [11] M. Stekelenburg, D. Ph, M.C.M. Rutten, D. Ph, L.H.E.H. Snoeckx, D. Ph, F.P.T. Baaijens, D. Ph, Dynamic Straining Combined with Fibrin Gel Cell Seeding Improves Strength of Tissue-Engineered Small-Diameter Vascular Grafts, *Tissue Eng. - Part A.* 15 (2009) 1081–1089.
- [12] A. Karimi, M. Navidbakhsh, A. Shojaei, S. Faghihi, Measurement of the uniaxial mechanical properties of healthy and atherosclerotic human coronary arteries, *Mater. Sci. Eng. C.* 33 (2013) 2550–2554.
- [13] A. Tajaddini, D.L. Kilpatrick, P. Schoenhagen, E.M. Tuzcu, M. Lieber, D.G. Vince, D.L. Kilpatrick, P. Schoenhagen, M. Tuzcu, M. Lieber, D.G. Vince, Impact of age and hyperglycemia on the mechanical behavior of intact human coronary arteries : an ex vivo intravascular ultrasound study, *Am. J. Physiol. Hear. Circ. Physiol.* 44195 (2005) 250–255.
- [14] D.A. Vorp, B.J. Schiro, M.P. Ehrlich, T.S. Juvonen, M.A. Ergin, B.P. Griffith, Effect of Aneurysm on the Tensile Strength and Biomechanical Behavior of the Ascending Thoracic

- Aorta, *Ann. Thorac. Surg.* 75 (2003) 1210–1214.
- [15] A. Martins, J. V Araújo, R.L. Reis, N.M. Neves, Electrospun nanostructured scaffolds for tissue engineering applications, *Nanomedicine (Lond)*. 2 (2007) 929–942.
- [16] A. Martins, R.L. Reis, N.M. Neves, Electrospinning: processing technique for tissue engineering scaffolding, *Int. Mater. Rev.* 53 (2008) 257–274.
- [17] T.-H. Nguyen, B.-T. Lee, The effect of cross-linking on the microstructure, mechanical properties and biocompatibility of electrospun polycaprolactone–gelatin/PLGA–gelatin/PLGA–chitosan hybrid composite, *Sci. Technol. Adv. Mater.* 13 (2012) 35002.
- [18] Y.M. Ju, J.S. Choi, A. Atala, J.J. Yoo, S.J. Lee, Bilayered scaffold for engineering cellularized blood vessels, *Biomaterials*. 31 (2010) 4313–4321.
- [19] C.M. Vaz, S. van Tuijl, C.V.C. Bouten, F.P.T. Baaijens, Design of scaffolds for blood vessel tissue engineering using a multi-layering electrospinning technique, *Acta Biomater.* 1 (2005) 575–582.
- [20] S.G. Wise, M.J. Byrom, A. Waterhouse, P.G. Bannon, M.K.C. Ng, A.S. Weiss, A multilayered synthetic human elastin / polycaprolactone hybrid vascular graft with tailored mechanical properties, *Acta Biomater.* 7 (2011) 295–303.
- [21] E. Pektok, B. Nottelet, J.-C. Tille, R. Gurny, A. Kalangos, M. Moeller, B.H. Walpoth, Degradation and Healing Characteristics of Small-Diameter Poly (epsilon-Caprolactone) Vascular Grafts in the Rat Systemic, *Circulation*. 118 (2008) 2563–2570.
- [22] S. de Valence, J.C. Tille, D. Mugnai, W. Mrowczynski, R. Gurny, M. Möller, B.H. Walpoth, Long term performance of polycaprolactone vascular grafts in a rat abdominal aorta replacement model, *Biomaterials*. 33 (2012) 38–47.
- [23] P.C. Caracciolo, M.I. Rial-Hermida, F. Montini-Ballarín, G.A. Abraham, A. Concheiro, C. Alvarez-Lorenzo, Surface-modified bioresorbable electrospun scaffolds for improving hemocompatibility of vascular grafts, *Mater. Sci. Eng. C*. 75 (2017) 1115–1127.
- [24] G.C. Yeo, A. Kondyurin, E. Kosobrodova, S. Weiss, M.M.M. Bilek, A sterilizable , biocompatible , tropoelastin surface coating immobilized by energetic ion activation, *J. R.*

Soc. Interface. 14 (2017).

- [25] S.M. Mithieux, S.G. Wise, A.S. Weiss, Tropoelastin — A multifaceted naturally smart material, *Adv. Drug Deliv. Rev.* 65 (2013) 421–428.
- [26] L.M. Maurer, B.R. Tomasini-johansson, D.F. Mosher, Emerging roles of fibronectin in thrombosis, *Thromb. Res.* 125 (2010) 287–291.
- [27] S.P. Vyas, B. Vaidya, Targeted delivery of thrombolytic agents: role of integrin receptors, *Expert Opin. Drug Deliv.* 6 (2009) 499–508.
- [28] S.G. Wise, H. Liu, A. Kondyurin, M.J. Byrom, P.G. Bannon, G.A. Edwards, A.S. Weiss, S. Bao, M.M. Bilek, Plasma Ion Activated Expanded Polytetrafluoroethylene Vascular Grafts with a Covalently Immobilized Recombinant Human Tropoelastin Coating Reducing Neointimal Hyperplasia, *ACS Biomater. Sci. Eng.* 2 (2016) 1286–1297.
- [29] A. Waterhouse, Y. Yin, S.G. Wise, D. V. Bax, D.R. McKenzie, M.M.M. Bilek, A.S. Weiss, M.K.C. Ng, The immobilization of recombinant human tropoelastin on metals using a plasma-activated coating to improve the biocompatibility of coronary stents, *Biomaterials.* 31 (2010) 8332–8340.
- [30] P.E. Tyllianakis, S.E. Kakabakos, G.P. Evangelatos, Colorimetric Determination of Reactive Primary Amino Groups of Macro- and Microsolid Supports, *Appl. Biochem. Biotechnol.* 38 (1993) 15–25.
- [31] N.A. Hotaling, K. Bharti, H. Kriel, C.G. Simon, DiameterJ: A Validated Open Source Nanofiber Diameter Measurement Tool, *Biomaterials.* 61 (2015) 327–338.
- [32] S.L. Martin, B. Vrhovski, A.S. Weiss, Total synthesis and expression in *Escherichia coli* of a gene encoding human tropoelastin, *Gene.* 154 (1995) 159–166.
- [33] A. Abdal-hay, A. Memic, K.H. Hussein, Y. Seul, M. Fouad, F.F. Al-jassir, H. Woo, Y. Morsi, Rapid fabrication of highly porous and biocompatible composite textile tubular scaffold for vascular tissue engineering, *Eur. Polym. J.* 96 (2017) 27–43.
- [34] M. Neufurth, X. Wang, E. Tolba, B. Dorweiler, Modular Small Diameter Vascular Grafts with Bioactive Functionalities, *PLoS One.* 10 (2015) 1–24.

- [35] M. Richard, R. Black, C. Kielty, PCL – PU composite vascular scaffold production for vascular tissue engineering : Attachment , proliferation and bioactivity of human vascular endothelial cells, *Biomaterials*. 27 (2006) 3608–3616.
- [36] F. Han, X. Jia, D. Dai, X. Yang, J. Zhao, Y. Zhao, Y. Fan, X. Yuan, Performance of a multilayered small-diameter vascular scaffold dual-loaded with VEGF and PDGF, *Biomaterials*. 34 (2013) 7302–7313.
- [37] D. V. Bax, A. Kondyurin, A. Waterhouse, D.R. McKenzie, A.S. Weiss, M.M.M. Bilek, Surface plasma modification and tropoelastin coating of a polyurethane co-polymer for enhanced cell attachment and reduced thrombogenicity, *Biomaterials*. 35 (2014) 6797–6809.
- [38] M. Ahmed, H. Ghanbari, B.G. Cousins, G. Hamilton, A.M. Seifalian, Small calibre polyhedral oligomeric silsesquioxane nanocomposite cardiovascular grafts: Influence of porosity on the structure, haemocompatibility and mechanical properties, *Acta Biomater*. 7 (2011) 3857–3867.
- [39] N. Monteiro, A. Martins, R. Pires, S. Faria, N.A. Fonseca, J. Moreira, R.L. Reis, N.M. Neves, Immobilization of bioactive factor-loaded liposomes on the surface of electrospun nanofibers targeting tissue engineering, *Biomater. Sci*. 2 (2014) 1195–1209.
- [40] C. Oliveira, A.R. Costa-pinto, R.L. Reis, A. Martins, N.M. Neves, Biofunctional Nanofibrous Substrate Comprising Immobilized 2 Antibodies and Selective Binding of Autologous Growth Factors, *Biomacromolecules*. 15 (2014) 2196–205.
- [41] L.A. Bosworth, W. Hu, Y. Shi, S.H. Cartmell, Enhancing Biocompatibility without Compromising Material Properties : An Optimised NaOH Treatment for Electrospun Polycaprolactone Fibres, *J. Nanomater*. 2019 (2019) 1–11.
- [42] S.J.P. Mcinnes, T.J. Macdonald, I.P. Parkin, T. Nann, N.H. Voelcker, Electrospun Composites of Polycaprolactone and Porous Silicon Nanoparticles for the Tunable Delivery of Small Therapeutic Molecules, *Nanomaterials*. 8 (2018) 1–12.
- [43] D. Cho, S. Lee, M.W. Frey, Characterizing zeta potential of functional nanofibers in a microfluidic device, *J. Colloid Interface Sci*. 372 (2012) 252–260.

- [44] K. Cai, M. Frant, G. Hildebrand, K. Liefelth, K.D. Jandt, Surface functionalized titanium thin films: Zeta-potential, protein adsorption and cell proliferation, *Colloids Surfaces B Interfaces*. 50 (2006) 1–8.
- [45] H. Chen, J. Huang, J. Yu, S. Liu, P. Gu, Electrospun chitosan-graft-poly (-caprolactone)/poly (-caprolactone) cationic nanofibrous mats as potential scaffolds for skin tissue engineering, *Int. J. Biol. Macromol.* 48 (2011) 13–19.
- [46] B. Vrhovski, A.S. Weiss, Biochemistry of tropoelastin, *Eur. J. Biochem.* 8 (1998) 1–18.
- [47] D. V Bax, U.R. Rodgers, M.M.M. Bilek, A.S. Weiss, Cell Adhesion to Tropoelastin Is Mediated via the C-terminal GRKRK Motif and Integrin $\alpha\beta 3$, *J. Biol. Chem.* 284 (2009) 28616–28623.
- [48] D. V Bax, Y. Wang, Z. Li, P.K.M. Maitz, D.R. Mckenzie, M.M.M. Bilek, A.S. Weiss, Binding of the cell adhesive protein tropoelastin to PTFE through plasma immersion ion implantation treatment, *Biomaterials*. 32 (2011) 5100–5111.
- [49] M.A. Hiob, S.G. Wise, A. Kondyurin, A. Waterhouse, M.M. Bilek, M.K.C. Ng, A.S. Weiss, The use of plasma-activated covalent attachment of early domains of tropoelastin to enhance vascular compatibility of surfaces, *Biomaterials*. 34 (2013) 7584–7591.
- [50] Y. Yin, S.G. Wise, N.J. Nosworthy, A. Waterhouse, D. V Bax, H. Youssef, M.J. Byrom, M.M.M. Bilek, D.R. Mckenzie, A.S. Weiss, M.K.C. Ng, Covalent immobilisation of tropoelastin on a plasma deposited interface for enhancement of endothelialisation on metal surfaces, *Biomaterials*. 30 (2009) 1675–1681.
- [51] S. Landau, A.A. Szklanny, G.C. Yeo, Y. Shandalov, E. Kosobrodova, A.S. Weiss, S. Levenberg, Tropoelastin coated PLLA-PLGA scaffolds promote vascular network formation, *Biomaterials*. 122 (2017) 72–82.

CHAPTER IV.

General Conclusions and Future Work

Chapter IV. General Conclusions and Future Work

4.1. General conclusions

Extensive research was made to develop functional biomechanical vascular substitutes for vascular bypass applications. Matched mechanical properties and rapid endothelialization are the most critical requirements that vascular substitutes should accomplish to suit the purpose of replacing vessels segments. Herein, the proposed work aimed at developing an electrospun tubular fibrous scaffold biofunctionalized with tropoelastin, as a biomimetic approach to address the vascular grafts needs.

The eTF scaffolds were successfully fabricated by electrospinning, presenting a porous luminal surface with fibers diameters ranging from submicron to several microns. The fibers were randomly organized, showing some degree of alignment in the axial direction. The porosity obtained was about 34%, the pore sizes ranged between 1 and 23 μm and the pore areas were up to 70 μm^2 .

The functionalization of the luminal surface of eTF scaffolds was carried, firstly, by NaOH treatment and, then, by aminolysis to insert oxygen-containing groups (-COOH and -OH) and -NH₂, respectively. The surface functionalization was effectively confirmed by the quantification of amine groups by Ellman 's reagent method, as well as the presence of different surface functionalities by the surface charge analysis. The surface treatments did not affect the fibers morphology, as confirmed by SEM, but promoted a decrease in the group of fibers with diameters lower than 1 μm . Uniaxial tensile tests were performed along the axial and radial directions, under dry and hydrated conditions, for untreated, activated and aminolysed eTF scaffolds. The radial tensile properties exhibited lower maximum stress and its corresponding strain when compared with the axial properties due to the presence of fibers axially aligned. Although the surface treatments have affected the maximum stress and the corresponding strain, their values were within the range of those of native vessels.

Taking advantage of the different surface functionalities, tropoelastin was immobilized on activated and aminolysed eTF scaffolds, and further confirmed by microBCA assay. The activated substrate presented a higher binding capacity of tropoelastin in comparison to the aminolysed substrate. The protein immobilization on eTF scaffolds surface with two different functionalities aimed at exposing the C-terminal and N-terminal of tropoelastin to, consequently, study their effect over ECs behaviour. The eTF scaffolds supported endothelial cell adhesion, spreading and

proliferation, as evaluated by MTS and DNA results. Generally, the presence of tropoelastin influenced positively the ECs behaviour. Particularly, exposing tropoelastin -COOH groups to ECs seemed to promote enhanced viability and protein synthesis at the early stages of culture, as well as the cells activity due to an apparent higher production of VEGF at day 7. On the other hand, exposing its -NH₂ groups stimulated endothelial cells to synthesize higher amounts of protein. ECs maintained their phenotype along the time-course of the experiment as confirmed by the staining of the endothelial cell adhesion molecule (CD31), being more evident for NH₂-TE condition at day 7. Regardless tropoelastin presence, eTF scaffolds supported cells adhesion and proliferation, as well as phenotype maintenance. Besides, after 7 days, the presence of an endothelial layer on the luminal surface, fully covering the surface, was confirmed by SEM analysis. In conclusion, our biofunctional eTF scaffolds possess mechanical properties similar to those of native vessels and enhanced cell-material interactions towards endothelialization, demonstrating to be a valid strategy for development of successful blood vessels replacement.

4.2. Future work

The work developed under the scope of this thesis produced promising findings and, thereby, can be complemented with other studies to ultimately confirm its suitability for vascular tissue engineering applications. Although these eTF scaffolds were biofunctionalized with an anti-thrombogenic protein and supported endothelial cell coverage, hemocompatibility studies could be also performed to give an insight of their thrombogenic properties. Particularly, a study of platelets adhesion, morphology, activation and coagulation activity could be conducted with fresh blood to understand the behaviour of these scaffolds, before and after the biofunctionalization with tropoelastin.

Since SMCs play an important role on blood vessels along with ECs, a co-culture system comprising ECs seeded in the luminal surface and SMCs seeded in the outer surface could be implemented. Additionally, these constructs would also benefit from dynamic cell culturing under physiological conditions (pressure and flow) for longer periods to understand the interaction of both cell types on tissue remodelling and ECM synthesis. Envisioning the future application, culture of fibroblasts could also be explored in an attempt to develop a highly functional vascular tissue, mimicking the native architecture and cell composition of blood vessels.

Considering the mechanical testing, biomechanical properties, such as burst pressure, dynamic compliance and suture retention strength should be also evaluated to assess the

mechanical response of eTF scaffolds. Moreover, performing this mechanical testing on human vessels would be a better strategy to compare directly with the scaffolds under the same conditions.

Finally, the evaluation of these constructs *in vivo* would be also of interest to assess their response in living tissues, as well as their function in replacing blood vessels. A study on *in vivo* compliance, intimal hyperplasia, patency, thrombosis, *in vivo* calcification, polymer degradation, mechanical properties maintenance and tissue regeneration of eTF scaffolds would be challenging, yet motivating, since only few studies have focused on the *in vivo* performance of synthetic vascular grafts.